Development of Polymer Based Electrospun Nano fiber Filters for Removal of Aerosols from the Petrochemical Industrial Exhaust

Submitted by

Syeda Irsa Mazhar

07/FBAS/PHDES/F-14

Supervised by

Dr. Maliha Asma

Department of Environmental Sciences (FC)

Co-Supervised by

Prof. Dr. Muhammad Raffi

National Institute of Laser and Optronics (NILOP, College, PIEAS)

Faculty of Basic and Applied Sciences
Department of Environmental Sciences (FC)
International Islamic University, Islamabad
(2022)

International Islamic University
CENTRAL LIBRARY
ISLAMABAD

PHD
661.804
SYD

Accession No. TH-25903

Petrochemicals -- chemical - engineering

Electrospun

Nano - fiber

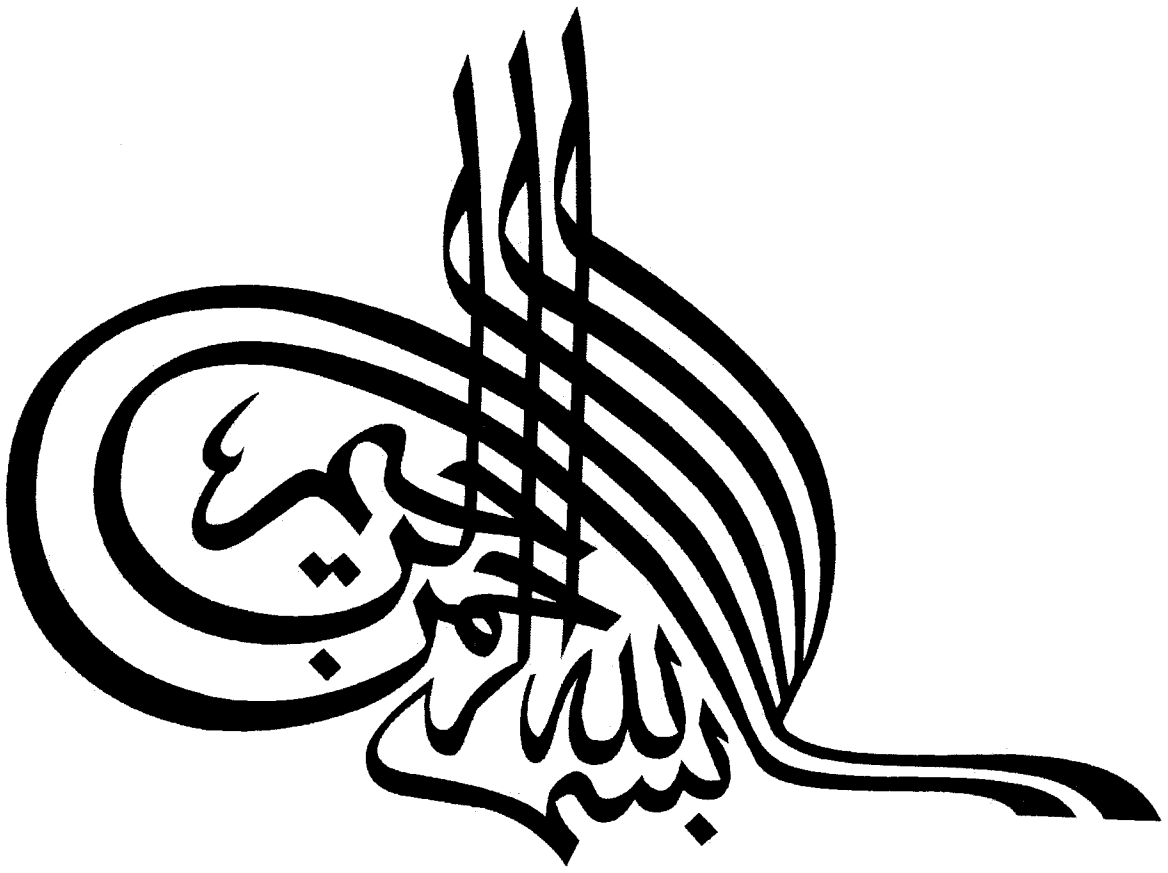

In the name of Allah,
the Most Beneficent,
the Most Merciful

Development of Polymer Based Electrospun Nanofiber Filters for Removal of Aerosols from the Petrochemical Industrial Exhaust

Syeda Irsa Mazhar

07/FBAS/MSES/F14

Thesis submitted to Department of Environmental Sciences,

International Islamic University, Islamabad as a partial

Fulfillment of the requirement for the award of the

Degree of PhD Environmental Sciences (FC)

June, 2022

Supervisor

Dr. Maliha Asma

Co- supervisor

Prof. Dr. Muhammad Raffi

DEDICATED

To

My Beloved Parents
To whom I owe everything

"Do not go where the path may lead,
go instead where there is no path and leave a trail"
Ralph Waldo Emerson

Department of Environmental Science (FC)

International Islamic University Islamabad

Dated: 21-06-2022

FINAL APPROVAL

It is certified that we have read the project report submitted by Syeda Irsa Mazhar. It is our judgment that this thesis is of sufficient standard to warrant its acceptance by the International Islamic University, Islamabad for the PhD Degree in Environmental Science.

COMMITTEE

External Examiner 1
Dr. Rohama Gill,
Professor,
Department of Environmental Sciences,
Fatima Jinnah Women University, Rawalpindi

External Examiner 2
Dr. Azeem Khalid,
Professor/Chairman
Department of Environmental Science
Institute of Soil & Environ Science, PMAS
Arid Agriculture University, Rawalpindi

Internal Examiner
Dr. Zafeer Saqib
Assistant Professor
Department of Environmental Science (MC), IIUI

Supervisor
Dr. Maliha Asma
Assistant Professor
Department of Environmental Science, IIUI

Co-Supervisor
Dr. Muhammad Raffi
Professor
National Institute of Laser and Optronics (NILOP)

Dr. Syeda Maria Ali
Assistant Professor/In charge
Department of Environmental Science (FC), IIUI

Dean
Prof. Dr. Muhammad Irfan Khan
Faculty of Basic and Applied Science, IIUI

DECLARATION

I hereby declare that the work presented in the following thesis is my own effort, except where otherwise acknowledged and that the thesis is my own composition. No part of the thesis has been previously presented for any other degree.

Dated 8-07-2022

Syeda Irsa Mazhar

ACKNOWLEDGEMENTS

Some feats cannot be accomplished alone

Praise to Almighty Allah, The Greatest, Gracious, Merciful and The Most Beneficent, Who granted me wisdom and perseverance for completing this Research study.

I am thankful to my supervisor, **Dr. Maliha Asma,** Assistant Professor Department of Environmental Science for her detailed review and advice in the preparation of this.

I consider it a proud privilege to express my deepest gratitude and deep sense of obligation to my co-supervisor, **Dr. Muhammad Raffi, Professor**, National Institute of Laser and Optronics (NILOP, college, PIEAS), who kept my morale high by his suggestions and appreciation. His motivation has lead me to this success; without his sincere and cooperative nature and precious guidance, I could never have been able to complete this task. I am grateful to Dr. Hafiz Zahid Shafi (Associate Professor), and other technical staff from Materials Division, NILOP-C for their continuous encouragement and technical support at all stages of this work.

I want to give heartfelt thanks to Acting Chairperson **Dr. Maria** and **Dr. Irfan Khan**, Dean, Faculty of Basic and Applied Sciences, IIUI for their cooperation extended during the study. I would also like to acknowledge Higher Education Commission (HEC) for granting me six month scholarship under **IRSIP** to visit **University of Florida, USA** under the supervision of **Dr. Chang Yu Wu** (Environmental Engineering Department). Through this scholarship I was able to complete my lab work and learnt a lot of other analytical techniques related to my research.

Finally, yet importantly, I would like to express my heartfelt thanks to my **beloved parents** for their blessings, morale support and financial help during my entire career that enabled me to complete my work dedicatedly, my friends (especially **Anjuman Shaheen (late), Seema, Dr. Waqar-un-Nisa, Dr. Rakshanda, madam Sajida and Tayyaba Sajjad,** for their help and wishes for the successful completion of this project.

Syeda Irsa Mazhar

FORWARDING SHEET

The thesis entitled "Development of Polymer Based Electrospun Nanofiber Filters for Removal of Aerosols from the Petrochemical Industrial Exhaust" submitted by Syeda Irsa Mazhar in partial fulfillment of PhD in Environmental Sciences has been completed under my guidance and supervision. I am satisfied with the quality of student`s research work and allow her to submit this thesis for further processes per IIUI rules and regulations.

_____

Dr. Maliha Asma

Development of Polymer Based Electrospun Nanofiber Filters for Removal of Aerosols from the Petrochemical Industrial Exhaust

Table of Contents

List of Figures

List of Tables

Abbreviations and Acronyms

AFM	Atomic Force Microscopy
BET	Brunauer, Emmett and Teller
CH_4	Methane
CuO	Copper oxide
°C	Degree centigrade
cm	centimeter
DC	Direct current
E %	High Efficiency
EDS	Energy dispersive spectrum
FE-SEM	Field emission scanning electron microscopy
FTIR	Fourier transform infrared spectroscopy
GC	Gas chromatography
HCHO	Formaldehyde
kV	kilovolt
LBDASA	Low-bond axisymmetric drop shape analysis
MERS	Middle eastern respiratory syndrome
MPPS	Most penetrating particle size
mL/h	Milliliter per hour
mm	Millimeter
mg	milligram
µm	micrometer

μS	Micro siemens
NO_2	Nitrogen dioxide
NF	Nanofiber
NiO	Nickel oxide
nm	Nanometer
PVA	Polyvinyl alcohol
PM	Particulate matter
PTFE	Polytetraflouroethylene
ΔP	Pressure drop
Pa	Pascal
PP	Polypropylene
PE	Polyethylene
PBI/PIM	Polybenzimidazde/poly imidazdate
PVDF/HFP/PVDF	Polyvinylidene fluoride/hexaflouroprpylene/ Polyvinylidene fluoride
PBI/PDA	Polybenzimidazde/polydopamine
QF	Quality factor
RMS	Root mean square
ROS	Reduced oxygen species
SARS	Severe acute respiratory syndrome
T.C.D	Tip to collector distance
TGA	Thermogravimetric analyzer
ULPA	Ultralow particulate air filter

UV	Ultraviolet
VOCs	Volatile organic compounds
WCA	Water contact angle
Zno	Zinc oxide
ZOI	Zone of inhibition

ABSTRACT

The abundant existence of air pollutants and its penalties on human health is a worldwide apprehension. The filter media conventionally used to capture PM from air are comprised of microfiber but with the limitations of not being able to remove multiple pollutants; volatile organic compounds (VOCs and microbes; virus& bacteria). Composite electrospun multifunctional air filtration nanofibrous membranes have gained more attention in the recent era because they are synthesized by simple and eco-friendly electrospinning technique. This research presents the development of PTFE-metaloxides based electrospun composite nanofibrous filter mats for capturing particulate matters, volatile organic compounds and microbes from air at a minimum air pressure drop and holding high quality by mimicking actual industrial conditions.

Physiochemical structural properties of the heat treated PTFE-Metal oxide nanofibrous filter mats improved by metal oxides doping like fiber diameter, porosity and hydrophobicity; mean fiber diameter decrease from 0.24 μm to 0.12 μm, porosity increase up to 88.73 %. Water contact angle also increased from 102 to 122 degrees respectively. Aerosol filtration efficiency (%) of composite filter mats enhanced up to the 97.71% for $PM_{2.5}$ and 99.33% for PM_{10}. Pressure drop for filter mats retained up to 42 Pa in comparison with commercial PTFE filter with pressure drop of 62 Pa. Quality factor of PTFE nanofibrous mats at 0.024(Pa^{-1}) meet the requirements of commercially available PTFE air filters. UV results demonstrated that surface adsorption of the VOCs by mats were effective in removing formaldehyde and toluene by (PTFE-ZnO) formaldehyde & acetone by (PTFE-NiO) from polluted air. Nanofibrous filter mats demonstrated excellent self-cleaning property which further aid in long term air filtration of hazardous pollutants from air. Hence, these surface modified hydrophobic multifunctional composite air filters can effectively be used in wide practical application in industries to ensure good indoor air quality.

Introduction

1.1 AIR POLLUTANTS AND AIR FILTERING MATERIALS

1.1.1 Introduction to Air Pollutants

Air pollution is one of the growing global concern for the scientists/researchers because air pollutants have complicated chemical composition, which make their removal from air a challenging task. Major air pollutants include particulate matter (PM), gaseous pollutants, biological pathogens and others. Release of these air pollutants led to many human (and other living organisms) and environmental problems. It is well known that discussing pollution is conscious of different unfortunate deaths, as well as their irreversible effects on the environment. World bank report published in 2012 depicted that individual percentage of 60% in economically successful nations live in discuss air quality levels that are possibly inconvenient to their wellbeing (V. V. Kadam, Wang, & Padhye, 2018; L. Li et al., 2015; Repace et al., 2011) and could even cause damages to agricultural crops. In the coming years by 2050 premature mortality from air pollution will be raised to estimated value of more than 6.5 million (Brook et al., 2010). Figure 1.1 shows the detailed classification of air pollutants. Particle Matter typically characterized into $PM_{2.5}$ with particles diameter smaller than 2.5 μm and PM_{10} with the size between 2.5–10 μm, respectively (Brook et al., 2010). Among them most specifically PM particles with smaller diameter are lethal air pollutants to be sieved having capacity to deeply move down into human lungs and bronchi (Betha, Behera, & Balasubramanian, 2014; Horton, Skinner, Singh, & Diffenbaugh, 2014; Wu et al., 2014; R. Zhang et al., 2013). Chemical composition of the particulate pollutants is organic and inorganic compounds, among organic for instance carbon derived species (CO_2 and CO) and in organic compounds composed of sulfur- and nitrogen-based (SO_2^{2-}, SO_4^{2-} , NO^{3-}) (Hailin

et al., 2008; Han & Naeher, 2006; Maricq, 2007). Additionally, various gaseous molecules are also part of particulate matter composition such as volatile organic compounds.

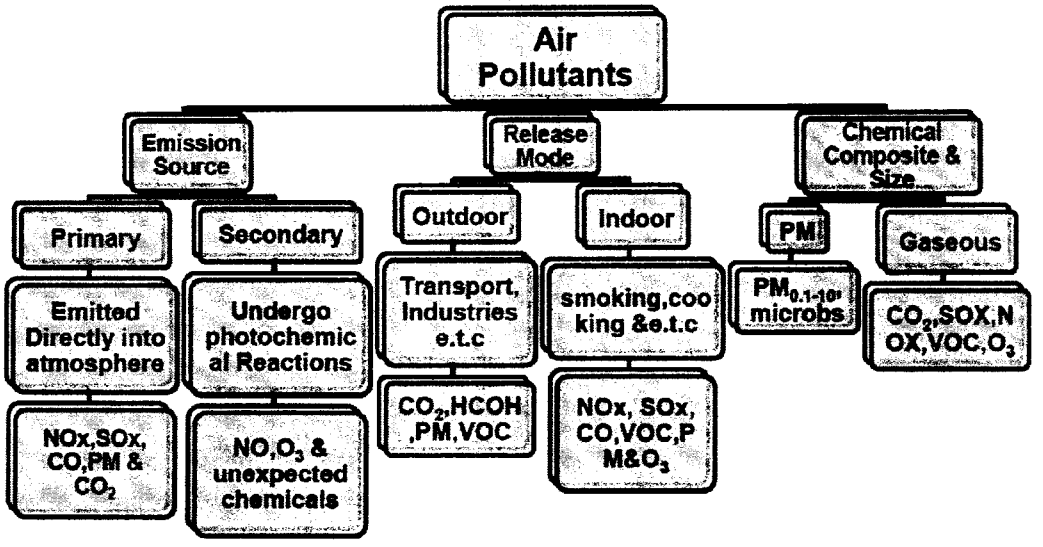

Figure 1.1. Classification of air pollutants

Bio-aerosols represents additional type of main air pollutant which greatly increases the risks to the public health as they can spread through polluted air (Jung et al., 2011; Vanangamudi, Hamzah, & Singh, 2015; Verdenelli, Cecchini, Orpianesi, Dadea, & Cresci, 2003). These bio aerosols cause both long-lasting and severe diseases that can be lethal, allergenic, contagious (Jung, Lee, & Kim, 2009; Main, 2003). Bio aerosol toxicity was proved through the discovery of Severe Acute Respiratory Syndrome (SARS) and Middle Eastern Respiratory Syndrome (MERS)(V. V. Kadam et al., 2018). Outdoor air pollution greatly desired the need of improving indoor air quality. Henceforth, the plea for high-performance multipurpose air-filtering materials that can simultaneously capture both particulate matter and gaseous/chemical pollutants particles along with the microbial contaminants is increasing dramatically.

1.1.2 Classification of Air Filters

Air filters are frequently used device to take out hazardous pollutants from air. Air filters are broadly used in various sectors like industries, residential, commercial sector and health sector. Conventionally, non- woven, porous, randomly oriented micro fibers air filters/film are chemically made of petroleum based materials. In the market there are commonly 3 different types of available air filters are: High Efficiency particulate air filter (HEPA), chemical (activated carbon) and anti-microbial capturing (nano particles surface modified) air filters as shown in Figure 1.2.

It is the need of the hour that presently working air filtration systems in order to obtain clean air from the outlet of air filter, utilizing all different types of air filters at the same time are critically needed. Using multiple filters could increase the pressure drop at the outlet of the air filters and as a result, consumption of a huge amount of energy and high cost for cleaning.

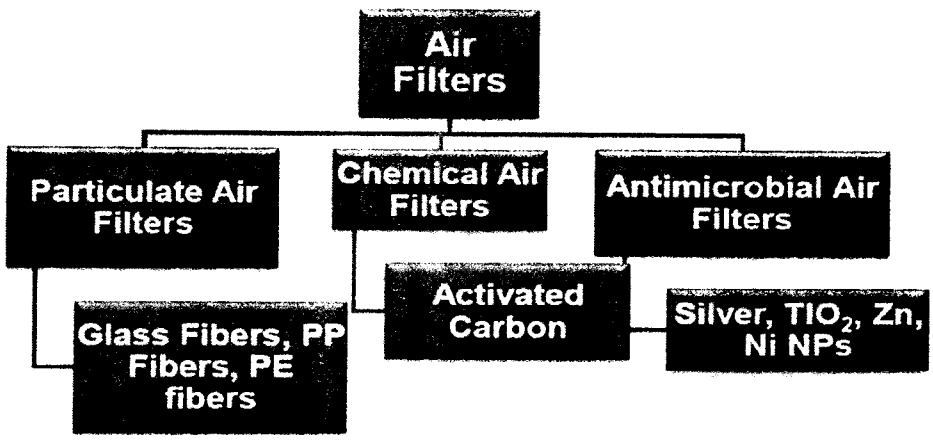

Figure 1.2 Classification of current air filters

1.1.2.1 Particulate Air Filters

Particulate matters filters chemically constituted manmade or materials made from petroleum based raw material. Those chemicals include polypropylene (PP) and fiberglass (FG), they are specifically fabricated to capture or target PM with different size ranges. In today's

industrialized world most frequently used air filters both in industries and home are high efficiency particulate air filters (HEPA). In case a filter to be categorized as HEPA filters; they need to meet certain requirements set by Department of Energy (DOE). First one include they should possess 99.97% or more (E) for filtering particle size range of 0.3 μm; (2) maintaining a pressure drop lower than 1.3" water (320 Pa)(DOE, 2005). Limitations of these filters include very limited chemical functionality, unsatisfactory interfaces with contaminants, and their dispose off cause's secondary environmental pollution. Particulate filtration is defined terms of: (1) performance evaluation/efficiency (E%); (2) air flow resistance; (3) quality factor (QF) (R. Brown, 1993). The filtration performance evaluation and pressure difference can be calculated with the help of air experimental setup shown in Figure 1.3. Definition of drop in pressure is; difference in pressure between inlet and outlet of air stream through air filter in the filtration system and it should be minimal to reduce the consumption of more energy by the system (Souzandeh, Johnson, Wang, Bhamidipaty, & Zhong, 2016; Souzandeh, Wang, & Zhong, 2016). Filter performance evaluation (E), pressure difference (ΔP) and quality factor (QF) are calculated by the following equations (i-iii):

$$E\% = \frac{(Cp - Cc)}{Cp} \text{ X100} \quad \text{(i)}$$

$$\Delta P = P_{up} - P_{down} \quad \text{(ii)}$$

$$Q = -\frac{In(1-\eta)}{\Delta P} \quad \text{(iii)}$$

In equation (i) C_p: denotes contaminants concentration in the air before filtration; C_c: denotes contaminants concentration in the air after filtration; ΔP is difference in pressure upstream air and downstream air flow; and Q: is the quality of filter (Uppal, Bhat, Eash, & Akato, 2013).

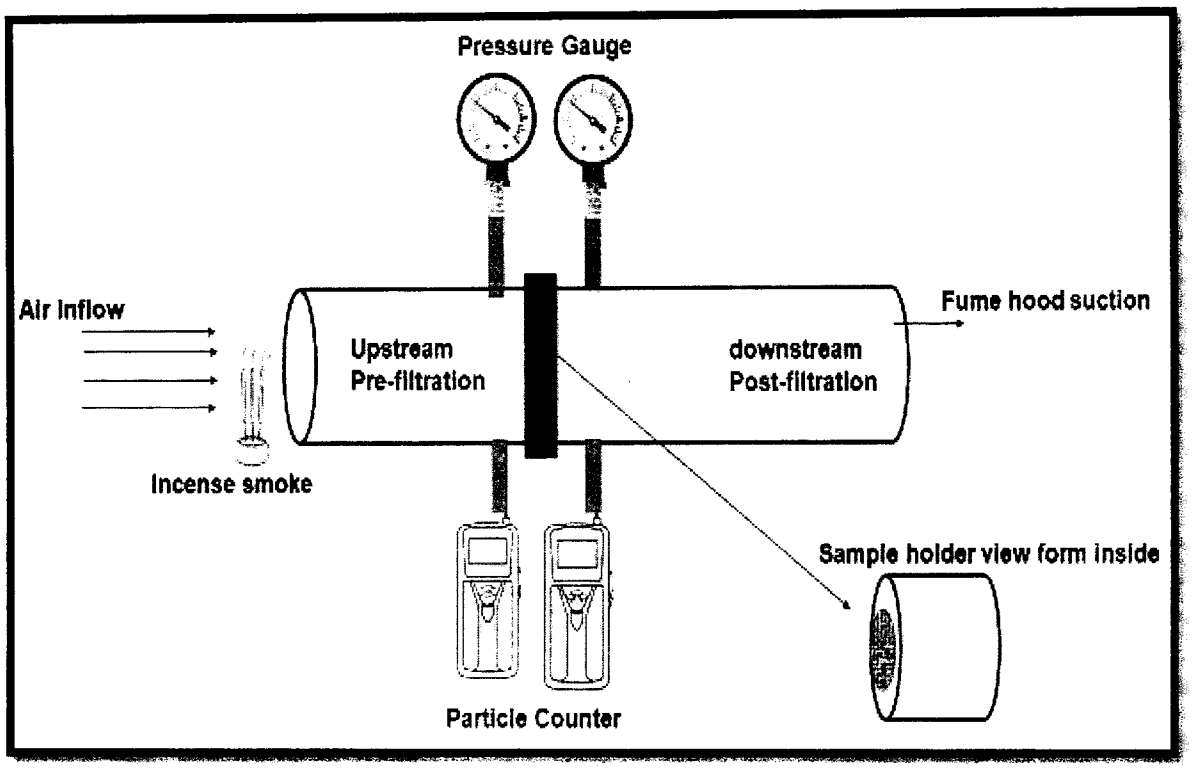

Figure 1.3. Air filtration measurement setup developed at NILOP comprising of DC fan, Differential pressure manometer, PM counters, burning incense as a pollutant source and nanofibrous mats holder.

1.1.2.2 Chemically modified Air Filters

Gaseous contaminants in air are mostly removed by chemically modified filters. Chemical air filters are synthesized from fibrous material which constitute high loading of powder material like activated carbon. Activated carbon is used because of its large surface area through which it can absorb/ adsorb chemical molecules from polluted air. However, it is noted that this type of air filters are design only to remove gaseous contaminants with low filtration performance. Due to complex and unstable nature of the contaminants, performance of filter is measured against a diluted chemical relative to time (Aluigi et al., 2009; Uyar et al.,2010). These diluted suspensions afterwards are characterized by employing different techniques;

UV Visible spectroscopy, (Chuang, Hong, & Chang, 2014), High Potential liquid chromatography (HPLC)(Kayaci & Uyar, 2014), gas chromatography (GC) (R. C. Brown, 2001) adsorption, gas sensors and others.

1.1.2.3 Antimicrobial Air Filters

Bio aerosol are among the most lethal impurities intimidating the human wellbeing; consequently, there is a need of an air filter with high capturing and disinfecting of these bio aerosols from polluted air. But in reality when these bio aerosols are captured by filters these bio aerosols accumulate on filter surface and start to sprout when it become moist (V. Kadam, Jadhav, Nayak, Wang, & Padhye, 2016; Sundarrajan, Tan, Lim, & Ramakrishna, 2014). The particulate matter and other organic impurities caught on the filter could additionally aid in the growth of the bio aerosols which may lead to a substantial decrease in filter proficiency and sooner or later decline in the quality of the filter. Secondary environmental pollution caused by the gases (volatile chemicals) released in to the air from the microbial metabolism which further deteriorate the filter(Sim, Park, Bae, & Jung, 2015; Woo, Kang, Kim, Kim, & Han, 2015). Antimicrobial air mesh are particularly intended to simultaneously capture both PM and bio aerosols from air. In conventional filters during the nanofibers filters fabricating processes to enhance its antimicrobial property different types of additives are added in the solution like metal oxides, heavy metals and titania (M. Jin et al., 2007; Jin, Jeon, Kim, & Youk, 2007) which are costly and can cause irrevocable compensations to the human health and environment.

1.2 CAPTURING MECHANISMS OF AIR FILTERS

Filtration mechanism is an approach through which contaminants are captured, stick/ absorbed by the filtration material. Filtration method of solid and gaseous contaminants is different. Their filtration depends on properties of both contaminants and filters. Solid particles and gaseous contaminants filtration is governed by physical parameters while those of gaseous is by chemical properties.

1.2.1 Particulate Capturing Mechanisms

Solid contaminants are filtered from air through size based methodology by blocking the pollutants on the surface of filters. Sieving being the most important mechanism is feasible for those pollutant particles having size lager than the pore size of the filter on the other hand where sieving is not effective; fibrous filters are able to retain the solid contaminates smaller than its pore size. Basic filtration mechanisms comprise of gravitation, inertial impaction, interception, diffusion, electrostatic attraction and intermolecular interaction on filter surface. In nanofibrous structure dominant filtration mechanism is interception and diffusion (R. Brown, 1993). Figure 1.4 schematically shows the filtration mechanisms around a single fiber.

Nanofibrous filters have two dominant filtration mechanism; Interception and diffusion. Interception is dominant when the particle size that interact with the fiber surface is 0.5 μm, diffusion is effective for less than 100 nm size particles. Through interception and Brownian motion particle with the size range of 50-500 nm are removed with the aid of nanofibrous filters (Maze, Tafreshi, Wang, & Pourdeyhimi, 2007; Mukhopadhyay, 2010).

TH-25903

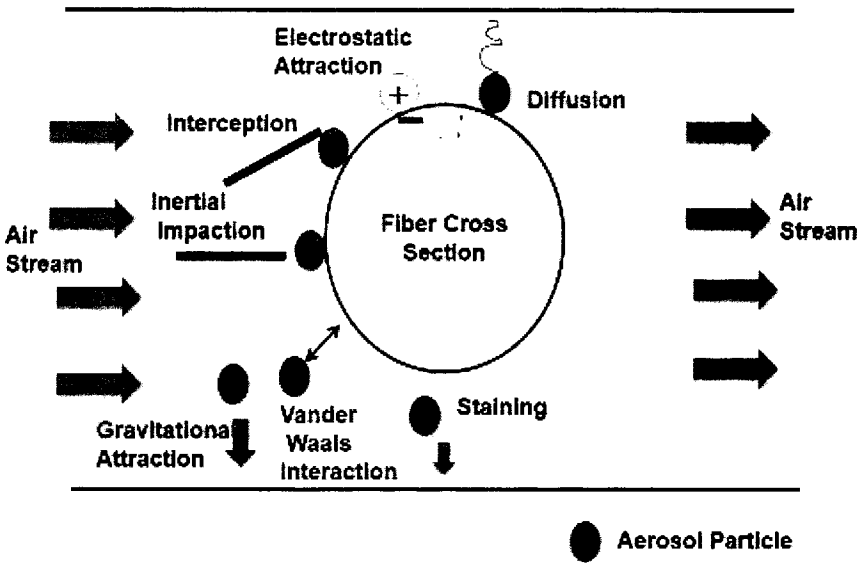

Figure 1.4. Longitudinal sectional view of fiber depicting particle capturing mechanisms

1.2.2 Gaseous Chemicals Capturing Mechanisms

Gaseous contaminants are captured by intermolecular interaction such as physisorption and chemisorption through polluted air stream. The removal of gas molecules from the air through a fibrous structure may involve one or more of the following mechanisms: (a) diffusion of gas on sorbent's surface, (b) gas adsorption by large pores, (c) gas molecule adsorption in internal pores (d) chemical interaction between the gas molecule and polymer structure, that can either be absorption or adsorption.

Physisorption refers to fibers structural surface pores seizing of gas molecules due to intermolecular attraction, i.e. weak forces (Van der Waals forces), polar interaction, hydrogen bonding, high specific surface area of nanofibers (Aluigi et al., 2009). Physisorption of gaseous pollutants sometimes depends on size of pollutant molecule and number of atoms involve in interaction as shown in figure 1.5. Chemisorption is a type of chemical action in which pollutants are converted in to simple compounds. The chemical action may be an acidic-basic reaction, nucleophilic outbreak, catalytic/non-catalytic, oxidation/reduction and polymerisation. Chemisorption is further selective in comparison with physisorption. It is the

chemical interaction of pollutant particles with active functional groups on the surface of the fibers (V. Kadam et al., 2016). Therefore, electrospinning of the functional nanofibers can be a useful approach for filtration of gaseous chemical pollutants.

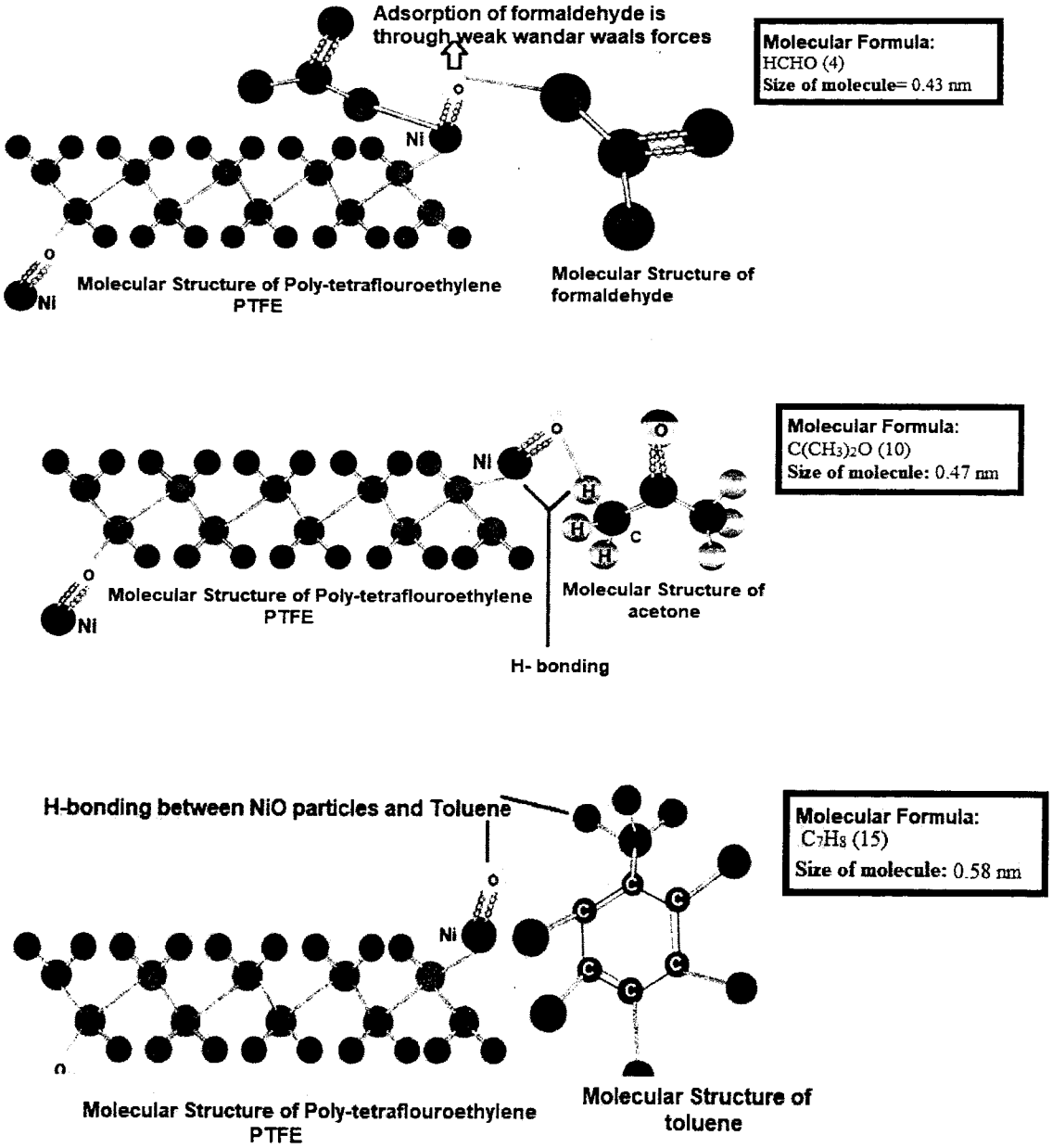

Figure 1.5. Physisorption mechanism of VOCs by PTFE-NiO composite fibrous mats

1.3 ELECTROSPINNING PROCESSING AND POLYMERIC NANOFIBERS

Nanofibers having nanometer scale diameters can be fabricated from various polymers, either

synthetic or natural, having different properties for several uses. The nanofibers diameter depends on two things; the type of polymer, fabrication method (Reneker & Chun, 1996). Traditional methods for nanofibers synthesis are, self-assembly (C. Zhang et al., 2014) template synthesis (Martin, 1994), drawing (Z.-M. Huang, Zhang, Kotaki, & Ramakrishna, 2003), thermal-induced phase separation (Ma, 2004) and electrospinning (Guibo, Qing, Yahong, Yin, & Yumin, 2013; C. Liu et al., 2015). All polymeric nanofibers possess very high specific surface area, noticeable mechanical properties, high permeability, flexibility and so forth in comparison with the conventional microfibers (Khajavi, Abbasipour, & Bahador, 2016). On the basis of these properties, nanofibers have been of great interest for many uses like in the field of tissue engineering (Riboldi, Sampaolesi, Neuenschwander, Cossu, & Mantero, 2005), wound dressing (Yang, Xu, Kotaki, Wang, & Ramakrishna, 2004), drug delivery (Sharifi et al., 2016), batteries (B. Zhang, Kang, Tarascon, & Kim, 2016), and air filtration (Kelly, Gao, & Sailor, 2011; Souzandeh, Johnson, et al., 2016).

1.3.1 Electrospinning

Among all the nanofiber fabrication techniques, electrospinning is the most extensively used process for the manufacturing of nanofibers because of its facile setup and ability for mass production of nanofibers from numerous polymers. Although electrospinning is a relatively well-known fabricating technique, currently, it is the most advanced processing method to manufacture high performance nanofibers with high feature percentage, specific surface area, and high pore interconnectivity(D. Li & Xia, 2004).

1.3.1.1 Process

Electrospinning is a simple but effective method for making uniform fibers ranging from micron and submicron fibers to ultrathin fibers with various nanofibers structure and

orientation via applying high voltage electric field(Nayak, Padhye, Kyratzis, Truong, & Arnold, 2012). In typical electrospinning process, a viscoelastic fluid is loaded in a plastic syringe mounted on a syringe pump. The fluid can be either a polymer solution or molten polymer. The polymer fluid then passes through a syringe and high electric field is applied to the fluid. A point come when charged fluid inside the syringe overcome the surface tension, the Tylor cone designed at the tip of the syringe. The fluid elongated and finally deposited on the grounded collector electrode. The jet experiences instabilities and fluctuates, which along with the fluid properties determine the structure of the collected fibers. The simultaneous stretching of fluid jet and subsequent solvent evaporation during electrospinning process lead to the arrangement of nanofibers with various diameters and shapes (Podgorski, Bałazy, & Gradoń, 2006; Sambaer, Zatloukal, & Kimmer, 2012).

Solution parameters; consistency, polymer solution conductivity, surface tension, molecular weight, solvent system together with electro spinning procedure parameters including electric current, fluid effusion rate and needle tip-to- grounded collector distance play very important roles in the electrospinning process and properties of nanofibers. Green electrospinning has gained importance now a days it requires usage of hazardous solvent free solutions for electrospinning technique. Water soluble polymer solutions are best suited for green electrospinning because they avoid creating secondary pollution during whole spinning process. In present research PTFE aqueous emulsion, PVA and Zinc oxide aqueous solutions were used for green electrospinning process. Electrospun nanofibers have tremendous potential in applications such as clean energy, health and environment areas, and air filtration.

1.3.2 Polymeric Nanofibers

An extensive variability of manmade polymers and biopolymers in the presence of or lacking of additives are appropriate for production of nanofibrous membranes via electrospinning

technique either at lab scale level or at industrial level. Examples of synthetic polymers include polyethylene (PE), polypropylene (PP), polystyrene (PS), polyacrylonitrile (PAN), polycaprolactone (PCL), polyurethane (PU), and so forth (Casper, Stephens, Tassi, Chase, & Rabolt, 2004; Dotti et al., 2007; Khajavi et al., 2016; Tsai & Schreuder-Gibson, 2003). Moreover, cellulose, collagen, gelatin, keratin, zein, chitosan and so forth are some examples of natural biopolymers used for production of nanofibers (De Vrieze, Westbroek, Van Camp, & Van Langenhove, 2007; Khajavi et al., 2016; Lala et al., 2007; Matthews, Wnek, Simpson, & Bowlin, 2002; Souzandeh, 2017; Souzandeh, Johnson, et al., 2016).

1.3.3 Composite Materials

Traditionally synthesized nanofibrous air filtration membranes from manmade polymers can be modified by the addition of certain specific additives to enhance their filtration efficiency. Now a days superhydrophobic multifunctional air filtration membranes functionalized with different additives are extensively studied by many researchers.

Polytetraflouroethylene (PTFE) is a fluoropolymer that is famous for its thermal and chemical stability, low surface energy (hydrophobic) and good electrical insulation due to its chemical structure as shown in Figure1.6 (E. N. Brown & Dattelbaum, 2005; Q.-l. Huang, Xiao, Hu, & Li, 2011; Kurose, Takahashi, & Koyama, 2004; F. Wang et al., 2016). Polyvinyl alcohol (PVA) has been chosen as a binder to prepare composite with PTFE polymer due to its favorable properties such as water soluble nature, non-toxicity, excellent chemical stability, gas permeability, low decomposition temperature (280°C) and lower cost which support spinning of polymer solution, eventually leading to control viscosity and minimize beading in the formed nanofibers (J-C Park et al. 2010Xu et al., 2019;Zhang et al., 2005; Huang and Rwei, 2012). Porous PTFE membranes (Meng, Ye, Mansouri, & Chen, 2014; Xiao et al., 2014; Zhou, Yao, Xiang, & Wu, 2014) and PTFE bag filters (Mao, Liu, Chang, & Sun, 2015; Nan, Xiang-yu,

Chen, & Qin-fei, 2017; Park, Kim, Jo, & Lee, 2012) have been used extensively as high-temperature air filters. Most of hot gas filter are made of nonwoven fabrics of PTFE, (Jaworek, Krupa, & Czech, 2007), Polyphenylene sulfide (PPS) (Tanthapanichakoon, Hata, Nitta, Furuuchi, & Otani, 2006) glass (R. Brown & Thorpe, 2001), ceramic (Leibold, Dirks, & Rüdinger, 1989)and metal fiber(Ryi, Park, Park, Lee, & Kim, 2007). Recently, nano composite blends membrane synthesis have attracted attention in different fields, for example (PBI/PIM) polybenzimidazole/ polymer imidazolate blends(Ignacz, Fei, & Szekely, 2018), (PVDF-HFP/PVDF) polyvinylidene fluoride/hexafluropropylene/ polyvinylidene fluoride blends (Meringolo et al., 2019), (PBI/PDA) polybenzimidazole/polydopamine blends (D. Zhao et al., 2019), (PEI/PVA) polyethyleneimine/poly vinyl alcohol blends (Abdul Mannan, Yih, Nasir, Muhktar, & Mohshim, 2019) and PSf/sPAEs blends (Jang, Yoon, Lee, & Choi, 2018) show great execution. In this regard PTFE composite blends still require further systematic investigation and research. Chemically modified surface of these PTFE fibers could further enhance their filtration performance. Recently PTFE based polymer membranes gained attention to be used as vacuum membrane distillation(Y. Huang et al., 2017), heterogeneous catalyst for dye degradation(W. Kang et al., 2016a), superhydrophobic air filtration membranes surface was modified by plasma method with silica nanoparticles (Y. Liang et al., 2018b). The commercially available expanded PTFE filter matrix was used and the surface of filter was homogenously seeded with zinc oxide nano rods by atomic layer deposition method (150-300 cycles). Filter application was for filtration of model particulate matters size range of 2.5 μm along with its antibacterial property (Zhong et al., 2015). An amphiobic (PFDAE)-grafted ZnO@PTFE membrane with enhanced antifouling functionality and high organic pollutants removal efficiency was prepared by Feng and his team in 2016. The PTFE membranes were modified by (ALD) atomic layer deposition method specifically for the removal of oily aerosol pollutants from air. For PTFE composite nanofiber membrane, it has potential as

multifunctional air filter media with surface modifications and so far little research has been reported about the application of Green electrospun process hydrophobic PTFE composite nanofiber membranes for PM and VOCs filtration along with good antibacterial property.

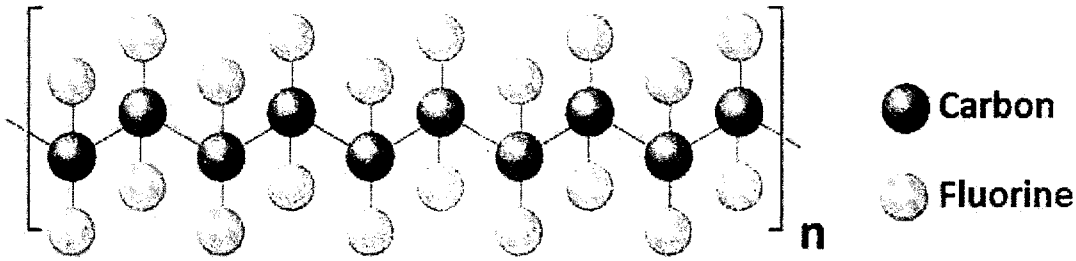

Figure 1.6 Molecular structure of polymer polytetraflouroethylene (PTFE).

1.4 Green Electrospinning

Traditional electrospinning produces nanofibers by stretching a viscoelastic fluid under the influence of electrostatic repulsions and solvent evaporation. The great majority of electrospinning precursor, primarily organic solvent, appears to evaporate, posing a significant barrier to large-scale electrospinning production. Meanwhile, the majority of organic solvents used in solvent electrospinning are toxic and harmful; solvent accumulation from solution evaporation during the electrospinning process causes serious environmental pollution that is hazardous to human health; additionally, residual solvent in the fibers limits many promising potential applications. As a result, traditional electrospinning should be further improved in order to maintain an environmentally friendly, green, and sustainable development plan. However, the vast majority of previous papers have described continuous nanofiber fabrication using organic solution electrospinning. Solvent-free electrospinning, aqueous solution electrospinning, and other greener approaches for fabricating green electrospun nanofibers have received little attention (Lv et al., 2018).

In the electrospinning history, there is no specific definition of green electrospinning. The main focus is on highlighting green electrospinning in the following aspects such as green materials (degradable materials), green solution (water based), and (solvent free) green electrospinning method. Natural polymer materials, chemical synthetic polymer materials, and biosynthetic polymer materials can be classified as natural polymer materials, chemical synthetic polymer materials, and biosynthetic polymer materials, according to the accessible supply of electrospun polymer materials. Natural materials are obviously green and biodegradable, as they are derived from nature and eventually returned to it. Microorganisms and chemical reactions, respectively, are used to make biosynthetic polymer materials and chemical synthetic polymer materials. All of these materials, whether natural or manmade, are biodegradable and environmentally friendly. Furthermore, because the electrospun nanofibers created using these green materials are green, sustainable, and easily recycled, they have a wide range of industrial applications.

A formulation of an aqueous polymer dispersion mixed with an amount of water-soluble polymer can be employed for electrospinning, according to the notion of green electrospinning. Because there is no organic solution residue in the nanofibers, the use of some toxic and harmful organic solutions could be avoided, resulting in a pollution-free and environmentally friendly electrospinning process. As a result, the applications of these green electrospun nanofibers could be expanded, particularly in the biomedical field such as tissue engineering, wound healing, drug delivery and aerosol filtration. Water-soluble polymers can be electrospun into ultrathin nanofibers from their aqueous solution, but only a small percentage of polymers are available. Taking this into mind, solvent-free electrospinning has been intensively developed, allowing solution evaporation to be avoided and electrospun nanofibers to be

created in a more environmentally friendly manner. Solvent-free/green electrospinning refers to an electrospinning technology that does not use standard organic solvents (Lv et al., 2018).

1.5 NANOFIBERS CHARACTERISTICS FOR AIR FILTRATION APPLICATION

Both physical and chemical characteristics of nanofibers play a significant part in filtration performance enhancement. Physical properties include; fiber diameter, pore size distribution, (SSA) specific surface area, areal density and thickness whereas chemical properties includes; structural functional groups, in tailoring the air filtration properties.

1.5.1 Physical Characteristics

1.5.1.1 Fiber Structure (Fiber Diameter and Pore Size)

Before going into the detail of fiber structure it is important to mention here about pore structure which is general term collectively used to explain about **the porosity, pore size, pore size distribution, and pore morphology of a porous medium**. Pore size and fiber diameter both play a very important role in filtration performance of a filter membrane. It has been reported that for removing particles size of 0.3 μm with efficiency above 99%, fiber diameter of nanofibers should be less than 300 nm (Vitchuli et al., 2010).

Recently research study of PAN air filter demonstrated that a decrease in average fiber diameter from 1μm to 200 nm resulted in a significant increase in particulate efficiency from 48.21 to 98.11% (C. Liu et al., 2015). Smaller pollutants particles diffuse easily into higher fiber diameters and in this case interception is dominate over diffusion. The small fiber diameter reduces the pore size and enhances the diffusion and direct-interception for the smaller particles. Not only average fiber diameter but also its distribution is very important as far as filtration performance of nanofibers membrane is concerned. In case of uni modal fiber

distribution air flow causes low resistance and normalized thickness compared with that of a wider or bimodal distribution with the same average fiber diameter (S. Zhang, Shim, & Kim, 2009). In the recent researches it has been reported that smaller fiber diameters (less than 100 nm) can provide improved aerodynamic slip where the collision between air molecules and nanofibers are almost eliminated. Therefore, this slip flow decreases the friction and the pressure drop does not elevate which was reported before (Balgis et al., 2015).

In addition to average fiber diameter and its distribution; pore size plays a critical role in filtration properties, particularly the pressure drop of a filter. In general, nanofibers can provide three different types of pores: (1) closed pores, which are not reachable; (2) blind pores, which are terminated inside the structure of the filter media; and (3) through pores, which are open and effects the filtration performance (Patanaik, Jacobs, & Anandjiwala, 2010). The smaller pore size results in a very high filtration efficiency but unfavorably higher air flow resistance and large pores have an opposite effect. Therefore, the pore size can influence the pressure drop intensely. It is reported recently that the gradient of different pore sizes can enhance the filtration performance of filtering media without largely increasing the pressure drop of the filter. This is because of created circulatory flow between large and small pores and more pathways for the air molecules to flow (Sambaer et al., 2012).

1.5.1.2 Fiber Areal Density and Thickness

Fiber areal density is defined as the mass of the nanofibers per unit area. The thickness of a nanofibers filter directly depends on the areal density of the nanofibers which linearly depends on the amount of the electrospun solution and electrospinning time (Y. O. Kang, Im, & Park, 2015). Higher area density of nanofibers coupled with thicker filter membrane lead towards achieving high filtration efficiency; however, it harmfully causes increase in pressure drop of filter. It is noted that increasing areal density and thickness of nanofibers layer does not enhance

the filtration efficiency beyond a certain limit, but continues to increase the air flow resistance and, as a result, fading the quality factor of the filter. Recent studies proposed that filtration performance of nanofibers can be boosted if they are stacked in layers compared with one thick layer of nano fabrics with low areal density and thickness(Hassan, Yeom, Wilkie, Pourdeyhimi, & Khan, 2013).

1.5.2 Chemical Characteristics of fiber structure

Physical properties of nanofibers control the filtration properties for removing PM while chemical properties control the capturing of gaseous chemical molecules from air. Polymer's chemical characteristics such as structural functional groups play a very important role in air filtration properties for gaseous chemicals. As it was discussed above, the commercial air filters are made of conventional polymers such as PP, PE and glass microfibers. The pollutants interaction with nanofibers in these air filters are mostly size based (Total numbers of atoms involved in interaction). Thus, because of lack of active functional groups in the structure of these materials, no interactions exist between fiber and gaseous pollutants. In order to address this issue, recently researchers focus on polymers with polar functional groups such as polyacrylonitrile (PAN), polyvinyl pyrrolidone (PVP), polyvinyl alcohol (PVA), polyamide (PA) and polyimide (PI) (C. Liu et al., 2015; J. Xu et al., 2016; R. Zhang et al., 2016). These materials have active functional groups with positive dipole moment that can interact and capture the gaseous pollutants. Therefore, nanofibers that have high amount of functional groups on their surface represent a promising solution for high performance air filtering materials. A few researchers incorporated metal oxide particles in electrospinning blends to enhance the surface area for adsorption of gaseous pollutants and physical filtration (molecular size based) of air pollutants through nanofibrous membranes. Like Huang et al., (Q.-L. Huang, Huang, Xiao, You, & Zhang, 2017) incorporated zinc oxide particle in PTFE electro spinning

solutions to obtain nanofibers membranes for vacuum membrane distillation purpose, and (W. Kang et al., 2016a) used iron oxide particles as heterogeneous catalysts on PTFE matrix. In another study (Y. Liang et al., 2018b) used silica particles on the surface of PTFE matrix to be used a functional groups for removing PM from air. But one of the major limitation of these particles is secondary environmental pollution chances and these particles are not easily available in cheap prices. So in the present study those metal oxide particles are used as functional group on PTFE nanofibers mats surface that have high selectivity towards VOCs trapping/ sorption.

1.6 CHALLENGING ISSUES OF AIR FILTERING MATERIALS

Major limitations in these air filtration systems are high pressure drop downstream, more energy usage due to depth aerosol filtration and cost of cleaning. Major issues linked with present commercial air filter production material are being studied in research labs are summarized below:

(1) **Materials:** All of the synthesized materials Polypropylene, glass fiber and many additives are not naturally disposable or environmentally friendly. And not all filters are hydrophobic, they can be a place favorable for microbial growth; these factors could be a possible reason to secondary environmental pollution.

(2) **Functionality:** Limited filtrations of various pollutants, because of (a) nonexistence of active chemical functional groups in the filtering materials; (b) high particles concentration loading (activated carbon or NP) into nanofibrous membranes may reduce particulate filtration performance or deteriorate the pressure resistance, which will increase the energy usage for active air exchange.

(3) **Processing:** Production of air filtration materials involves various complicated and costly processes, especially production of chemical and antimicrobial air filters.

(4) **Filtration mechanisms:** Current filtration process in air filters are through physical interaction, which is only effective for large pollutant particles. These air filters are inadequate for the removal of toxic gaseous chemicals (usually various polar molecules) and antimicrobial components.

Therefore, the development of cost-effective surface modified composite hydrophobic multi-functional air filtering materials through green electrospinning with high removal efficiencies for variety of pollutants (particulate matters, toxic chemicals, microbes) while maintaining low air flow resistance represents a challenging task for the development of advanced materials for air filtration systems.

1.7 OBJECTIVES AND SIGNIFICANCE

The aim of this dissertation is to fabricate PTFE based high-efficiency, hydrophobic, multi-functional composite air filtering materials through green electrospinning. The specific research **objectives** are:

1) Synthesis of PTFE based surface modified hydrophobic composite electrospun nanofibrous mats through green electrospinning. Surface modified by doping PTFE-PVA matrix with metal oxide; zinc oxide and nickel oxide respectively.

2) Study physiochemical properties of nanofibrous mats by FESEM, AFM, FTIR, Raman and UV-Vis spectroscopy. Static water contact angle calculated by sessile drop method and self-cleaning ability was studied through simple dust method.

3) Performance evaluation of synthesized nanofibrous mats for the removal of particulate matters (PM) and volatile organic compounds (VOCs) and pathogenic germs from air stream and comparison with commercially available PTFE air filters.

The **significance** of this dissertation can be summarized as follows:

(1) For environment: Hydrophobic material PTFE polymer is selected to be used for fabrication of high-performance hydrophobic composite multifunctional air filtering materials. This dissertation presents two types of PTFE based composites one with the Zinc oxide metal (PTFE-ZnO) and the other with porous nickel oxide particles (PTFE-NiO). These metal oxide were selected due their easy availability and secondly due to their high selectivity towards gaseous air pollutants. The composites are to be fabricated via facile, reproducible eco-friendly green electrospinning technique. The use of water soluble polymer is environmentally friendly and cost-effective materials can avoid the secondary pollutions to the environment at their disposal after use.

For new filtration capability: It is a breakthrough in generating extra filtration performance without relying on the addition of any other agents, such as capturing toxic (gas state) chemicals via the plenty of functional groups. As a key component in air cleansing systems, air filtering materials play an important role in removing pollutants, including both particulates and toxic chemicals, from the air. Previous studies on air filtration application as well as commercial air filters in the market have simply focused on removing only one or two types of pollutant. In this dissertation, novel nanofibrous morphologies are utilized to create multifunctional air filtering materials that are able to efficiently remove different types of pollutants simultaneously and combine various types of air filters into one single filtering mat without the addition of any active costly materials.

This research will finally give rise to multi-functional air filtering materials which can be used in numerous air filtration applications.

MATERIALS AND METHOD

In the present study 8 samples of PTFE-PVA (Control), PTFE-ZnO and PTFE-NiO (four samples each) composites were prepared through green electrospinning. It was done by preparing four series of solutions; one without metal oxide doping (control) and other with different weight % of metal oxides. Then these blends were electrospun into nanofibrous filter mats. For this purpose following procedure was adopted. It is important to mention here that combination of two polymer solutions is named as "suspension", mixing of 3 solutions in one beaker make a "blend" and end product obtained after heat treatment is named as "composite" filter mats.

2. Materials

Polytetrafluoroethylene (PTFE 60 wt% dispersion in water, Sigma-Aldrich, Germany), PVA (polyvinyl alcohol, M_w35000, degree of polymerization 1700, and degree of alcoholysis 88% BDH, Germany), Zinc Acetate Dihydrate (Zn $(CH_3COO)_2$. $2H_2O$) Sigma-Aldrich Germany), Nickel Actatate Tetrahydrate by Merk, germany, Formaldehyde HPLC $\geq$ 99.9% (Merk, USA), Toluene AR $\geq$ 99.5% (Merk, USA) and Acetone (HPLC $\geq$ 99.9% purity, Sigma-Aldrich, Germany), Commercial PTFE filters(37mm diameter, pore size 3.0μm) Zefon International, USA, PTFE/PP support filters(37mm Diameter, pore size 3.0 μm)Pall Corporation California, USA and Deionized (DI) water. All reagents were used as received from the suppliers without further processing.

2.1 Nanofibrous Filter Mats preparation and Characterization:

2.1.1 Electrospinning Solutions preparation

Electrospinning solutions of PTFE-ZnO were prepared by mixing three solutions namely A,B and C. PTFE-PVA quantity in the solution was fixed and only zinc oxide nano particles loading was varied (experimental schematics shown in Figure 2.1). Solution A was prepared by adding 0.2 g PVA (10wt%) powder in 2 ml distilled water which was magnetically stirred(WiseStir,

Germany) for 3h at room temperature. Solution B consists of 4ml PTFE dispersion whereas Solution C was prepared by dispersing10, 15 and 20 wt% of zinc acetate dihydrate in 2ml distilled water. Subsequently, solution A,B and C were mixed together in a 100 mL beaker by magnetic stirring for 24h at room temperature. Electrical conductivities of resultant solutions were measured (Milwaukee-MW301, Hungary) which were1864 µs/cm (PTFE-PVA) whereas 1852, 1841 and 1848 µs/cm for PTFE-ZnO composite containing 10.0, 15.0 and 20.0 wt% of ZnO respectively. In case of PTFE-NiO solution preparation same protocol was followed as described in the above paragraph except the ratio concentration of nickel oxide added in the solution were 2, 4 and 6 wt%. It is important to mention here that combination of two polymer solutions is named ad "suspension" and mixing of 3 solution in one beaker make a "blend". The term green electrospinning is used in the present research for making water soluble polymer blends/suspensions which are eco-friendly and do not cause any secondary pollution during spinning process (detail mentioned in introduction portion 2.1)

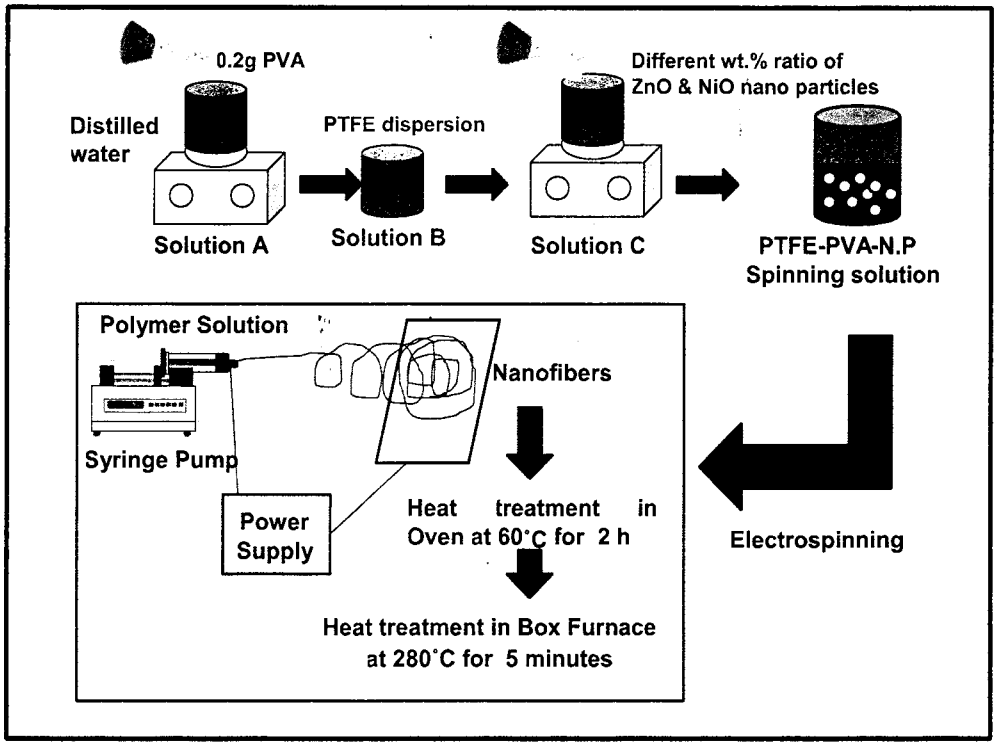

Figure 2.1 Schematics of Experimental, solution preparation and electrospinning process.

2.1.2 Synthesis of Electrospun Nanofibrous Filter Mats

Electrospinning is an electro hydro dynamical phenomenon, employed for producing fibers in the range of nanometer and micrometer from polymer solutions or melts. The easy accessibility of electrospinning process to fabricate economical fibers from different kinds of polymers is a huge improvement in nano- or micro-scale technology. The collected fibers diameters range from 2 nm to several micrometers. Electrospinning technique offers a unique capability to produce novel structures with controllable pore characteristics and mat morphology (Huang et al., 2006).

2.1.3. Electrospinning principle

During the electrospinning process, polymer spinning solution is loaded into a plastic syringe, which is then attached to an infusion pump. A high voltage power supply is then linked to the tip of the syringe using clips, as illustrated in Figure 2.2. Current will charge the solution inside the syringe and after a certain threshold voltage, repulsive force between the charged particles in the solution will overcome the surface tension. Taylor cone will formed and it will be stretched towards the collector plate due to the presence of opposite charge Huang et al., 2006).

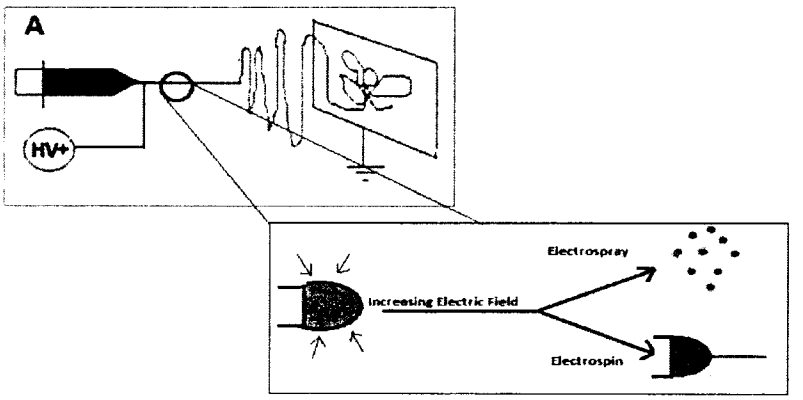

Figure 2.2 Illustration of Electrospinning principle.

If electro-spinning solution viscosity is high, taylor cone jet will not break into droplets and electro-spinning will continue. On the other hand if solution viscosity is low, then jet will break up into small droplets called electro-spraying. The collected fibers structure, morphology and other characteristics are based on the electro-spinning operating conditions. For instance nozzle and collector distance from each other is varied mostly between 5 and 30 cm. The solution infusion rate and the applied potential are normally from 0.1 to 100 µl/min and 5 to 25 kV, respectively (Hohman, Shin, Rutledge, & Brenner, 2001).

During the normal operation of electrospinning, jet stretched and find its way towards the collector. During this stretching process jet can undergo instability; electrically induced

bending instabilities and whipping instability. Diameter of electrospun fibers are smaller than those fibers produced via conventional techniques. Electrospinning process can be carried out at different environment like in controlled environment (vacuum chamber) and at room temperature. By manipulating electrospinning parameters fiber structure can be controlled. The parameters can be categorized as: 1) solution parameters, solution concentration, viscosity, surface tension, electrical conductivity, 2) process parameters, needle tip to collector distance, applied voltage and effusion rate 3) ambient parameters, such as temperature and humidity (Schiffman & Schauer, 2008).

2.1.4. Electrospinning apparatus setup

The electrospinning set up used in this study was horizontal spinning configuration as shown in Figure 2.3. In order to synthesize electrospun nanofibrous mats, PTFE-PVA-metal oxide solution was loaded into a disposable plastic syringe equipped with a 23-gauge stainless steel needle. The filled syringe was fixed on a syringe pump (Parker Position System, USA).A circular copper disc (diameter 20cm) wrapped in aluminum foil was used for the collection of fibers. The needle of the syringe was connected to the positive terminal of 50 kV high-voltage DC power supply (DEL Electronic Corporation, USA) whereas negative terminal was connected with the copper collector plate. Electrospinning process was performed at a solution effusion rate of 0.3 ml/hr, tip to collector distance (T.C.D) of 12cm and at 18kV applied voltage. The as prepared electrospun PTFE-ZnO and PTFE-NiO with different wt% of zinc oxide and nickel oxide loaded samples were heat treated in lab oven (Memmert VO 200, Germany) at 60°C for 2h to remove the moisture. These nanofibers were then heat treated in the box furnace (KSL-1200X-J, USA) at 280°C at a heating rate of 5°C/min for 5min to remove carrier polymer PVA from the PTFE matrix. Schematic of electrospinning growth process is shown in Figure 2.3.

Figure 2.3 Illustration of Electrospinning Setup comprising of Effusion Pump, power supply and grounded collector.

2.2. Nano Fibrous Filter Mats Characterization

2.2.1. Scanning Electron Microscopy (SEM)

SEM considered as the most popular microscopic techniques to study the morphological characteristics of the samples, because of the simplicity in sample preparation and general simplicity of image interpretation. In SEM microscopy sample surface is scanned by the high energy electrons beam. Sample image can be scanned at scales from 0.1mm up to a few nm. In general principle, Surface features of the sample are obtained through the interaction of the atoms of the sample with the incoming electrons. For obtaining surface morphology sample must be conductive, it is coated mostly with the thin layer of heavy metal (e.g gold) in a sputter coater. Coating is necessary in order to reduce the surface charging and make SEM scanning of the sample possible.

After coating the sample is placed in a vacuum chamber of the equipment. For scanning a high energy electron bean is produced which travel down through a column of magnetic lenses. And at last focus on a fixed point of analysis on the surface of sample by producing secondary electrons. These secondary electrons are further collected by a detector and then

translated into signals. These signals are then amplified, analyzed, and translated into images for the surface topography of the sample (Michler, 2008).

In the current research work, SEM samples were prepared by direct electro spinning of the polymers nanofibers on wire gauge then followed by Au sputtering (SPI- Module sputter coater, Division of structure probe, Inc) for better conductivity and to avoid surface charging during imaging. The morphology of the electrospun fibers were investigated by (FESEM, JEOL JSM 6400 JEOL, Japan). Scanning electron micrographs were obtained at an applied voltage of 20 kV. The Mean fibers size distribution were determined by measuring over 50 fibers selected randomly from the SEM images using image analysis software IMAGE J software Ver. 1.38 x and results were plotted in software ORIGIN.

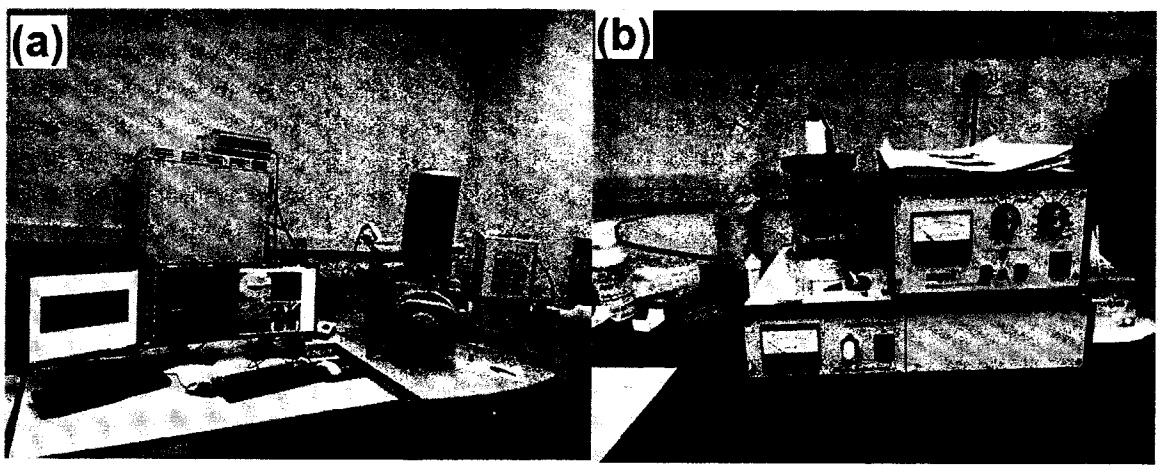

Figure 2. 4 (a)Field Emission Scanning Electron Microscope (b) Gold Sputtering Unit (NANOSCALE RESEARCH DIVISION) University of Florida

2.2.2. Atomic Force Microscopy (AFM)

Atomic force microscopy is doubtfully the most versatile and powerful microscopic technic for studying samples at nano scale. The versatility of AFM include providing three dimensional topographic images of samples. AFM is a powerful tool which with minimum

sample preparation can generate images at atomic resolution with angstrom scale resolution height information.

Samples in AFM are scanned by a very sharp tip cantilever that moves over the surface of the sample. When the tip of the cantilever reaches close to the surface of the sample due to force of attraction cantilever moves under the force of attraction towards the sample surface. When the tip is brought closer to the surface than force of repulsion is dominant and cantilever started deflecting away from the surface of the sample. Laser beam inside AFM detect the deflections of cantilever which is then monitored by the PSPD. By using a feedback loop to control the height of the tip above the surface thus maintaining constant laser position the AFM can generate an accurate topographic map of the surface features as shown in Figure 2.5 (https://ccem.mcmaster.ca/atomic-force-microscope/). In the present study Surface roughness of the samples was measured by an Atomic Force Microscope (AFM,QScope™ 350). All the samples were scanned over an area of 10μm × 10μm in a tapping mode. WS × M 2.0 SPM software was used for image analyses. RMS root mean square surface roughness of the sample was measured through software in the AFM.

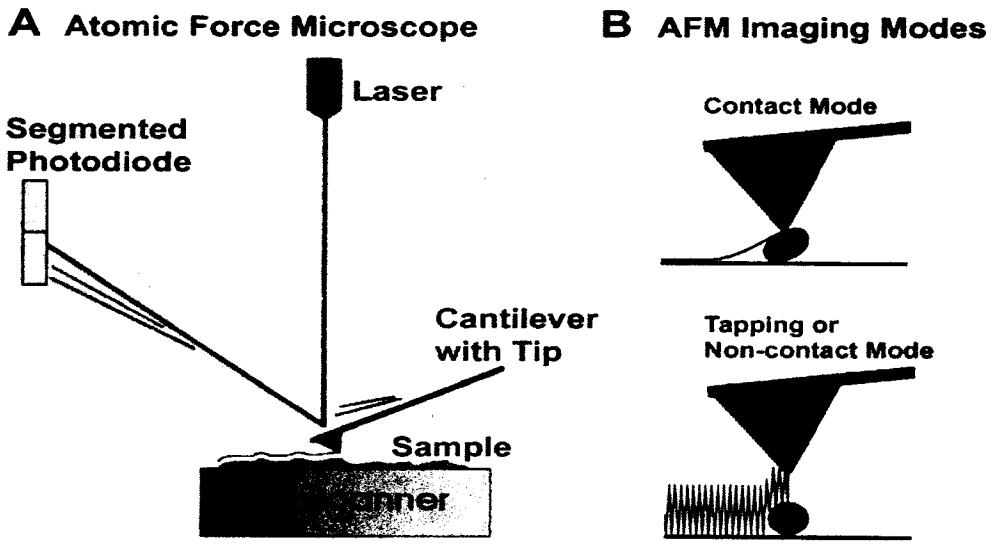

Figure 2. 5 Schematics of Atomic Force Microscopy

2.2.3. Thermal Investigations

To study the thermal features of electrospun nanofibers, nanofibers blends and nano composites TGA is the most effective technique. The glass transition temperature, melting temperature, enthalpy of fusion, degree of crystallinity and thermal degradation are a sign

of structural change which might be occurred after electrospinning/blending and heat treatment. Therefore, thermo gravimetric analysis (TGA) was investigated to study the thermal behavior of the electrospun fibers after electrospinning. TGA gives both information of thermal behavior and about compatibility of polymer blend. Additional information obtained from TGA is influence of blending on crystal behavior of sample and mechanical property of the fibers. The first order derivative of TGA refers to the temperatures at which the maximum weight loss occurs (Loganathan, Valapa, Mishra, Pugazhenthi, & Thomas, 2017). Thermo-gravimetric analysis was performed using (TGA Q5000 V3.17 Build 265) under a nitrogen flow. About 5 mg of sample was heat-treated from 25- 800°C at of 5 °C/min heating rate. All the graphs were plotted for temperature against the mass loss (Y-axis). Schematics of TGA graphs is shown in Figure 2.6.

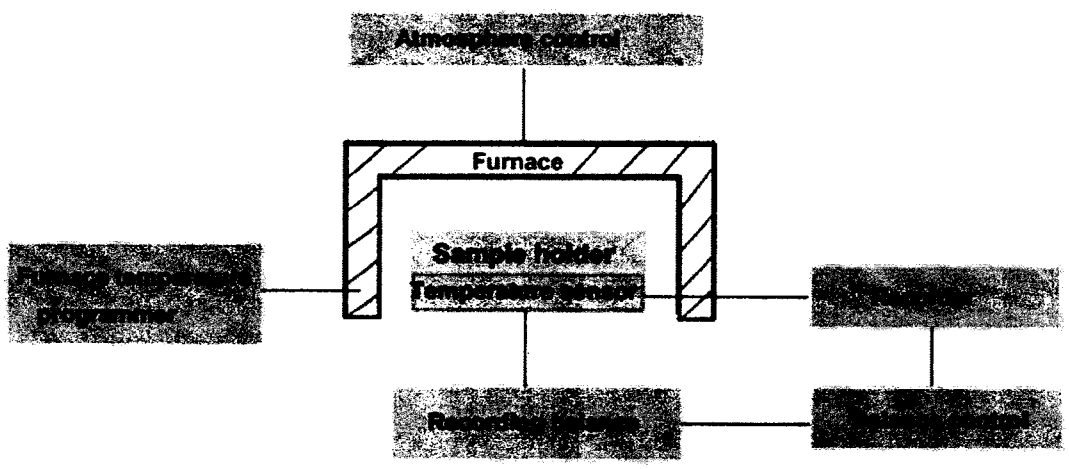

Figure 2. 6 Schematics of experimental set up of TGA

2.2.4. Fourier Transform Infrared spectroscopy (FTIR)

To study the functional groups and structure clarification of both organic and inorganic compounds Fourier transform infra-red spectroscopy is extensively used tool for this purpose. Infra-red radiations originate vibrations in the bonds which connects atoms or groups of atoms which constitute the sample. During IR analysis process, high wavelength IR is passed through the sample and its transmittance or absorbance is measured using an IR spectrometer. Graph obtained showing variation in transmittance and absorbance percentage is called IR spectrum. The dip in the spectrum is known as peak and represents IR transmittance or absorbance at that frequency. In the spectrum hundred percent transmittance means zero percent absorption and vice versa (Kansiz, Domínguez-Vidal, McNaughton, & Lendl, 2007). FTIR spectrum obtained for the present research study is shown below in Figure 2.7. IR spectra of both pure and composite electrospun nanofibrous mats were obtained using an FTIR Spectrometer Nicolet 8700 equipped with a fixed 100 μm diameter aperture and a mercury-cadmium-telluride (MCT) detector was used to analyze the absorbance in the wave number range 500- 4000 cm^{-1} in a transmittance mode.

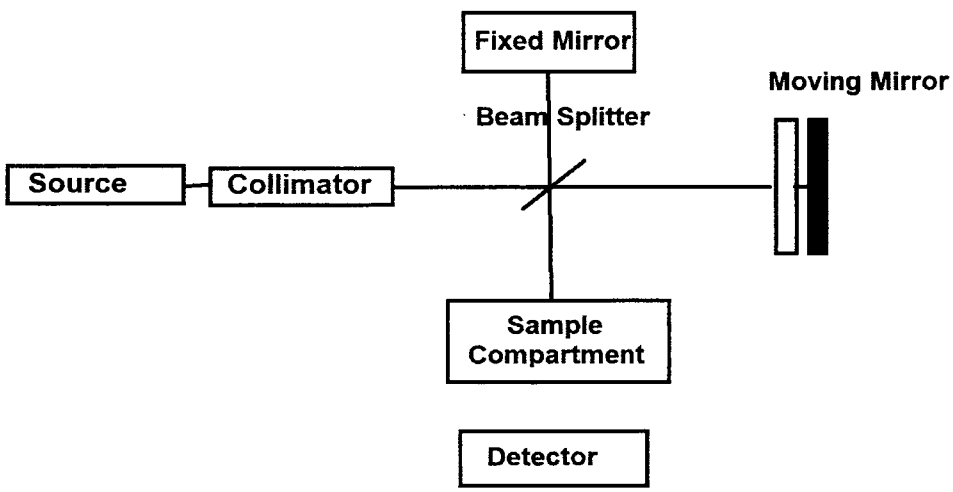

Figure 2. 7. Schematics of Fourier Transform Infra red Spectrometer (FTIR).

2.2.5. Raman Spectroscopy

In Raman spectroscopy molecular vibration in the components of the sample is through the transfer of light energy by scattering. Raman spectrometer detect the scattered light energy and give resultant finger prints of the sample. Spectral information obtained through this process is essential for characterizing material property of the sample. When a light beam hits matter, it interact with it in a specific way, dependent on the interplay between the light waves and the atoms and molecules that make up the matter. The interaction may leave the energy of matter and light unchanged (refraction, reflection, elastic scattering) or lead to an energy exchange between both as shown in Figure 2.8. All vibrational spectroscopies characterize molecular vibrations and to a smaller extent also molecular rotations. The forces keeping the molecule together will act like springs connecting the atoms as illustrated in Figure 2.8 (a) (Hollas, 2004). Current research study Raman spectroscopic analysis was done by Dongwoo Optron's micro-Raman spectrometer with 532 nm as an excitation laser source. Spectral analysis range was from 100 to 2000 cm^{-1} and exposure time was 7 s.

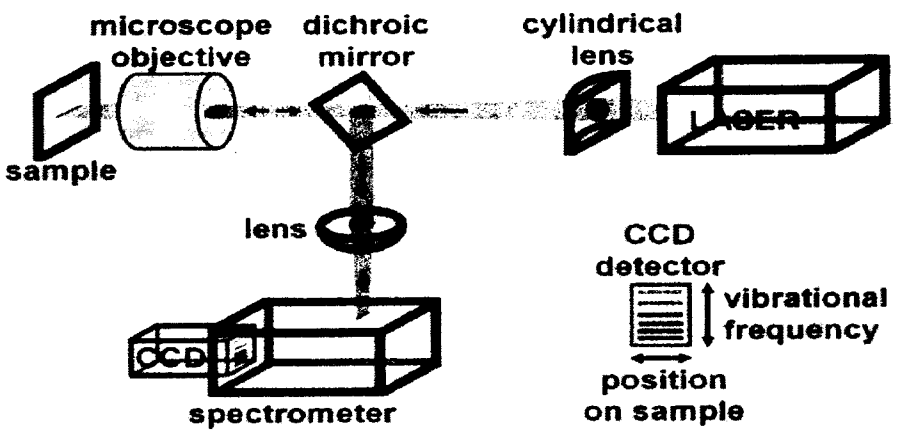

Figure 2. 8 Schematic of Basic principle of Raman spectroscopy

2.2.6. UV-Visible Spectroscopy

UV-Visible spectroscopy is an analytical laboratory method that give both qualitative and quantitative analysis of a substance. Those atoms which absorb the light in the UV and visible regions of the electromagnetic spectrum UV-Vis spectroscopy probe their electronic transition of molecules. The absorption of UV and Visible light by different species can be define as, the species which have extended system of alternation double and single bonds they will absorb UV light, and species having color they will absorb visible light as shown in Figure 2.9. In this way, it makes UV-Vis spectroscopy applications over wide range of samples in multidiscipline fields (Perkampus, 2013).

The quantification of gas adsorption capacity is relatively complex compared to the measurement of PM filtration efficiency (De Coste, J.B. and G.W. Peterson, 2014). The VOC adsorption capacity evaluation is done under two ways. The first technique is to determine the residual concentration of VOC in the air by gas chromatography. The second method is to extract filter media adsorbed VOC in a suitable solvent and analyse through techniques like high performance liquid chromatography (HPLC) (Noreña-Caro, D. and M. Álvarez-Láinez, 2016), UV-VIS spectrophotometry (Uyar, T., et al., 2009) and BET adsorption isotherm (Scholten, E., et al., 2011).

UV spectroscopy in comparison with other techniques is rather simple which can be used to evaluate VOC adsorption capacity. The characteristic absorbance of a specific VOC in a suitable solvent can be determined and calibrated. The adsorbed VOC by filter media can be extracted in the same solvent. UV spectrum of the samples can be compared with the calibration, and VOC adsorption per mass unit of the filter can be calculated. On the other hand, UV spectroscopy can also be used to determine the change in absorbance when the sample is immersed in the solution containing gaseous pollutant (Uyar, T., et al., 2009).

In the present study the concentrations of extracted VOCs in the solution were determined using UV-Vis spectroscopy using a UV-Vis (Hitachi U-4001) spectrophotometer at a characteristic absorbance of 275, 287 and 300 nm as shown in Figure 2.10 (b-c). VOCs adsorption experiment detail is in figure. 2.10 (a). A standard calibration curve with a correlation coefficient of R_2=0.9999 was obtained for formaldehyde, R_2= 0.9977 for toluene and R_2= 0.9998 for acetone by using different calibration standard concentrations 0, 20, 40, 60, 80and 100 mg L^{-1}. A linear relationship is found between absorbance and VOCs concentration with a good correlation coefficient. The regression equation was used to convert absorbance values of VOCs expressed as VOCs adsorption per unit mass (μg/mg) of fabric sample.

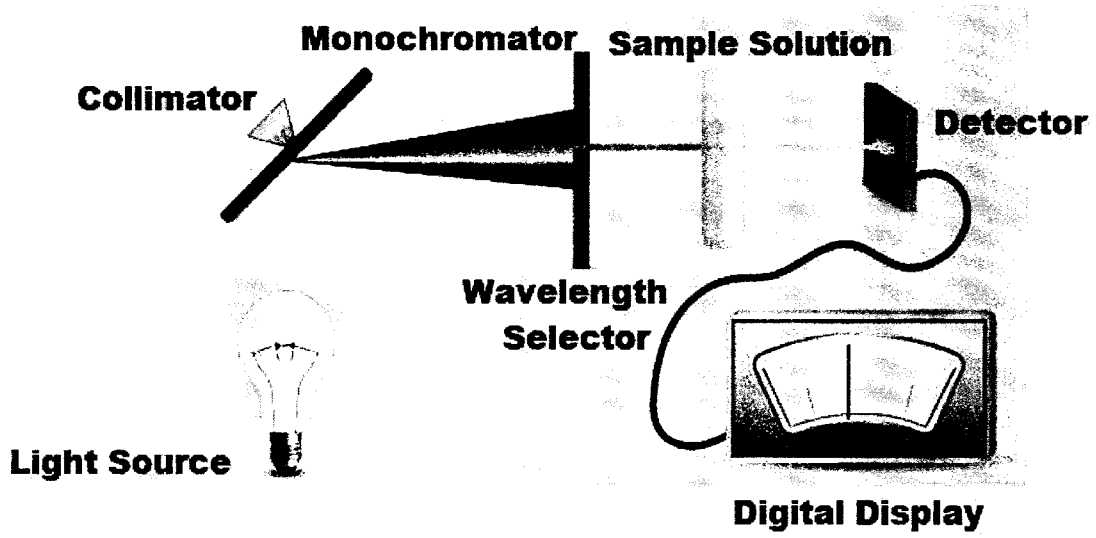

Figure 2. 9 Basic instrumentation of UV-Vis spectroscopy

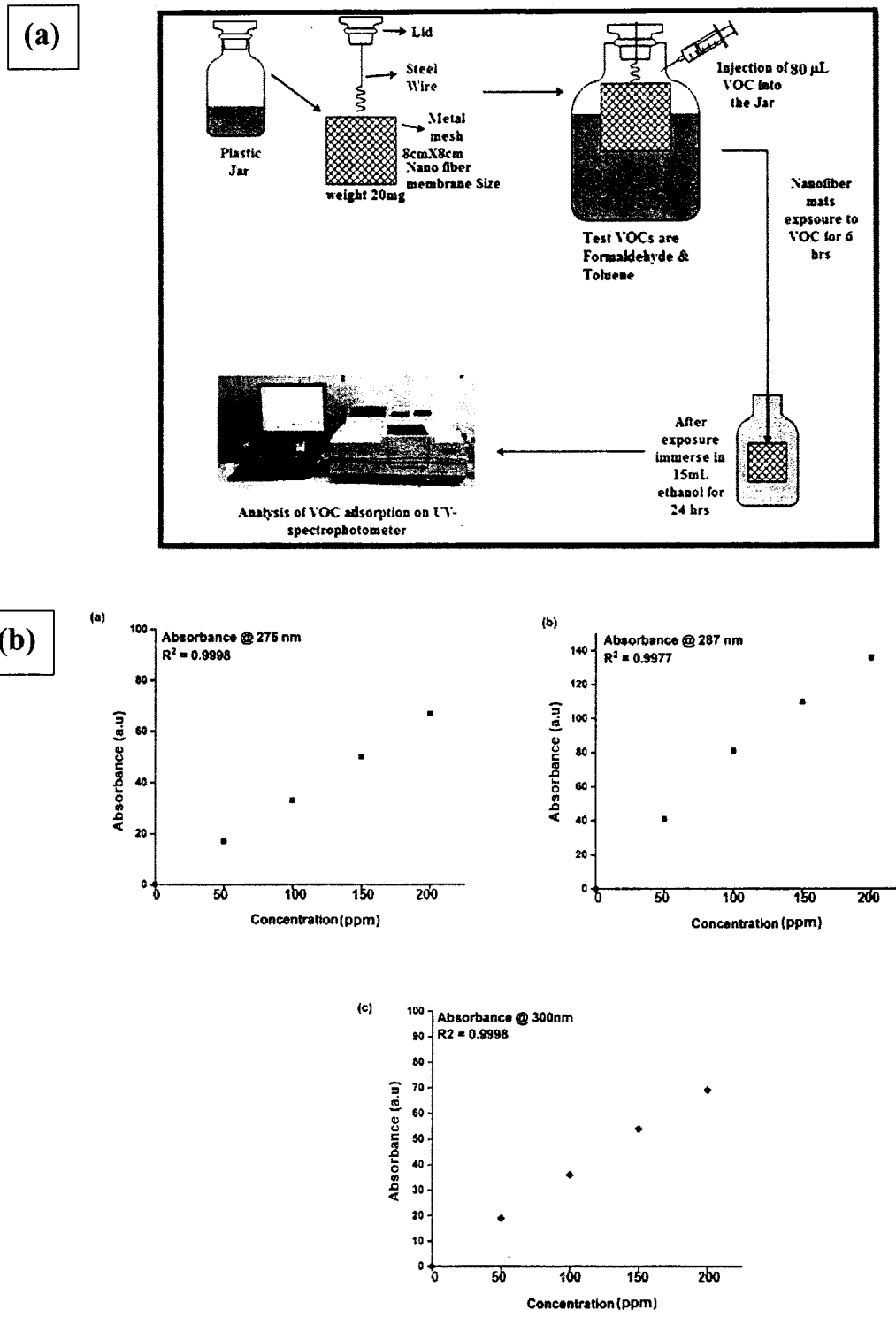

Figure 2.10. (a) Schematics of UV adsorption experiments of VOCs, (b) Standard calibration curves of VOCs at different solvent concentrations. Correlation was found at an absorbance of 300, 287 and 275 nm respectively for formaldehyde, toluene and acetone using UV-Vis spectroscopy.

2.2.7 Air Filtration Experiment

The performance test ($PM_{2.5}$ and PM_{10} removal efficiency and pressure drop) of the PTFE-metal oxides nanofibrous mats was performed by using an air filtration measurement system. The PTFE- metal oxide based air filter was fabricated directly on circular metal wire gauge 37mm diameter. The PM particles generation source was from mosquito coil smoke, according to literature, incense smoke has wide PM size distribution from< 0.3 μm to>10.0 μm (Jeong et al., 2017; C. Liu et al., 2015). Small DC fan was used to draw polluted air in to the air filtration system with a flow rate of 2.25m/s (DFH4007C, Dongguan Xingdong Electronics Co., Ltd.). The PM concentration was monitored by Air quality analyzer (HT-9600, China) and the PM filtration efficiency was calculated by comparing the PM concentration before and after filtration by nano-filters. The pressure difference of the air filter was calculated by a differential pressure manometer (HT-1890, max. pressure range 10 psi, resolution 0.01). All experiments were performed in a controlled laboratory environment at room temperature with 40% relative humidity. The air resistance/ permeability coefficient was calculated using the following formula;

$$\beta = \Delta P/U \qquad (4)$$

where β (Pa-s/m) is regarded as the air resistance coefficient, ΔP (Pa) is the pressure drop, and U (m/s) is the face velocity(Xia, Bian, Zhang, & Chen, 2018).

Pore structure is a collective term used to define **about porosity, pore size and its distribution and pore morphology**.

The porosity (ε) of electrospun nanofibrous filter mats was calculated using the following Equation (5) (Reshmi, Sundaran, Juraij, & Athiyanathil, 2017)

$$\left(\frac{\rho 0-\rho}{\rho 0}\right)X100 \qquad (5)$$

ρ is the density of polymer raw material PTFE is 2.2 g/cm^3, ρo is the density of nanofibrous membrane. The density of electrospun nanofibrous membrane was calculated by determining the mass (mg), thickness(mm) and area(cm^2) of electrospun mat. The thickness is calculated using a micrometer. Mean pore radius (r) of electrospun nanofibrous membrane was calculated using the following equation (Reshmi et al., 2017).

$$R = \sqrt{\pi}/4\left(\frac{\pi}{2\log\left(\frac{1}{\epsilon}\right)}-1\right)d \qquad (6)$$

The removal efficiency of air filters for PM is calculated by the following formula:

$$E\% = (PM_{in} - PM_{out}) / C_{in} * 100\% \qquad (7)$$

Where PM_{in} and PM_{out} represent the cumulative mass concentration of aerosol at the incoming chamber and outgoing chamber. The air filtration set up is shown in Figure 2.11. The overall performance of the air filters is assessed by quality factor (QF).

$$QF = \ln(1-\eta)/\Delta P \qquad (8)$$

where η represents the removal efficiency of PM and ΔP represents the pressure drop (Canalli Bortolassi et al., 2019).

Surface free energy can be calculated based on contact angle measurement using liquids with different surface tensions. Notably, the surface free energy depends on the polymer chains organization that is related to the manufacturing methods to produce films and fibers (Lugscheider & Bobzin, 2001). In this study, the obtained contact angle data on polymer nanofibers surface with water was used to calculate surface free energy based on the Owens–Wendt model (Senturk Parreidt, Schmid, & Hauser, 2017) with polar and dispersive contributions.

$$(1+\cos\theta)\Upsilon_L = 2(\sqrt{\Upsilon_l^d \Upsilon_s^d} + \sqrt{\Upsilon_l^p \Upsilon_s^p}) \qquad (9)$$

The two unknowns, Υ_s^d and Υ_s^P, were calculated by determining the contact angle of the material using liquid (deionized water in the current work). The surface tension values Υ_L, Υ_l^d and Υ_l^P (in mJ/m^2) for water are 72.8, 21.8 and 51.0 (X. Wang, Li, Lin, Hodgson, & Wen, 2008) . Original values were obtained from a free ware software image J plug in LBADSA drop analysis. The Low-Bond Axisymmetric Drop Shape Analysis (LBADSA) method uses an image energy approach to fit a first-order approximation of the Young-Laplace equation to the whole image data instead of first detecting the drop contour (Stalder et al., 2010). All the values calculated in triplicate through different equations in the present study and standard error was calculated through standard deviation.

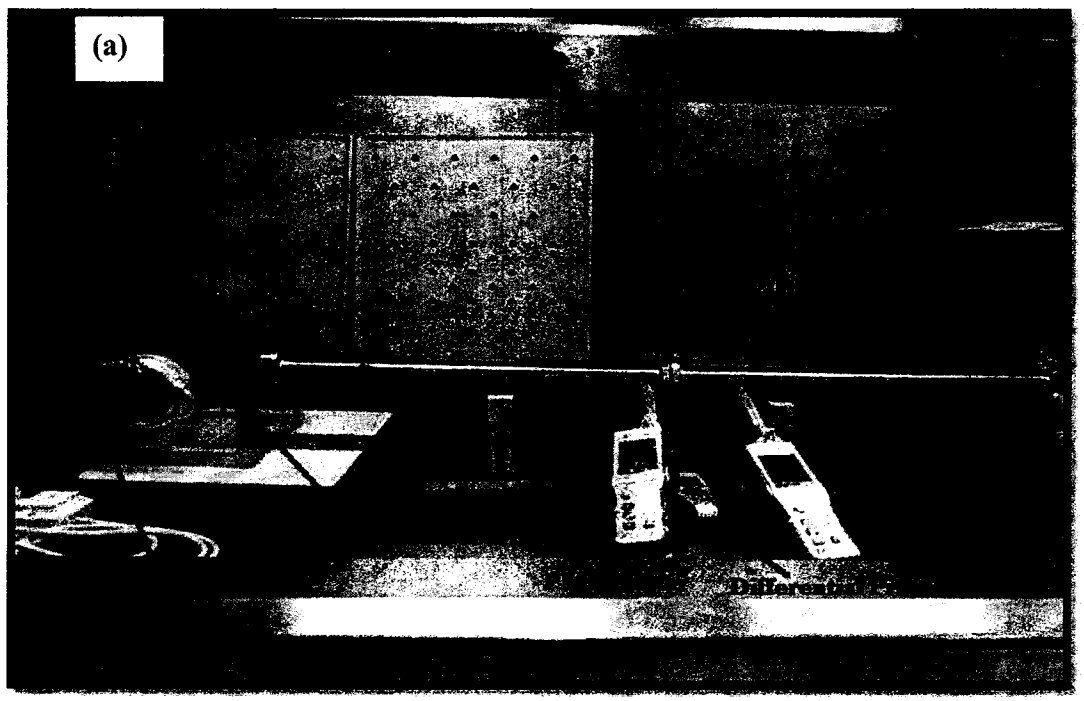

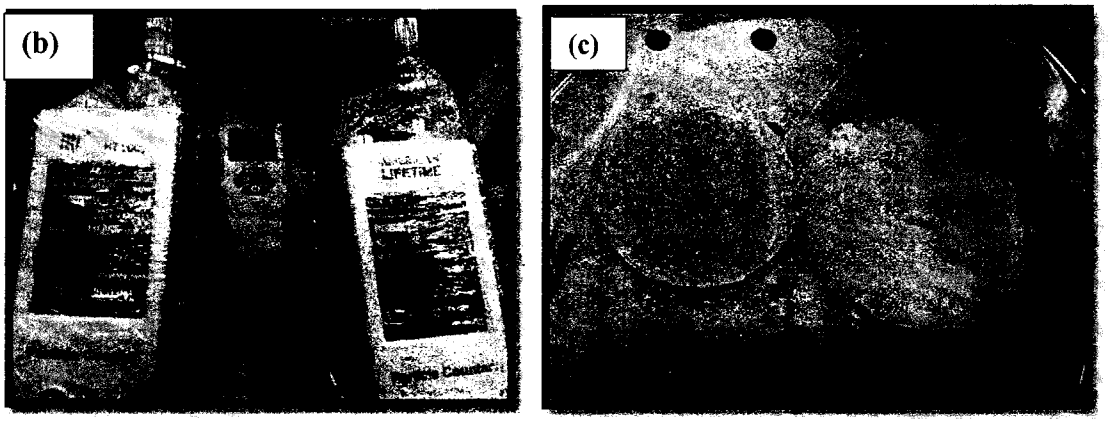

Figure.2.11 (a) Schematics of experimental set up for measuring particulate matters removal and pressure drop from polluted air by nanofibrous mats, (b) Mass concentration of PM in inlet and outlet of air filtration system and (c) Synthesized nanofibrous mats before and after Aerosols Filtration.

2.2.9 Antibacterial Activity of Nanofibrous Filter Mats

To assess antimicrobial capability of air filters in a lab quantitative antibacterial test analysis was done by using two bacterial strains of Bacillus sp and E. coli. Single colony of bacterial strains was grown in a nutrient broth medium for bacterial suspension preparation. Agar plate was prepared by dipping the cotton swab in the suspension culture and carefully and homogenously spread that on plates. The antibacterial activities of control solution and PTFE-Zno (10%, 15%, and 20%) and PTFE-NiO composite nanofibrous mats (2%, 4%, and 6%) were then determined. Each sample was placed onto an inoculated agar plate. The solution of PTFE-PVA was used as a control. The samples and inoculated agar plates were incubated for 24 h at 37°C. The zone of inhibition (ZoI) was determined as the total diameter (mm) of PTFE-ZnO and PTFE-NiO filter paper. All measurements were performed in PTFE-ZnO and PTFE-NiO with various concentrations and then compared with control solutions.

PART I

Physio-chemical Characterization of Electrospun Composite PTFE-ZnO Nanofibrous Filter Mats

Electrospun filter mats of PTFE-PVA-ZnO were synthesized by fixing the ratio of PTFE dispersion and PVA, however, the amount of ZnO loading varied from 10-20wt% in the precursor solutions. The PTFE-PVA was labeled as control solution, PTFE-PVA-ZnO as spun and PTFE-ZnO as heat treated. Process and solution parameters used in this study for the synthesis of nanofibrous filter mats are given in table 1 (Detail mentioned in section 2, sub section 2.1.1-2.1.3). This chapter deals with the detailed Physio-chemical characterization of PTFE-PVA (matrix) and PTFE-ZnO composite filter mats as following:

3.1. FESEM Analysis

FESEM was used to analyze the surface morphology of as-spun and heat treated PTFE-ZnO nanofibrous filter mats whose representative micrographs are illustrated in Figure 3; alongside are also shown the mean diameters of nanofibrous filter mats. The process parameters were kept constant for the growth of these samples, however, the concentration of zinc oxide loadings in solution varied from 10-20wt%. It can be seen in these micrographs that continuous and uniform fibers with varying degree of beaded structure were formed in the grown compositions (Figure 2 (a1-d1)). However, the extent of beading increased with increasing wt% of ZnO loadings in solution which was attributed to non-homogeneity of ZnO in the electrospinning solutions. The mean diameter of PTFE-ZnO nanofibers and their size distribution is shown in Figure 3(a3-d3). The estimated fibers mean diameter ranged from 0.24 μm±15.10 to 0.17μm±30.50 in these samples. It is pertinent to mention here that fiber diameter was influenced by both the solution viscosity and conductivity of the spinning solution; and

both of these factors had competing effect on fibers diameters (Ahmed et al., 2018; Nataraj et al., 2008). Higher viscosity results into formation of thicker fibers whereas; higher conductivity leads to evolution of fibers having finer diameters. The addition of Zn acetate into the spinning solution increased both viscosity and conductivity. However, up to 10wt% Zn acetate loading, effect of viscosity was dominating that thus resulted into rise in fiber diameter. Nevertheless, when Zn acetate content in the spinning solution was increased beyond 10wt%, effect of conductivity starts dominating which lead to formation of fibers of finer diameters for the compositions containing 15 and 20wt% Zn acetate. As shown in table 1, solution conductivity increased from 1861 to 1884 μS/cm upon addition of zinc acetate in the spinning solution. The increase in conductivity resulted in considerable stretching of the polymer jet that resulted in to formation of finer fibers for the solutions containing 15 and 20wt% Zn acetate loadings as shown in Figure 3 (a3-d3) (Huang et al., 2017).

As stated by (Huang et al., 2017) the non-Newtonian index (n) was observed to decrease with an increase in zinc acetate beyond 20wt% Zn acetate loading in the spinning solution. The authors mentioned that the value of 'n' reached a maximum zinc acetate up to 20 wt% Zn acetate loading suggesting good Newtonian flowing properties that indicated solutions were stable during electrospinning process up to 20wt% Zn acetate loadings only. For the aforementioned reason, Zn acetate loadings beyond 20wt% were not taken into consideration. Figure 3 (a2-d2) shows micrographs of nanofibrous filter mats which have been heat treated at 280°C for 5min in the box furnace. The purpose of this heat treatment was threefold; firstly, to remove supporting PVA from the nanofibrous filter mats matrix, secondly, to allow fusion of PTFE and ZnO particles embedded on the surface of PTFE and thirdly coarsening of fiber surface which was credited to the densification of PTFE fibers as observed in the Figure 3(a2-d2) (Huang et al., 2017). EDX data succinctly revealed the presence of zinc oxide (observed as

Zn and oxygen), carbon and fluorine on the surface of nanofibrous filter mats as shown in Figure 3(e1).

Table 1. Solution and Process parameters used during electrospinning.

a) Solution parameters		**b) Process parameters**	
Solution compositions	**Solution conductivity (μS/cm)**	Applied voltage	18kV
PTFE-PVA	1852±1	Tip to collector Distance	12 cm
PTFE-ZnO 10wt.%	1861±2	Flow rate	0.3mL/h
PTFE-ZnO 15wt.%	1872±1	Temperature	25°C
PTFE-ZnO 20wt.%	1884±1	Humidity	40%

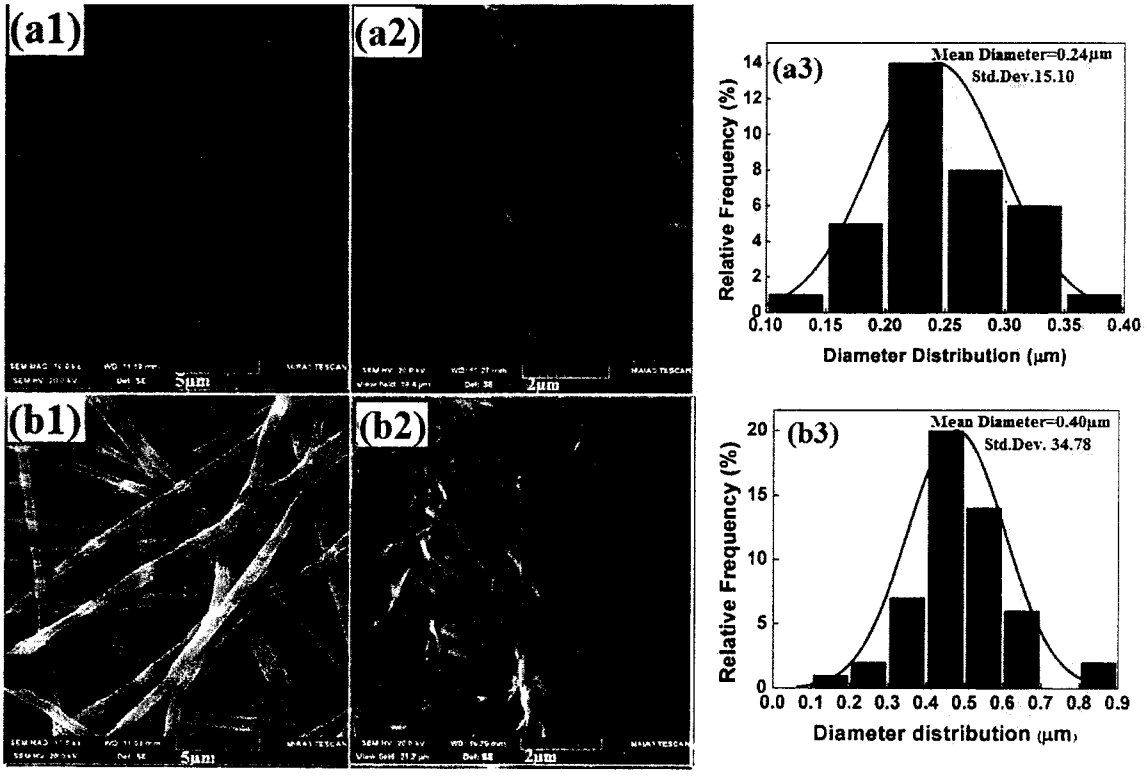

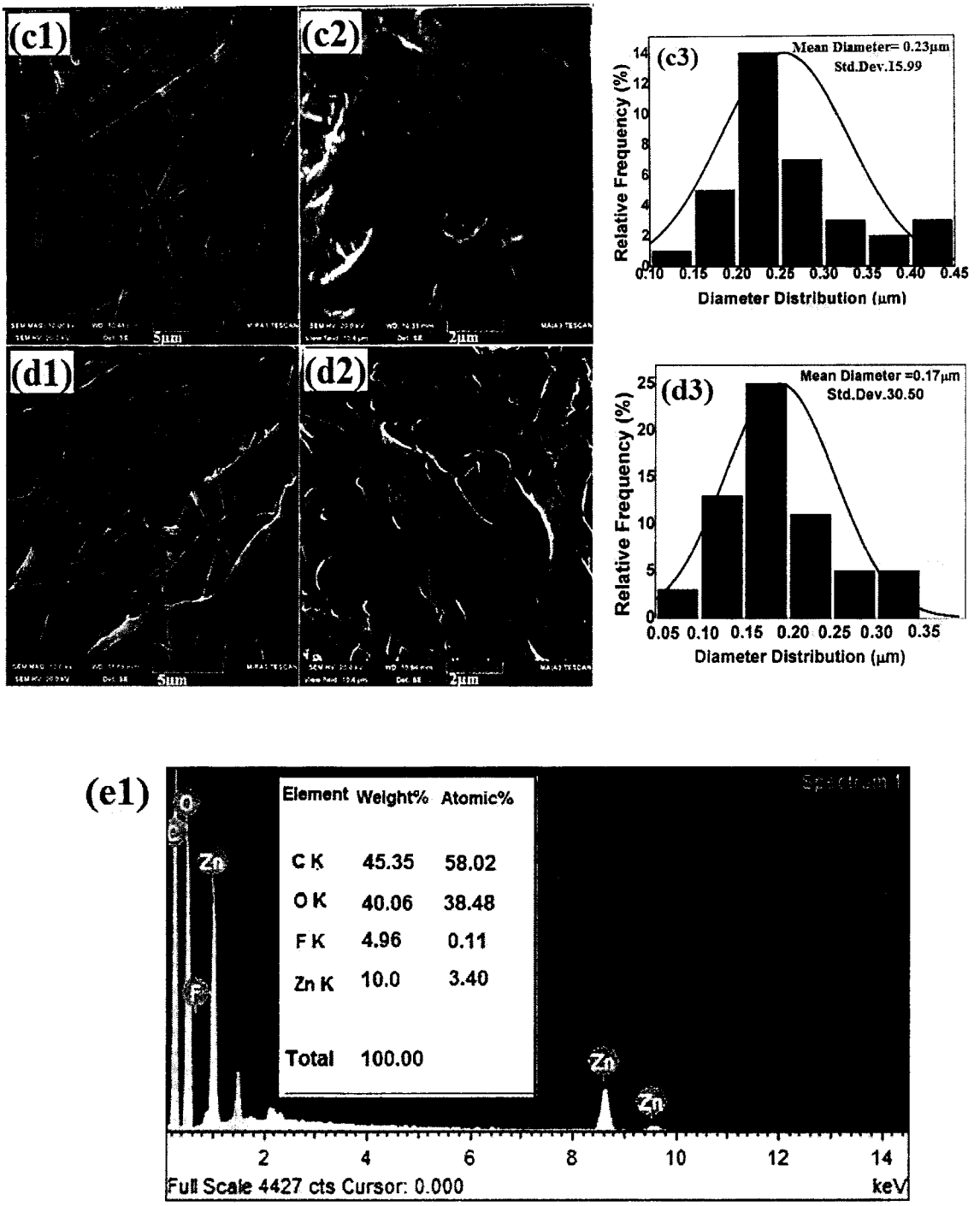

Figure 3.1 FESEM micrographs of nanofibrous filter mats: As spun pristine PTFE-PVA (a1), PTFE-ZnO 10wt% (b1), PTFE-ZnO 15wt%(c1), PTFE-ZnO 20wt% (d1) and their subsequent nanofibrous filter mats heat treated at 280°C for 5 min (a2-d2), Mean size distribution of nanofibers (a3-d3) and EDX spectrum of PTFE-PVA-10wt% ZnO nanofibrous filter mat (e1).

3.2. Atomic Force Microscopy (AFM) Analysis

Atomic force microscopy is a sensitive technique used to measure roughness of surfaces. In this work, AFM was employed to investigate surface roughness of heat treated PTFE and PTFE-ZnO nanofibrous filter mats containing 10, 15 and 20 wt% ZnO loadings. Figure 3.2 portrays Root Mean Square (RMS) roughness of pure PTFE and PTFE-ZnO nanofibrous filter mats. RMS roughness of filter mats without ZnO loadings (pure PTFE filter mats) was found to be 112 nm, whereas RMS roughness was found to be 193, 573 and 623 nm for specimens with ZnO loadings of 10, 15 and 20 wt % respectively. These results clearly revealed that pure PTFE filter mats show significantly lower RMS roughness and RMS surface roughness increases greatly with increasing the wt% of zinc oxide loadings in fibrous filter mats. Thus the presence of ZnO particles on the surface of fibers increases surface roughness, which in turn, further enhances the hydrophobicity of filter mats containing ZnO particles (Liang et al., 2018). It is worth mentioning here that loading of zinc oxide particles not only increase the surface roughness of fibrous filter mat but also provide more active sites for removal of pollutants (VOCs) from air.

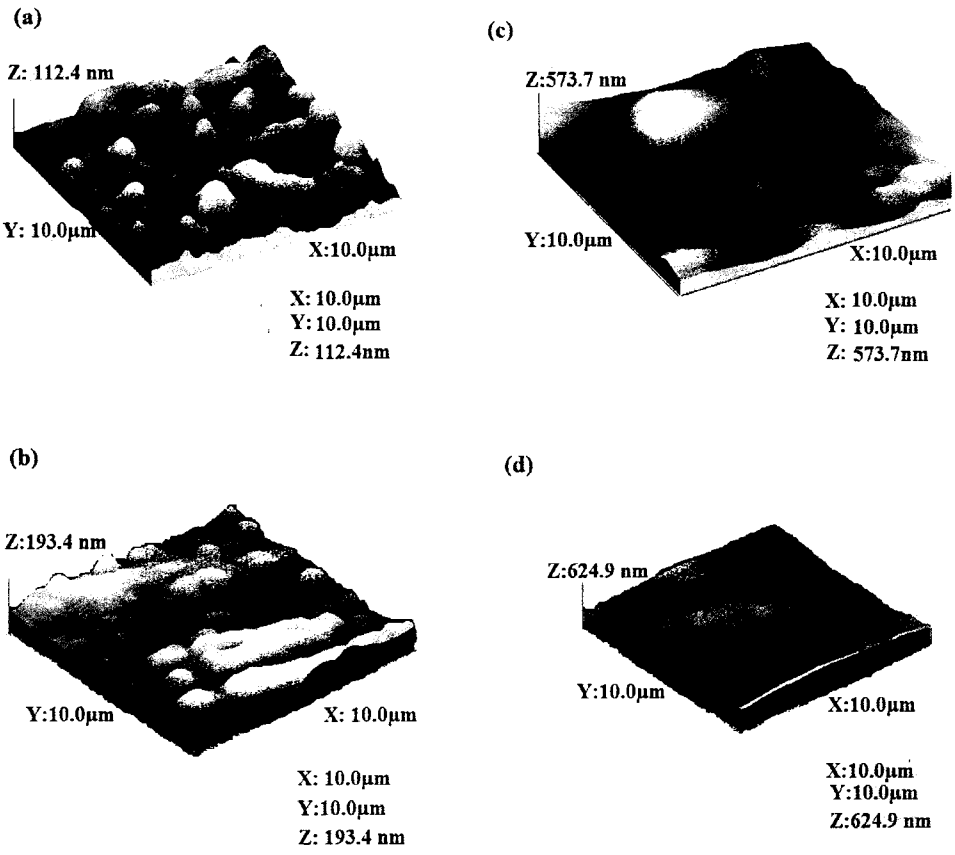

Figure.3. 2 AFM images showing Root Mean Square (RMS) roughness profile of nanofibrous filter mats heat treated at 280°C (a) Pristine PTFE mats (b) PTFE-ZnO with 10wt% (c) 15wt% and (d) 20wt% ZnO loading.

3.3. Thermo Gravimetric Analysis (TGA)

TGA is a well-established analytical technique that is used to investigate thermal stability of materials. The thermal properties of PTFE-ZnO composite nanofibrous filter mats (containing 10wt% ZnO loading) were evaluated by Thermogravimetric analyzer and Differential Temperature Analyzer as shown in Figure 3.3. The weight loss of PTFE-ZnO filter mat as a function of temperature was validated by the TG curve. As shown in Figure 3.3(a), there are two weight losses observed in the TG curve that have been represented by the red dotted vertical

marker lines. The first weight loss perceived between 290-350°C was attributed to complete decomposition of polyvinyl alcohol (Zhu et al., 2020) whereas the second weight loss between 400-500°C was assigned to the decomposition of PTFE.

These results have manifested that PTFE molecules remained preserved around 450°C due to their thermal stability, which is in agreement with the already reported literature (Hondred, Yoon, Bowler, & Kessler, 2013; Odochian, Moldoveanu, & Maftei, 2014). DTA curve of PTFE-ZnO nanofibrous filter mat is shown in Figure 4(b), which shows broad exothermic peak appeared at 290°C as a result of dehydration and decomposition of PVA from these composite nanofibrous filter mats while at 450°C PTFE started to decompose. It can be distinguished that PTFE nanofibrous filter mats have demonstrated exceptional thermal stability up to 450°C. Similar results on thermal stability of PTFE nanofibers have been described in the literature (W. Kang et al., 2016b; X. Li et al., 2019b; H. Xu et al., 2019). Based on these results heating temperature was fixed at 280°C for all the PTFE composite compositions.

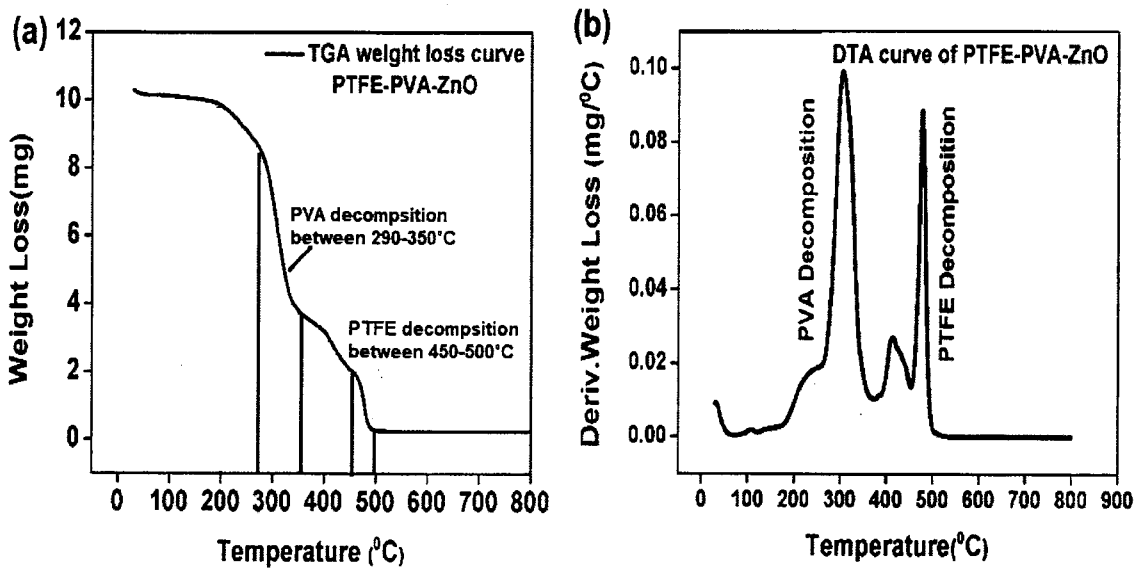

Figure 3. 3 (a) TGA and (b) DTA profile of as spun PTFE-PVA-ZnO nanofibrous filter mat containing 10wt% ZnO loading.

3.4. Fourier Transform Infrared Spectroscopy (FTIR) Analysis

Compositional characterization on both as-spun and heat treated PTFE-ZnO nanofibrous filter mats was performed by FTIR spectroscopy on these samples under transmittance mode, as shown in Figure 3.4. This was accomplished by identifying characteristic functional groups present in both as-spun and heat treated samples. Peaks observed at 1121 and 1235cm^{-1}were identified as characteristic peaks of symmetric and asymmetric-CF_2 stretching modes, whereas peak at 604cm^{-1} assigned to the deformation mode of -CF_2 bonds in both as spun and heat treated samples. The aforementioned three peaks were characteristics of PTFE present in these electrospun mats (X. Li et al., 2019b). In addition, the strong absorption bands noted at 2934 $cm^{-1}$and 3361cm^{-1} were associated to the stretching of -CH_2 bonds and -OH stretching in PVA (Y. Huang et al., 2017). It was evident from the FTIR spectra that absorption band (2934 and 3361cm^{-1}) associated with PVA disappeared after the heat treatment at 280°C while only strong absorption peaks perceived at 1121, 1235 and 604cm^{-1} were associated to the stretching of -CF_2 bonds preserved in both as-spun and heat treated samples.

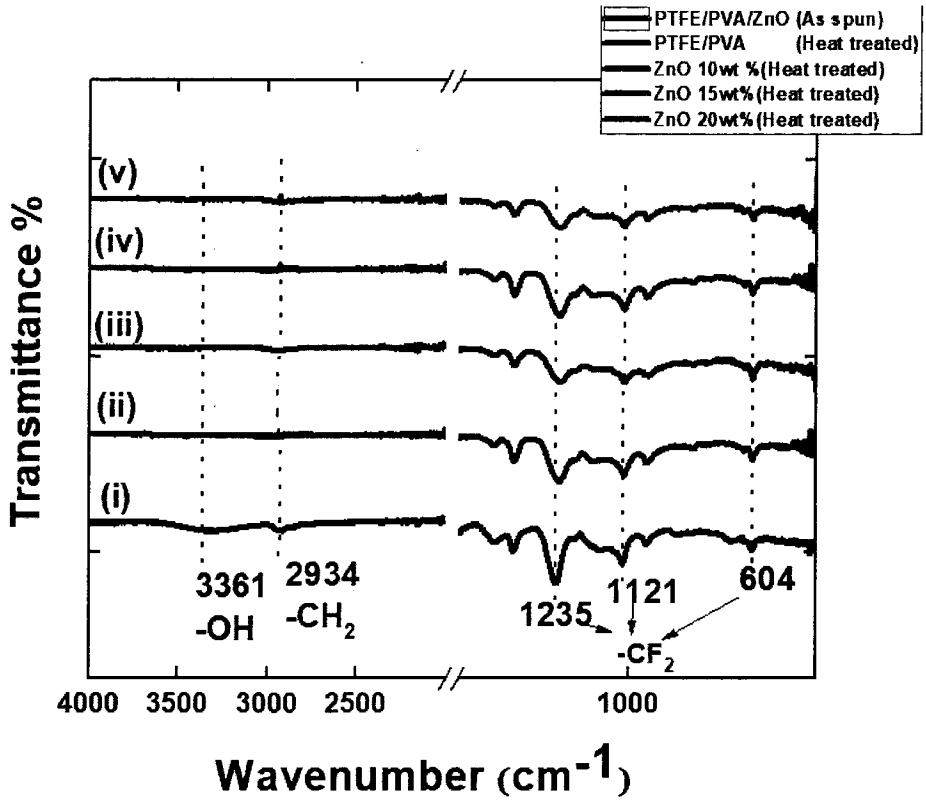

Figure 3. 4. FTIR spectra of PTFE-PVA-ZnO as spun nanofibrous filter mats (i) and PTFE-ZnO heat treated at 280°C for 5 min with different wt% of ZnO loadings (ii-v).

3.5 Raman Spectroscopy Analysis

Raman spectroscopy is a highly sensitive technique to study crystallinity and defects in the structure of materials. Raman spectra of both as-spun and heat treated nanofibrous filter mats of PTFE-ZnO are shown in Figure 6. The vibrational modes of PTFE at room temperature have the factor-group *D(14π/15),* whose modes are distributed among the symmetry species as: A_1(Raman-active, polarized), *A2* (infrared-active), *E1*(infrared- and Raman-active; depolarized in the Raman spectra), and E_2 (Raman-active, depolarized)(Koenig & Boerio, 1969). Reportedly, Raman bands observed at 1382,1379,1213 and 198cm^{-1} are attributed to the characteristics of PTFE which are recognized as symmetric stretching vibrations of A_1class CF_2 polymer, anti-symmetric stretching vibrations of CF_2 and stretching of E_1 class (Kereszturi,

Szabó, Tóth, Marosi, & Szépvölgyi, 2008; Koenig & Boerio, 1969). However, in this study Raman bands observed at 184, 1120 and 1385cm^{-1}were associated to E_1 Raman active band constituted due to stretching of CF_2 bonds, symmetric stretching vibration of -CF_2 bonds, and Raman active polarized groups arising from the symmetric stretching vibrations of A_1 class of CF_2 group.

Zinc oxide hexagonal shape structure belong to C^4_{6v} ($P6_3mc$) symmetry group. According to the Group theory zinc oxide crystal structure consist of eight sets of center zones having optical phonons. These zones are classified as Γ = A1 +2B1 +E1 +2E2. In these Phonon zones polar modes are A1 and E1 that split into transverse optical (A1T and E1T) and longitudinal-optical (A1L and E1L) phonons, while two Raman active modes of E2 mode consists of low- and high-frequency phonons (E2L and E2H) and B1 modes are silent modes (Bhunia, Jha, Rout, & Saha, 2016; Gültekin & Akbulut, 2016; Khan, 2010). The strong band noticed at 587 cm^{-1} in the literature was known as Raman active optical phonon mode, namely, E_1-low (E_1-LO) and has been reported to be associated to the crystal defects present in ZnO structure (Bhunia et al., 2016; Gültekin & Akbulut, 2016; Khan, 2010).

The low temperature heat treatment (280 °C) of nanofibrous filter mats had induced crystal imperfections in ZnO attributed to E1 low infrared active polar phonon modes of ZnO crystal. When subjected to heat treatment, blue shift in Raman signals from 587cm^{-1} (reported for hexagonal phase) to 622cm^{-1} has been observed in the present study. This blue shift in Raman peaks has been attributed to higher degree of crystalline imperfections in these samples including absence of oxygen, interstitial Zn and the free carrier deficiency (Gültekin & Akbulut, 2016; Horzum, Tascioglu, Özbek, Okur, & Demir, 2014).

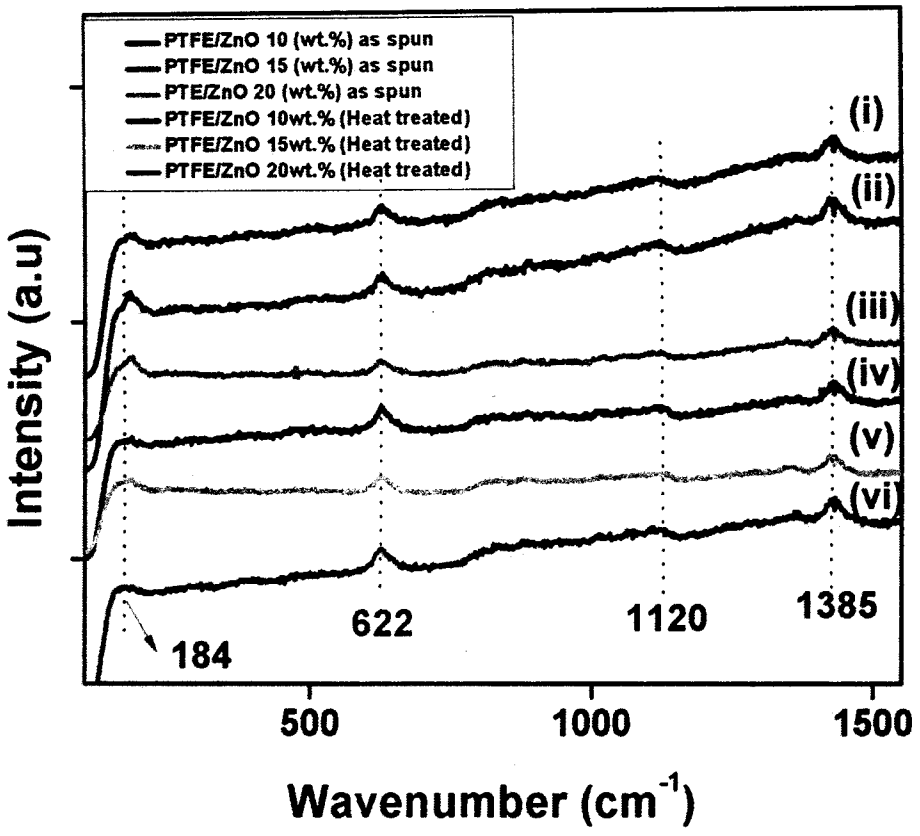

Figure 3. 5. Raman spectra of nanofibrous filter mats of PTFE-PVA-ZnO (i-iii) As-spun, (iv-vi) PTFE-ZnO heat treated at 280°C for 5 min.

3.6 Hydrophobicity Analysis

Hydrophobicity is an important property of nanofibrous filter mats which is attributed to lower surface energy and higher surface roughness. These two features are greatly desirable in the nanofibrous filter mats for tailoring their aerosol filtration and self-cleaning properties. On the bases of wettability, surfaces are classified as hydrophilic (water-loving) or hydrophobic (water-repelling) when they do interact with liquid droplets, specifically of water. In case of a hydrophilic surface, due to high surface energy water droplet wets the surface resulting in water contact angle values less than 90°. However, a hydrophobic surface maintains lower surface energy that leads to exhibit water contact angle value more than 90° which results into beading up of water droplet on such a surface (Simpson, Hunter, & Aytug, 2015). The -CF_2- group of

PTFE holds up low surface energy (0.019 N/m) (X. Li et al., 2019a) that gives ultra-hydrophobicity to the surface of PTFE- nanofibers. Figure. 3.6 (a) shows the schematics of water droplet penetration response on the rough surface of PTFE nanofibers attributed to the presence of spaces on these surfaces. Therefore, higher surface roughness and high adhesive forces give rise to more spaces which make nanofibrous filter mat surface highly hydrophobic by impeding diffusion of water droplet in to the surface (Tran & Webster, 2013).

In contrast, relatively smooth nanofiber surfaces with low adhesive forces (pure PTFE) cannot effectively avert water droplet from penetration into the spaces available on their surface, consequently leading to emergence of smaller values of water contact angle, as shown in Figure 3.6 (a)(B. Wang, Zhang, Shi, Li, & Guo, 2012).This argument is considerably presented in support of PTFE-ZnO nanofibrous filter mats (higher RMS values) which exhibit ultra-hydrophobicity that makes them a favorable candidate for development of VOC filters (Y. Liang et al., 2018a). The water contact angles (WCA) evaluated from the surfaces of both as spun and heat treated PTFE-ZnO filter mats are shown in Figure 3.6 (b) and Table 3.

The evaluated WCA of as-spun PTFE-PVA (control) nanofibrous filter mats was 82.16°±2.30, whereas these values computed for as-spun PTFE-PVA-ZnO filter mats were slightly higher which worked out to be 86.52°±1.20 and 87.15°±1.10 respectively with the rising ZnO content from 10 to 20wt% in PTFE matrix. Furthermore, WCA of heat treated PTFE-PVA nanofibrous filter mats was found to be 102.56°±2.40, while WCAs of heat treated PTFE-ZnO filter mats were determined to increase remarkably from 104.78°±1.90 to 121.55°±2.20 with the rising ZnO loading. Improvement of WCA in these samples has been ascribed to the removal of PVA (hydrophilic) from the PTFE matrix besides consolidation of porosity in the fibril structure after heat treatment which eventually led to escalation of hydrophobicity. The improvement in hydrophobicity and roughness can primarily be attributed to the formation of bead-like structure such as bulging of zinc oxide particles on the surface of nanofibers which are shown

in Figure 3.1. Moreover, higher value of hydrophobicity in filter media helps protecting them against moisture and airborne germs besides it also discourages the irreversible attachment and accumulation of microbes on them. Another favorable aspect of higher hydrophobicity in such surfaces is aversion against adhesion of dust particles which is important for fibrous materials designed to be used as air filter (Choi et al., 2018).

Self-cleaning characteristics of both as spun (PTFE-PVA) and heat treated PTFE-ZnO nanofibrous filter mats have been determined which are shown in Figure 3.6(c). To ascertain this quality of samples, carbon black was placed on their surfaces which were rinsed by flowing water droplets effused through a syringe. After cleansing the samples, it was observed that surface of pure PTFE filter mats remained wet with water droplets and clogged with particles of carbon black as well but contrarily, heat treated PTFE-ZnO surfaces became cleaner quickly and remained dry, as shown in Figure 3.6 (c). These results are in conformity with the reported outcomes of hydrophobicity and self-cleaning investigations of Liang et al. (Y. Liang et al., 2018a).

For better understanding of a physical process going on within a porous medium, full characterization of certain properties of porous material is necessary like pore structure, pore size and pore connectivity. Pore structure is a collective term used to explain about **porosity, pore size and pore morphology of a porous medium**. There are variety of pores present in electrospun nano membranes such as closed pores, blind pores and through pores (Patanaik, Jacobs, & Anandjiwala, 2010). Non accessible ones are closed pores, and blind pores terminate inside the nano membranes structure itself and are therefore no use for filtration application. The most important pores that provides open passage to air through nano membrane thickness and are critical for air filtration are through pores. By and large, pore size is not alike, but instead there is a distribution in their size which determines through pore characteristics. Electrospun nano

membranes having small pores can increase filtration efficiency but affects both air permeability and pressure drop. As clearly mentioned above, Particulate matter size can influence filtration efficiency and pressure drop which eventually effects quality factor. Nano membranes with 185 nm fiber diameter are more efficient in capturing PM less than 0.1 μm due to the natural diffusion (Hung, C.H. and W.W.F, 2011). However, for particles of the size range 0.1–0.4 μm, nano membranes with fiber diameters of 94 nm showed a higher quality factor which is due to the dominance of the interception mechanism. The smaller fiber diameter reduces the pore size by decreasing the pore aperture and enhancing the direct-interception mechanism for particle capture (Wang et al., 2010). In case of more grooves and structural pores on the surface of fiber VOCs get adsorbed in these grooves due to difference in energy. They easily get desorbed by applying suitable kinetic energy.

Porosity of the nanofibrous filter mats was measured by standard gravimetric method as shown in Figure 3.7. Gravimetric method is commonly used to determine the weight in membranes pores versus dry membrane weight without liquid. Porosity of filter mats increases with the increase in doping amount of zinc oxide particle on the surface of the filter mats. Porosity vary from 48 to 88% for pure PTFE and zinc doped PTFE nanofibrous filter mats.

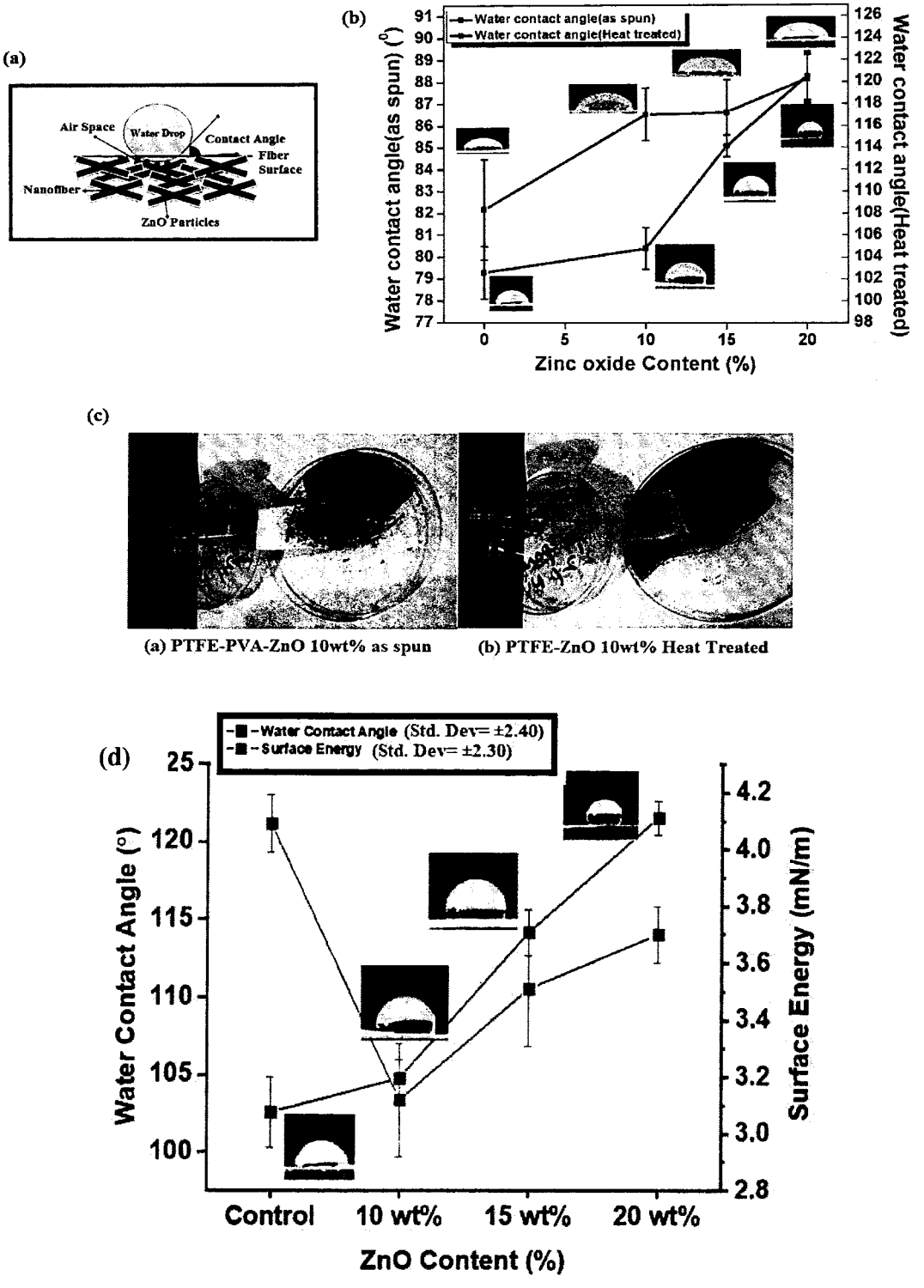

Figure3.6. (a) Schematics of water droplet behavior on a rough surface (b) Water contact angle of both as spun PTFE-PVA-ZnO (S.D *±1.20)* and heat treated PTFE-ZnO nanofibrous filter mats with different loadings of ZnO (S.D *±2.40)*, (c) Self-cleaning behavior of pure PTFE (as-spun) and heat treated PTFE-ZnO nanofibrous filter mats, (d) Surface free energy calculation of all synthesized compositions heat treated filter mats.

Table 2. Water contact angle and surface tension of both as spun and heat treated PTFE-ZnO composite nanofibrous filter mats.

Sample Composition	Water Contact Angle (WCA) (as spun)	Water Contact Angle (WCA) (Heat treated)	Surface Energy (mN/m)
PTFE-PVA	82.16°,S.D ±2.30	102.56°, S.D ±2.40	4.09
PTFE-ZnO (10wt%)	86.52°, S.D ±1.20	104.78°, S.D ±1.90	3.12
PTFE-ZnO (15wt%)	86.81°, S.D ±1.50	114.14°, S.D ±1.00	3.51
PTFE-ZnO(20 wt%)	87.15° ,S.D ±1.10	121.55°, S.D ±2.20	3.70

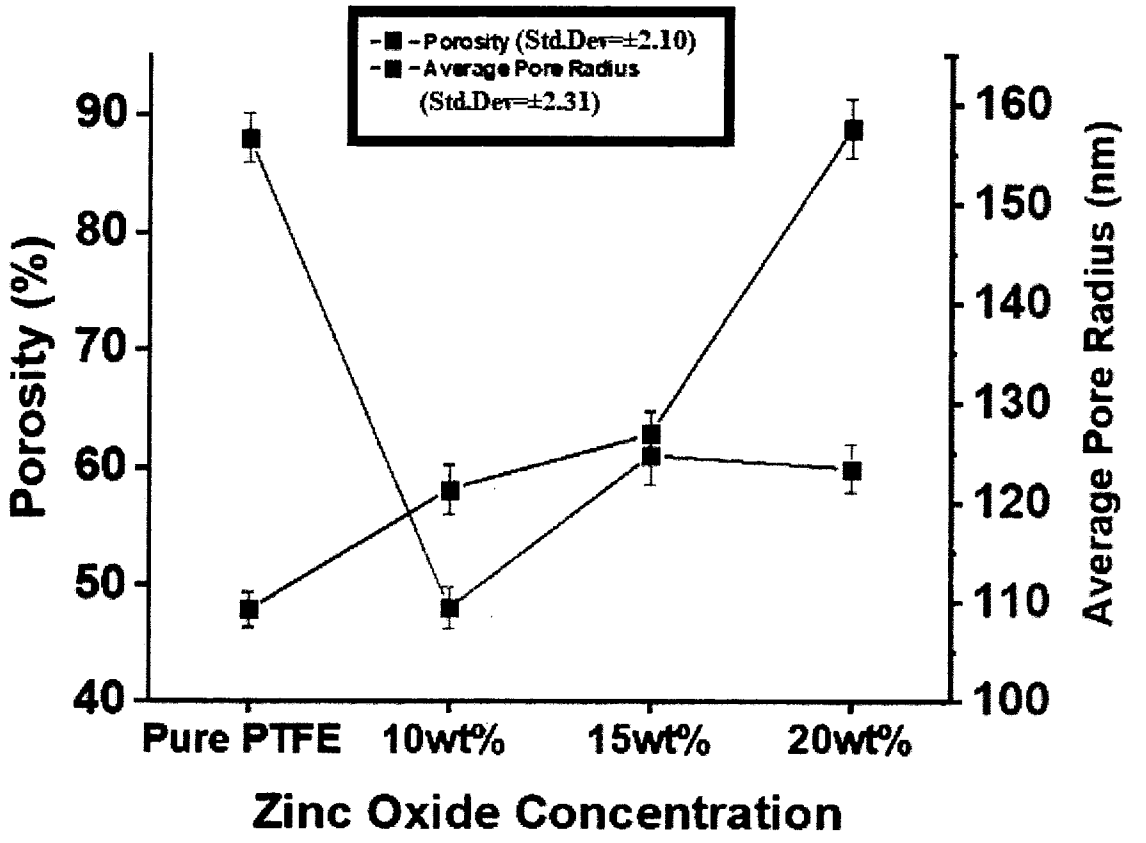

Figure 3.7 Porosity and average pore radius calculated for heat treated PTFE-ZnO nanofibrous filter mats.

3.7 Surface Free Energy (SFE) measurement

Surface energy values can be calculated indirectly using various liquids with known surface energy and their polar and non-polar components (Lugscheider & Bobzin, 2001). Contact angle of a drop (maximum 5 drops) is measured by placing it on a solid surface. Based on the number of components, the most common surface energy theory is two-component model—Owens/Wendt theory (equation 9 in methodology section).

In the present study, data calculated through contact angle on polymer nanofibrous filter mats(heat treated) with water was used to calculate surface free energy (Senturk Parreidt, Schmid, & Hauser, 2017). The two unknowns, Υ_L^D and Υ_L^P of (water drop on nanofibrous filter mats surface) were calculated by determining the contact angle of liquid (deionized water in the current work). The surface tension values Υ_L, Υ_L^D and Υ_L^P (in mJ/m^2) for water are 72.8, 21.8 and 51.0 (X. Wang et al., 2008) . Table 3 is showing the calculated values of surface free energy (mN/m) of pure PTFE and PTFE-ZnO composite heat treated nanofibrous filter mats.

Table 3. Surface Free Energy (SFE) of pure PTFE and PTFE-ZnO nanofibrous filter mats with varying loadings of zinc oxide particles. SFE calculated through Owens–Wendt theory for liquid (water) by analyzing the images in drop shape analyzer software.

Nanofibrous mats Composition	**Surface Free Energy (mN/m)**
Pure PTFE	4.09
PTFE-ZnO 10wt%	3.20
PTFE-ZnO 15wt%	3.51
PTFE-ZnO 20wt%	3.70

3.8 Summary:

In this study, effects of varying amount of ZnO loadings on physio-chemical structural properties of the filter mats were investigated through FESEM, EDX, AFM, FTIR, Raman spectroscopy, TGA and Water contact angle goniometry. The results have suggested that with increasing content of zinc oxide loadings in the electrospinning solution, electrical conductivity of solution increased which resulted into formation of nanofibers of finer mean diameters, higher RMS roughness and enhanced hydrophobicity when compared to the pure PTFE nanofibers. These characteristic improvements resulted into significant enhancement of their aerosol filtration ability.

Part II

Physiochemical Characterization of Electrospun Composite PTFE-NiO Nanofibrous Filter Mats

This part of the chapter describe in detail the Physio-chemical characterization of both as prepared PTFE-PVA-NiO and heat treated PTFE-NiO composite filter mats as following:

4.1 Nanofibers Morphology *Analysis*

The FESEM micrographs of PTFE-NiO composite nanofibers of as prepared and heat treated and their respective diameter distribution are shown in Figure 4.1. It can clearly be seen from SEM micrographs that continuous fibers with porous surface morphology were obtained for all the compositions studied only somewhere beads are visible which might be due to non-heterogeneity of electrospinning solutions (see Figure 4.1 (a1-d1)). In addition to beads in (all compositions PTFE-PVA,PTFE-NiO 2-4 wt%) only one composition of PTFE-NiO 6wt% concentration showed unique web shape morphology after electrospinning as shown in Figure. 4.1 (d1-d2). In the present study fiber mean diameter of as prepared PTFE-PVA-NiO nanofibers range from 0.34±218.61 to 0.23±102.12 μm and their counterpart heat treated PTFE-NiO range from 0.25±24.12 to 0.12±85.75 μm. The fiber diameter first increase and then started decreasing as shown in Figure 4.1 due to two possible reasons; first increase in the concentration of nickel oxide wt% in the electro spinning solutions, secondly increase in the applied voltage to the electrospinning solutions. (Lin, Pan, & Wu, 2007; Wu & Pan, 2006).

According to the theory of 'electro hydrodynamic (EHD)' (Mituppatham, Nithitanakul, & Supaphol, 2004) jet diameter is directly proportional to the surface tension and inversely proportional to the solution conductivity. Addition of salt content in spinning solution increases the solution conductivity. During the process of electrospinning controlling final diameter of

nanofibers there exists a competition between the surface tension and solution conductivity. In the presence of a suitable dopant or if the solution is itself very conductive due to addition of salt, an increase in the solution conductivity can overcome the surface tension effect and leading towards decrease in nanofiber diameter (Khalil & Hashaikeh, 2014).

After heat treatment fiber diameter was reduced due to densification of PTFE grains in the fibers, complete degradation of the organic phase and release of water vapors that had been suspended in the fiber texture. It is important to mention here that a unique porous morphology was observed in heat treated PTFE-NiO composite nanofibers as shown in Figure 4.1 (b4-d4). Energy dispersive spectrum of PTFE-NiO composite nanofibers confirms the presence of nickel oxide particles in the fibers as depicted in Figure. 4.1 (a4).

Table 4. Solution and Process parameters used during electrospinning of PTFE-NiO nanofibrous filter mats.

a)Solution Parameter		**b)Process parameters**	
Solution compositions	Solution Conductivity (μS/cm)	Applied voltage	20 kV
PTFE-PVA	1852±1.5	Tip to collector Distance	12 cm
PTFE-NiO 2wt.%	1889±2.5	Flow rate	0.3 mL/h
PTFE-NiO 4wt.%	1894±1.0	Needle gauge	23SS
PTFE-NiO 6wt.%	1897±1.8	Temperature	25 °C

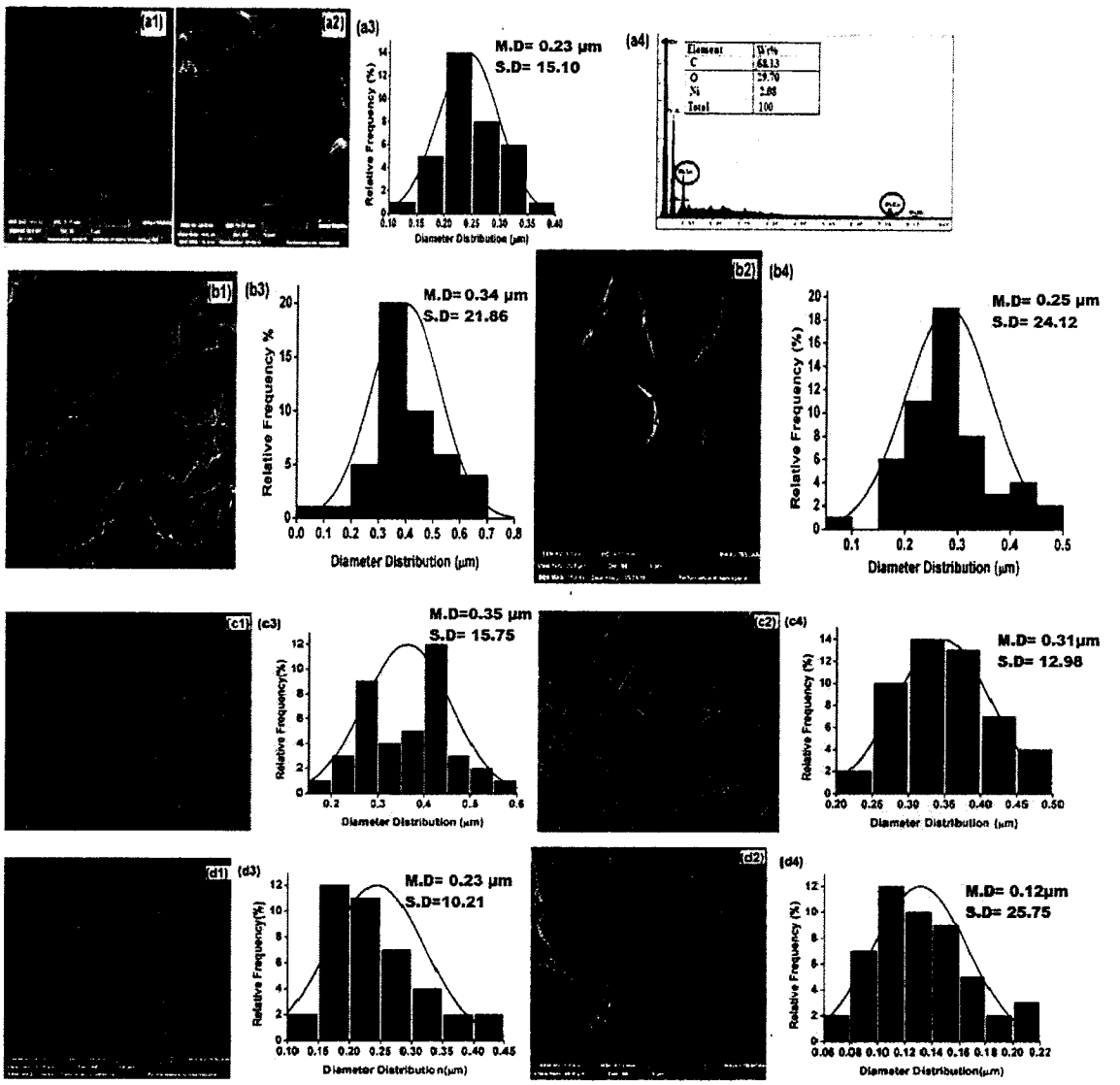

Figure 4.1 FESEM micrographs of nanofibrous filter mats: As spun pristine PTFE-PVA (a1), PTFE-PVA-NiO 2wt% (b1), PTFE-PVA-NiO 4wt%(c1), PTFE-PVA-NiO 6wt% (d1) and their subsequent PTFE-NiO nanofibrous filter mats heat treated at 280°C for 5 min (a2-d2), Mean size distribution of nanofibers (a3-d3). µm

4.2 Thermal Analysis of nanofibers

The thermal properties of PTFE-PVA-NiO composite porous nanofibers (containing 2wt% NiO loading) was evaluated by TGA and DTA as shown in Figure 4.2.

The weight losses with respect to temperature change in the PTFE-PVA- NiO nanofiber filter mats are indicated by dotted arrows in the TG curve (green line) in Figure 4.2. The first weight loss occurred at 75 °C because of water molecules removal from the sample, the second peak attained at 280 °C which corresponds to the decomposition of PVA, and the third weight loss peak attained at 475 °C, which is ascribed to the decomposition of PTFE (Grosvenor, Biesinger, Smart, & McIntyre, 2006). The thermal transformation temperature of nickel nitrate hexahydrate to nickel oxide is from 170° C to 290° C (Sarlak, Nejad and Shakhesi, 2012) as shown in Figure 4.2, TG curve represents the dehydration of nickel nitrate hexahydrate to nickel hydroxide around 170°C, and the thermal events between 200°C and 300°C is the indication of transition of nickel hydroxide to nickel oxide. The complete process is as follows (Song et al., 2010),

$$Ni(NO_3)_2.6H_2O \longrightarrow Ni(OH)(NO_3)_2 \longrightarrow Ni(OH_2)NO_3 \longrightarrow NiO\ OH \longrightarrow NiO \quad \text{(Eq.10)}$$

The DTA curve shown in Figure 4.2 (blue peaks) depicted broaden exothermic peak at 280 °C that could be attributed to the decomposition of acetate along with the degradation of PVA by dehydration on the polymer side chain. The peak at 475 °C corresponds to the decomposition of main chain of PVA (Khalil & Hashaikeh, 2015). It was clear from the TGA curve that all the PVA and organic group of nickel nitrate were removed completely at around 450°C, resulting metal oxide composite phase.

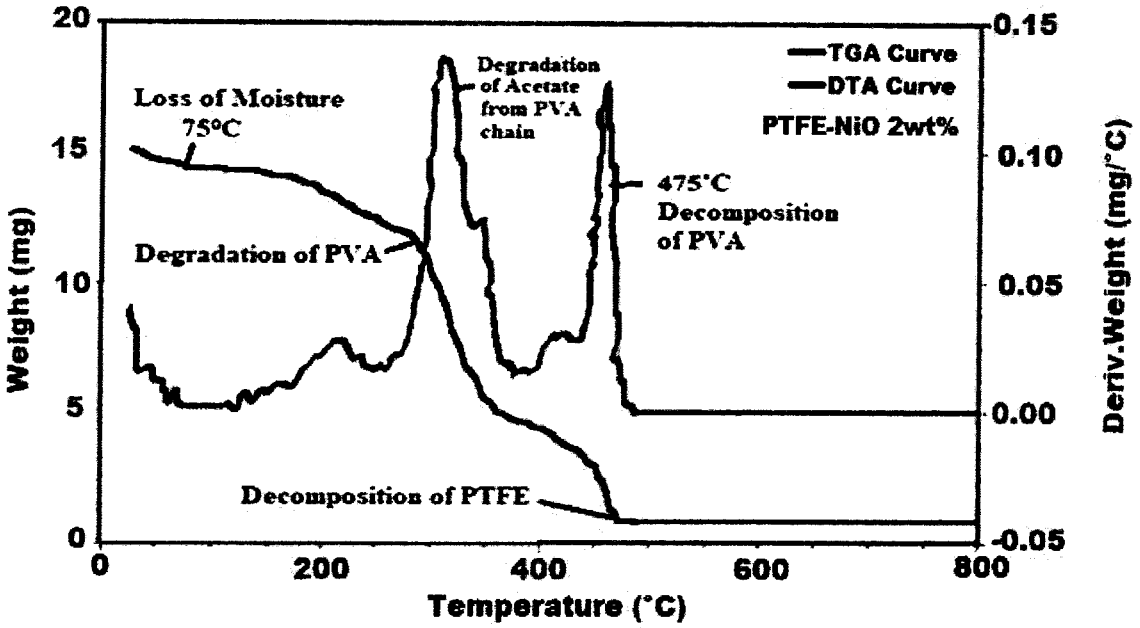

Figure 4.2. TGA and DTG scan of as-spun PTFE-PVA-NiO nanofibrous filter mats containing 2 wt% of nickel oxide particles.

4.3 FTIR analysis

Functional groups of both as spun PTFE-PVA-NiO and heat treated PTFE-NiO composite nanofibrous filter mats were identified by FTIR analysis as shown in Figure 4.3. The bands at 1015, 1231 cm^{-1} corresponds to the characteristics band of PTFE due to CF_2 stretching and the bands at 3331 cm^{-1} is assigned to the H–OH stretching which corresponds to the stretching vibrations of PVA (Vellingiri, Kumar, Deep, & Kim, 2017). Bands at 590 and 1362 cm^{-1} belongs to NiO particles (Ji et al., 2013; Y. Liu, Jia, Li, Hao, & Pan, 2018). After sintering at 280 °C for 5 min, the characteristic peaks of PVA disappeared completely while the bands associated with the stretching of $-CF_2$ bonds and those belonging NiO particles preserved in both as spun and heat treated samples as shown in Figure 4.3.

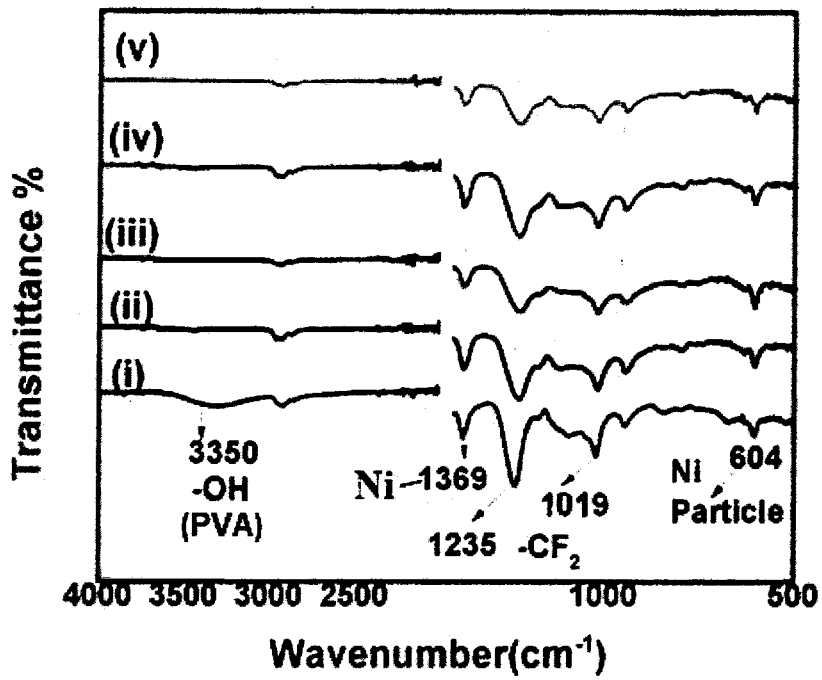

Figure 4.3. FTIR spectra of PTFE-PVA-NiO (i) as spun nanofibers (ii-v) and PTFE-NiO heat treated at 280 °C for 5 minutes.

4.4 Raman spectroscopy analysis

Raman spectroscopy is a technique to study chemical composition, crystal structure as well as the defects in the crystal structure. Raman spectra of both as spun and heat treated nanofibers of PTFE-NiO are shown in Figure 4.4. Due to anti-ferromagnetic nature of nickel oxide ; it has two types of magnons and their nature depends on the structure of nickel oxide at ground state (George & Anandhan, 2014; Kaganov, 1981). Two Raman peaks are located at about 570 and 1100cm^{-1} in the range of 200–2000cm^{-1} in the literature but in the present study peaks shifted towards 625 cm^{-1}. There are two phonon scattering modes recognized for nickel oxide particles; one-phonon (1P) longitudinal optical (LO) and two-phonon (2P) 2LO, the first mode is below 600 cm^{-1} and the second ones above 600 cm^{-1} range (Liu et al., 2012). The peak at 180 cm^{-1} is known as forbidden phonon scattering and its due to 1-phonon scattering (Mironova-Ulmane et al., 2007).

There are two major reasons reported for this peak is; after heat treatment presence of lattice weaknesses, the non-stoichiometry in the composition of oxygen in the crystal structure (George & Anandhan, 2014). The intense peak at 625 cm^{-1} has also originated from the defects (Mironova-Ulmane et al., 2007) as shown in Figure 4.4. Raman bands at 1382 cm^{-1}were characteristics of PTFE which were recognized as symmetric stretching vibrations of A_1class CF_2 polymer (Koenig & Boerio, 1969;Kereszturi, Szabó, Tóth, Marosi, & Szépvölgyi, 2008). In the present study, Raman bands were observed at 1431cm^{-1} associated to E_1Raman active band due to stretching of CF_2 bonds. Peak intensity increases with the heating temperature the reason might be the grain growth and nanofibers densification during heat treatment (Biju & Khadar, 2003).

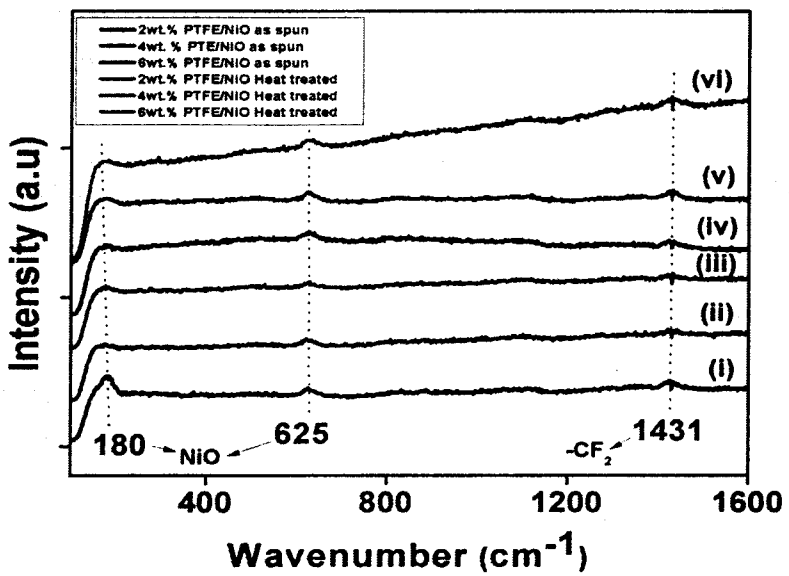

Figure 4.4. Raman spectra of composite nanofibers of PTFE-PVA-NiO as-spun (i-iii) and PTFE-NiO heat treated samples (iv-vi).

4.5 Hydrophobic Characterization of nanofibers

A surface is classified as hydrophilic (loving water) or hydrophobic (water repelling) by how it interacts with water droplet. If a water drop has a contact angle of greater than (90°) with the

surface it's called hydrophobic and hydrophilic if less than (90°) (Simpson, Hunter, & Aytug, 2015). Electrospun PTFE nanofibrous membranes are well known for their hydrophobicity due to their higher surface roughness with low surface energy. Not all applications requires hydrophobicity and in some cases, it is preferred that the electrospun membrane must be hydrophobic like in air filtration. Meanwhile, a single membrane/nanofibrous material hardly possesses all the desirable properties such as thermo stability, chemical stability, dust/pathogens resistance and good mechanical properties at the same time. Composite nanofibrous membrane are highly desirable for practical applications especially for air filtration purpose.

The $-CF_2-$ group of PTFE possesses very low surface energy (0.019 N/m) (X. Li et al., 2019) that give high hydrophobicity to the surface of PTFE-based composite nanofibers filter mats. The water contact angles (WCA) and overall surface energy of heat treated PTFE-NiO nanofibers filter mats are shown in Figure 4.5 (a) and Table 5. The water contact angle of the heat treated control PTFE nanofibers filter mats was 102.56°±2.40, whereas WCAs of heat treated PTFE-NiO composite nanofibers mats increase from 112.78°±1.90 to 121.55°±2.20 with an increasing NiO loading from 2-6 wt%. This increase in WCA(from Pure PTFE to PTFE-NiO 2-6wt%) was a result of heat treatment that not only removed the carrier polymer PVA (hydrophilic) from the nanofibers matrix but also consolidated the porous structure of nanofibers by densification of PTFE grains in fibers; eventually, both of these effects lead to enhancement of hydrophobicity of heat treated filter mats. In addition, it was also observed that WCA increased slightly with an increasing NiO loading in the electrospun nanofibers by making the surface of nanofibrous mats rougher. Higher water contact angle (more than 110°) means better hydrophobic property, which is important for the composite nanofibrous filter

mats for avoiding the negative influence of moisture and polar air pollutants adsorption on their surface (Y. Liang et al., 2018a).

Calculated surface free energy of water droplet on fibrous surface is shown in Figure 4.6(a). As the contact angle of nanofibers increases surface free energy (mN/m) decrease from 21.03±2.14 to 14.63±3.01 for heat treated PTFE-NiO samples with different weight content of nickel oxide particles. Pure PTFE sample showed surface energy of 21.03 mN/m and when nickel oxide particles incorporated in to the nanofibers the surface free energy decreases to 14.63 mN/m as shown in Figure. 4.5(a). The surface free energy data reveal that electrospun nanofibers may differ due to low polar components at the surface of nanofibers. The low polar component proposed that the liquid interactions with electrospun fibers can be related to the dispersive part including van der Waals forces, enhanced by the large surface area created by the small diameter of fibers (Żenkiewicz, 2007). Higher hydrophobicity of nanofibers also facilitate (air) filters rejecting dust and discourages the irreversible attachment and accumulation of microbes on the surface of air filters (Y. Liang et al., 2018a).

The self-cleaning tests are shown in Figure 4.5 (b) for both as spun and heat treated PTFE-NiO nanofibers filter mats. Carbon black was sprinkled on the surface of samples and was then cleaned by flowing water droplets with the aid of syringe. The as spun nanofibers remained wet and got clogged with carbon black particles in contrast the heat treated PTFE-NiO surface became rapidly cleaner and stayed dry and retained wettability represented by red dot as shown in Figure 4.5(b).The above results demonstrate that the surface of the heat treated PTFE-NiO electrospun nanofibers filter mats possesses excellent hydrophobicity and self-cleaning properties. These results are in-line with the hydrophobicity and self-cleaning results analysis of (Liang et al., 2018). Porosity of the nanofibrous mats was measured by standard gravimetric method as shown in Figure 4.6 Porosity of filter mats increases with the increase in doping

amount of nickel oxide particle on the surface of the mats. Porosity vary from 50.21 to 77.36% for pure and nickel doped filter mats. Pore radius range from 77.44 to 100 nm for both pure PTFE sample and composite PTFE-NiO nanofibrous filter mats as shown in Figure 4.6 in detail.

(a)

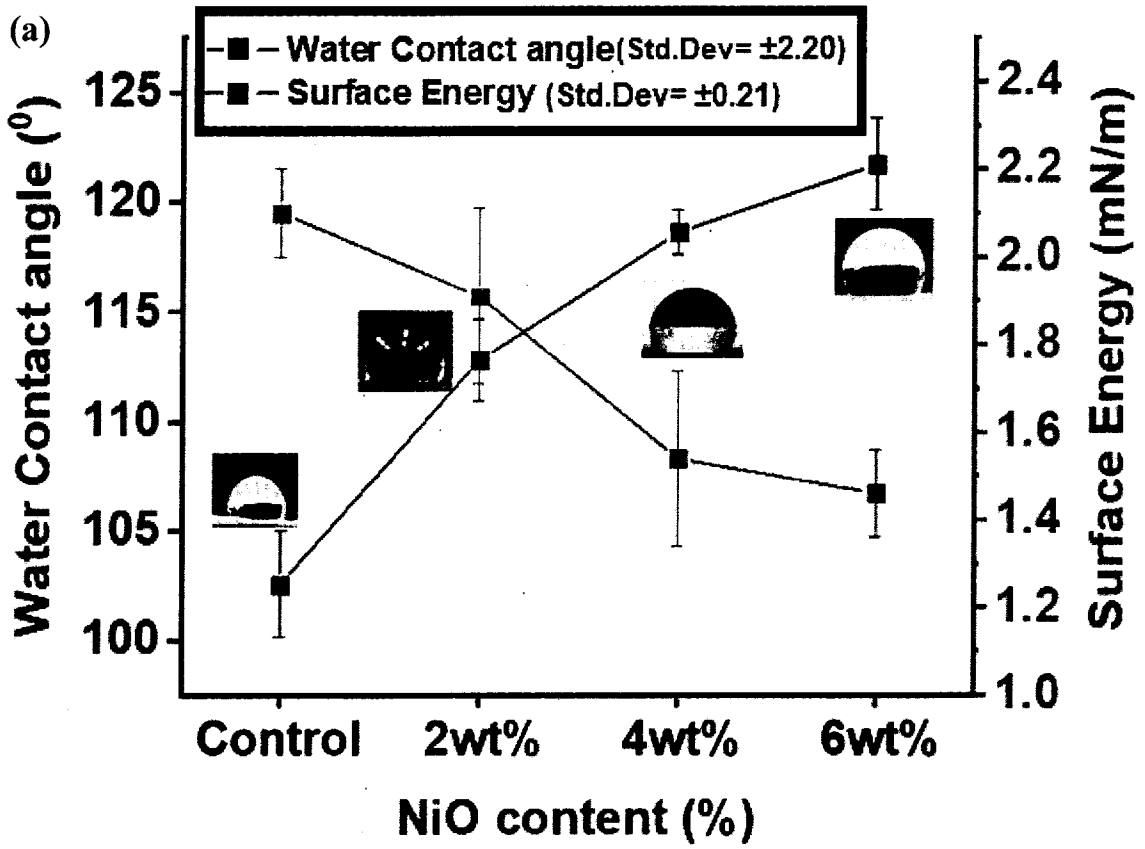

(b)

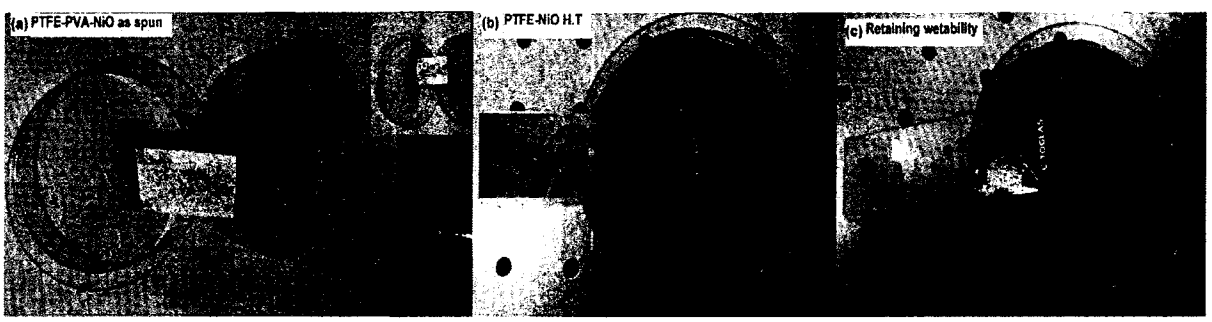

Figure4.5. (a) Water contact angle and surface free energy of heat treated PTFE-NiO nanofibrous filter mats (b) self-cleaning ability of as spun PTFE-NiO and PTFE-NiO heat treated nanofibrous filter mats.

Table 5. Water contact angle and surface free energy of heat treated PTFE-NiO composite nanofibrous filter mats.

Sample Composition	Water Contact Angle (WCA)(Heat treated)	Surface Energy (mN/m)
PTFE control	102.56°, S.D±2.40	2.10
PTFE-NiO (2wt%)	112.78°, S.D ±1.90	1.90
PTFE-NiO (4 wt%)	119.14°, S.D ±1.00	1.54
PPTFE-NiO (6 wt%)	121.55°, S.D ±2.20	1.46

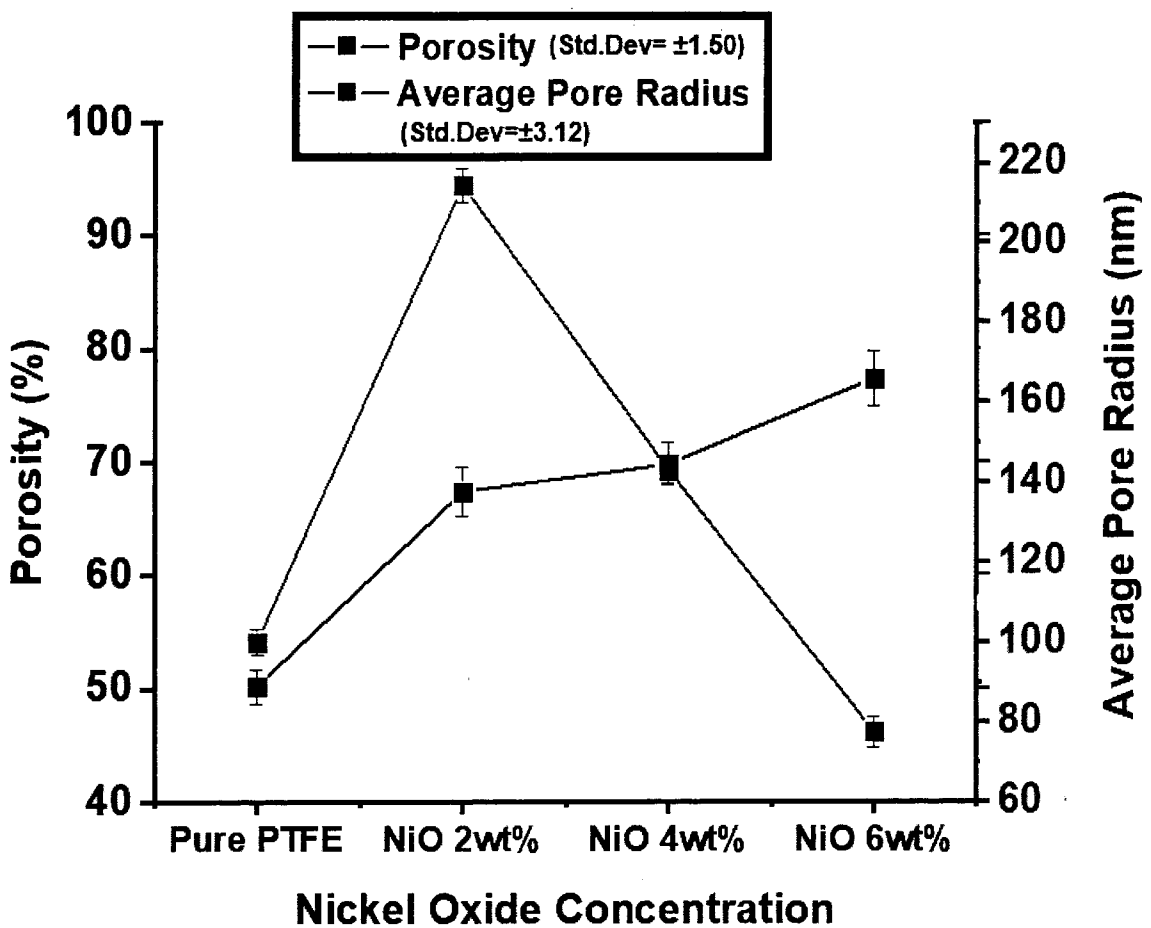

Figure 4.6. Line graph showing porosity (%) and pore radius (nm) of both Heat treated pure PTFE and composite PTFE-NiO nanofibrous filter mats with varying amount of nickel oxide.

4.7 Summary:

Surface property of nanofibers were modified by doping varying amount of nickel oxide particles (2, 4 and 6 wt %) in the electrospinning blend. Effects of varying amount of NiO loadings on physio-chemical structural properties of nanofibers were investigated through FESEM, Raman, TGA and water contact angle. The results suggested that with increasing amount of Nickel oxide loadings in electrospinning blend, conductivity of the spinning solution increased which resulted in fibers formation with finer diameters, percentage of porosity and enhanced hydrophobicity when compared to pure PTFE nanofibers. Web shaped unique morphology was obtained in only 6wt% of PTFE-NiO composite filter mats due to increase in applied voltage. These improvements in surface properties of filter mats resulted in significant enhancement of aerosols filtration on the surface/through pores of composite PTFE-NiO nanofibrous filter mats.

Part III

Performance Evaluation of Electrospun Synthesized PTFE composites Nanofibrous Filter Mats for Aerosol Filtration

(a) Composite PTFE-ZnO Nanofibrous Filter mats

In this chapter of the thesis aerosol filtration performance evaluation of fabricated PTFE-PVA (control), PTFE-ZnO and PTFE-NiO composite nanofibrous filter mats in comparison with the commercially available PTFE air filters was done in specially customized designed air filtration setup mimicking industrial exhaust. Design, working and parameters used during filtration of VOCs and PM are discussed in detail methodology section 2 sub sections 2.2.6 and 2.2.7. Along with the filtration tests antibacterial property of synthesized composite nanofibrous filter mats was also studied on two bacterial strains.

5.1 Adsorption of Volatile Organic Compounds

The aerosol filtration study has been carried out using three model VOCs, namely, toluene, acetone and formaldehyde (at ambient temperature and pressure) that encompasses molecules of VOC compounds of both aromatic and aliphatic hydrocarbons, which are extensively used in a wide array of industrial applications.

The results shown in Figure 5.2 manifesting that adsorption of molecules of model VOCs was deficient on pure PTFE nanofibrous filter mats, however, with the growing ZnO loading in these filter mats, adsorption of VOCs has depicted an increasing trend on the surfaces of PTFE-ZnO. Pure PTFE filter mats have demonstrated adsorption of 48, 16 and 16 μg/mg of VOCs of toluene, acetone and formaldehyde whereas these adsorptions have been found to 80, 31 and 30 μg/mg; 121, 48 and 49 μg/mg, and 141, 62 and 64 μg/mg for the mats containing 10, 15 and 20wt% ZnO.

These results revealed that adsorption of toluene, acetone and formaldehyde have increased ten, seven and three folds on the surfaces of nanofiber samples containing 20wt% ZnO loading when compared to pure PTFE filter mats and the values reported in the literature. The interaction of PTFE-ZnO nanofibers test membrane building blocks with the VOC compounds determines their adsorption capacity and selectivity against the tested VOCs. This can further be analyzed by considering the polar nature of tested VOC compounds and their predisposition towards interaction with the filtration medium of PTFE-ZnO nanofibers. Furthermore, selectivity of VOCs' molecules on the surface of PTFE-ZnO nanofibers has been attributed to the fiber structural properties, especially finer mean diameters, internal porous structure and presence of ZnO on the surface of nanofibers (H. Xu et al., 2019).

The sequence of VOCs filtration can be described in the following manner in which initially; maximal adsorption of VOC molecules has taken place on the surface of nanofibers. As the diameter of nanofibers has been found to be decreasing with the rise in ZnO loading which provided greater surface area and additional active sites for adsorption of VOCs molecules, as shown in Figure 5.1. Subsequently, VOC molecules partially got diffused into the pores available at the surface of the nanofibers which acted as core adsorption sites for the VOCs (table 2). In these samples, porosity has been found to increase from 47.88 to 88.73% with the rise in ZnO content from 0 to 20 wt.% in the PTFE matrix which resulted into enhanced adsorption of VOCs, as shown in Figure 3.9 of UV analysis of adsorption. Finally, molecules of VOCs have got adsorbed on the PTFE-ZnO nanofibers with characteristic intermolecular van der Waals forces, revealed in Figure 3.8.

The physisorption of VOCs and ZnO molecules on the surfaces of nanofibers could be polar and nonpolar. As after sintering of nanofiber filter mats, their surfaces retain residual organic species, therefore, the sensitivity of ZnO to the VOCs was ascribed to the interaction of residual surface carbonaceous species with the VOC molecules through non polar exchanges.

Conversely, the polar oxide surface features could effectively associate with polar organic compounds, such as acetone and formaldehyde (Scholten, Bromberg, Rutledge, & Hatton, 2011), as given in Figure 5.1. While in case of polar interaction, the possible nearest strong bond formed between the ZnO and VOCs is established among the oxygen atom of ZnO and hydrogen atom of VOCs designated as O_{surf}-$H_{toluene}$. The values of bonding energy of O_{surf}-$H_{toluene}$, adsorption distance ($d_{surf\text{-}molecule}$) and the change in average bond-length ($\Delta(C_{ben}$-$C_{CH2/3})^{ave}$) of toluene have been reported to be -1.17 eV and 2.389 Å respectively, on the surface of ZnO. If one atom of a compound is involved in the intermolecular interaction, then the value of bonding energy will be positive. The negative values of bond length indicate strong adsorption energy between the adsorbed molecules (H) and the surface of ZnO (Nugraha, Saputro, Agusta, Akbar, & Pramudya, 2019). As mentioned earlier in Raman spectroscopy analysis (Figure 3.5), ZnO particles embedded in PTFE matrix possess hexagonal wurtzite crystal structure in which zinc ions are surrounded by tetrahedra of oxygen ions. The coordination between zinc ion and oxygen ion results in tetrahedral symmetry and polarity accordingly along the axis. Charge difference appeared on zinc and oxygen atom due to the Zn–O polar bonds. In this bonding Zn atom is partially positive for that reason, ZnO can be considered as Lewis acid (Jiye et al., 2013). Thus, lone pairs on the alcoholic compounds tend to be attracted toward the positively charged metal atoms. Oxygen vacant sites may be considered as trapping sites for interaction with pollutants, VOCs in this case (Horzum et al., 2014).

Nugraha et al., (Nugraha et al., 2019) demonstrated that benzene, toluene and xylene (BTX) adsorption on ZnO surface are not originated from the orbital interaction between the BTX and the surface. Instead, the bonding comes from the contribution of weak van der Waals forces interaction between the surface and the molecule. These authors have verified that the toluene

adsorptions on ZnO (100) surface are indeed in a physisorption state that is established via only weak interaction with the surface of ZnO.

This weak interaction has been reported to be caused by the donation of 0.09-0.1 e^- to the ZnO surface from BTX molecules. However, H-atom in acetone ($H_{acetone}$) and formaldehyde ($H_{formaldehyde}$) can easily undergo formation of H-bonding, when available in the vicinity of oxygen atoms present on the surface of ZnO (O_{surf}). Thus, acetone and formaldehyde are adsorbed due to H-bonding between O_{surf} and, $H_{acetone}$ and $H_{formaldehyde}$ forming bonds O_{surf}-$H_{acetone}$ and O_{surf} -$H_{formaldehyde}$ respectively. The quantitative results of significant improvement in adsorption of VOCs on surfaces of these nanofiber mats was attributed to growth of porosity with the concentration of Zinc oxide which are given in Figure.3.7. Furthermore, the highest adsorption of toluene for the same compositions can be validated on the bases of higher number of atoms it contains and the larger size of toluene molecule when compared to acetone and formaldehyde. Similarly, the minimal amount of formaldehyde has adsorbed on the surface of PTFE-ZnO mats, in comparison to toluene and acetone, which can be justified on the rationale of its molecular structure which is composed of relatively lesser number of atoms of smaller size, as given in table 6.

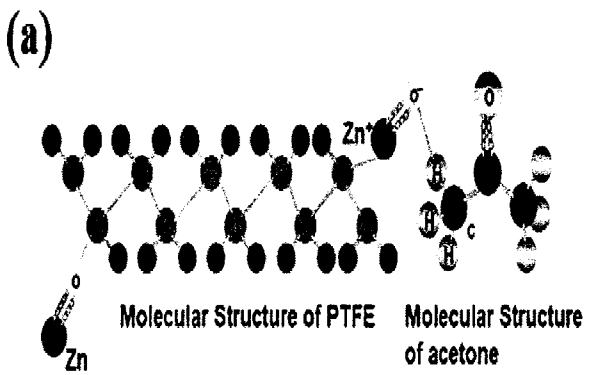

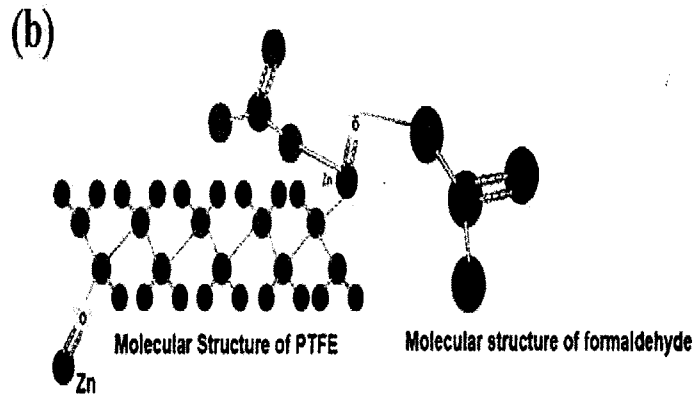

Figure 5.1. VOCs adsorption mechanism (intermolecular interaction) on the surface of heat treated PTFE-ZnO nanofibrous filter mats. Hydrogen bonding between (a) acetone and (b) formaldehyde

Table 6. Important parameters for the three modal VOCs used in this study

VOCs	**Size of molecule (nm) [Ref: Nidhi Sharma et al.]**	**Molecular formula of VOC**	**Adsorption mechanism**
Toluene	0.585	C_7H_8 (15)	van der Waals
Acetone	0.47	$C(CH_3)_2O$ (10)	H-bonding
Formaldehyde	0.43	HCHO (4)	H-bonding

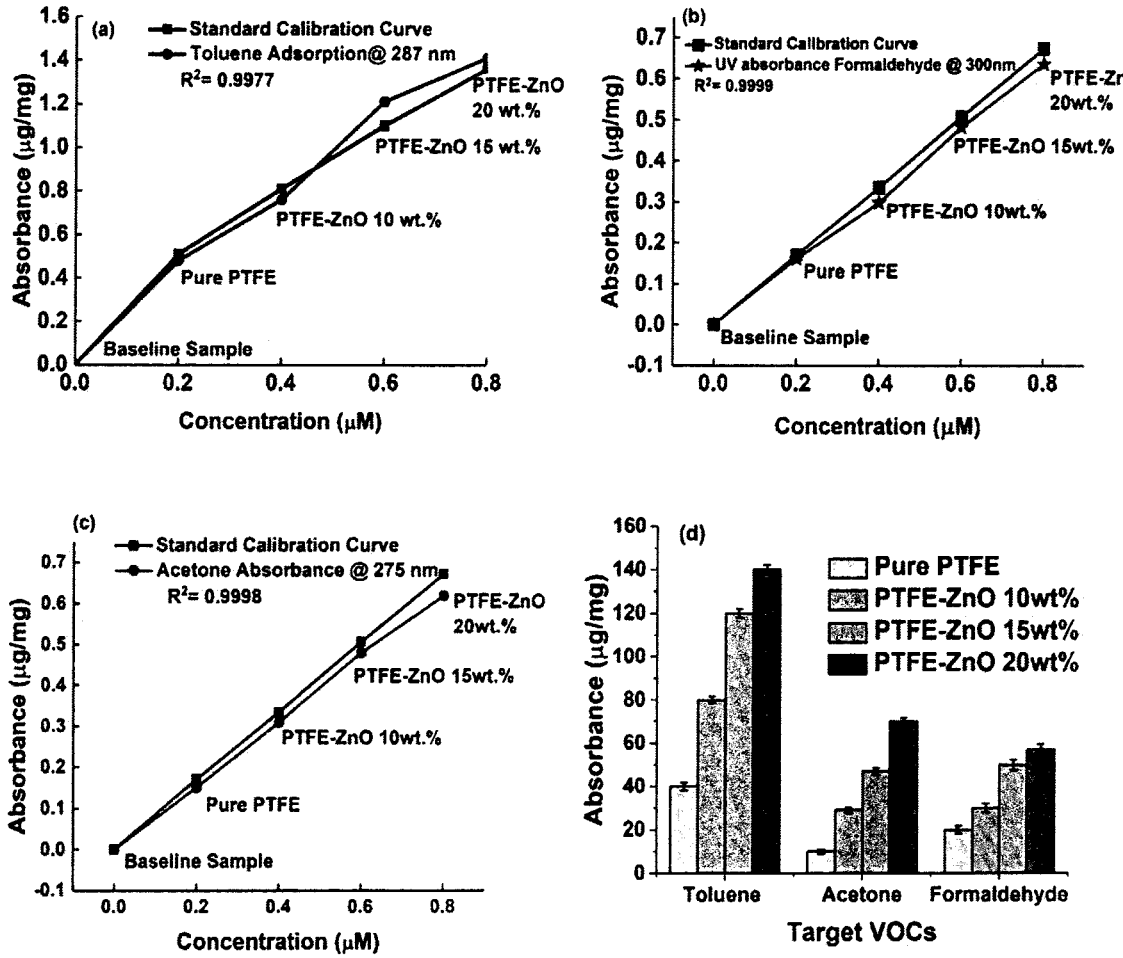

Figure 5.2. Bar chart showing relative adsorption (µg/mg) of the three model VOCs studied for all the synthesized nanofibrous filter mats at different solvent concentrations.

5.2 Aerosol filtration performance evaluation test

Due to high dust filtration capability membrane filtration technique has importance in air filtration field. Filtration efficiency and self-cleaning ability are one of the most interesting properties of the filter material, which can be calculated by the pressure difference inlet and outlet of the filter material to be measured and the particle size of the test particle. The filtration efficiency test was carried out on electrospun synthesized heat treated pure PTFE and PTFE-ZnO nano fibrous filter mats with different loading of Zinc oxide particles. In the present study, the test conditions were as following, temperature 20 °C, relative humidity 40.6%, air flow rate

2.25 m/s, filter diameter 37mm and PM pollutants source was (burning mosquito coil). The setup was in situ customized in lab mimicking industrial exhaust.

The synthesized nanofibrous filter mats of PTFE-ZnO with different zinc oxide weight percentage loadings filtration efficiency is shown in Figure 5.3. Quality Factor (QF) was also calculated to determine filtration performance of the nanofibrous filter mats. Filtration efficiency of the filter mats range from 91.71±0.24 to 97.99%±0.20 for PM $_{2.5}$ and 92.83±1.50 to 99.29 ± 2.25 for PM $_{10}$ as shown in Figure 5.3(a). Pure PTFE nanofibrous filter mats without metal oxide loading showed 91.71 % filtration efficiency for particulate matter 2.5 and 92.83% for particulate matter 10. With the increase in loading of zinc oxide in nano fibrous filter mats filtration efficiency increased from 95.57 to 97.14% for PM $_{2.5}$ whereas for PM $_{10}$ filtration efficiency increased from 97.80 to 99.29% as depicted in Figure 5.3.

After 25 minutes of filtration time there was no significant change in the filtration performance of composite filter mats but commercial filters efficiency reduced to 1% as shown in Figure 5.4. High filtration efficiency of nano fibrous filter mats is due to the fiber structural properties, like decrease fiber diameter, maximum pore radius, high percentage of porosity and high surface roughness as compared with the commercial PTFE filters (Canalli Bortolassi et al., 2019; W. Liang et al., 2019).

Pure PTFE samples showed satisfactory filtration efficiency but with the increase in the zinc oxide loading in the nanofibrous filter mats air filtration efficiency increased significantly in the present study due to four possible reasons; first structural changes like fiber diameter decreased that in turn provide more surface area of interaction to air pollutants, secondly surface roughness is showing increasing trend from 193 to 623 nm by increasing the zinc oxide loading in the mats as shown in Figure 3.2, thirdly pore radius decreased from 156 nm to 124 nm in size that helps in physical filtration (Diffusion and interception) of pollutants and last but not the least porosity increased from 58.15 to 88.73% with zinc oxide loading (Table.2).

The present research results data indicates physical mechanism of filtration is dominant for the large pollutant particles capturing. In case of smaller particulate matter PM $_{2.5}$ filtration efficiency increased due to interaction based mechanism capturing of small particulate matters from the air stream. The critical contribution of the functional groups in the zinc oxide structure for interaction-based mechanisms cannot be ignored.

Rough surface membranes in contrast to smooth surface membranes have high pollutants capturing efficiency due to increase front area fabricated (Souzandeh, 2017). Rough surfaced filtration membranes generate pressure gradient across the pores results in a more streamlined fiber geometry. This whole structure results in lower pressure drop in comparison with the smooth membranes, reason behind is increased stagnation region formed by boundary layers made around the rough fiber (Bian, Wang, Ting, Chen, & Zhang, 2018) (X. Zhao, Wang, Yin, Yu, & Ding, 2016). It can be concluded from the published facts that rough surface membranes have high filtration capability coupled with lower pressure drop which are in line with the present study results as clearly depicted in Figure 5.3 (a-b). Further membranes efficiency can be improved by modifying the surface with metal oxide. On the other hand, the pressure loss of the PTFE membrane decreased as the pore size increased, but in the present research results pressure drop of PTFE-ZnO nanofibrous filter mats remained the same (lower values as compared to the commercial filters) This shows the important role of mass ratio of zinc oxide in PTFE – PVA nanofibrous filter mats for decreasing the pressure drop as shown in Figure 5.3 (b).

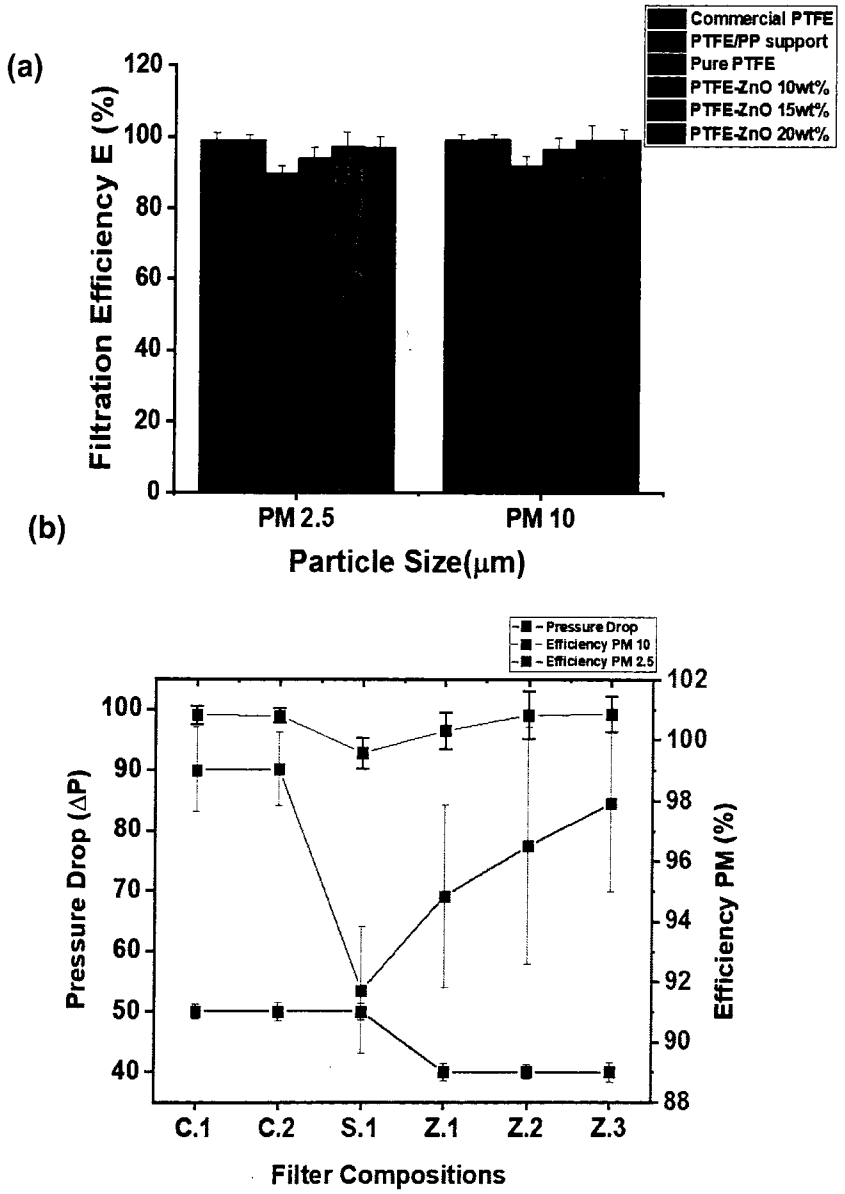

Figure 5.3 (a) Graph showing comparative analysis of Filtration Efficiency (E%) $PM_{2.5}$, PM_{10}, for all synthesized heat treated compositions, **(S.D ±0.24** $PM_{2.5}$, S.D±**2.25** PM_{10}**) (b)** Comparative analysis of Pressure drop (ΔP) of commercial filters and synthesized Nanofiber filter mats, in graph, c.1 represents commercial filter no.1 and S.1 represents synthesized nanofibrous mats, **(S.D ΔP±0.02, S.D ±0.24** $PM_{2.5}$, S.D±**2.25** PM_{10}**).**

5.3 Air Resistance test

Air resistance is another important aspect while bearing in mind the performance evaluation of air filters. Results clearly indicate that high filtration efficiency of PTFE-ZnO with low pressure drop at 40 Pascal. Here, air resistance coefficient (calculated through eq.1) of the PTFE-ZnO nanofibrous filter mats was compared with the commercially available PTFE air filter reported in (Xia et al., 2018) under the similar conditions. The air resistance coefficient of PTFE-ZnO filter mats was 176 Pa s/m with the $PM_{2.5}$ removal efficiency of 97.14% and with the PM_{10} removal efficiency of 99.29%. Inversely, the air resistance coefficient of the commercial PTFE air filter reported in (Xia et al., 2018) was 491 Pa s/m with the filtration efficiency of 99.96%. It is apparent that the air resistance of the PTFE-ZnO nanofibrous filter mats was much lower than that of the commercial PTFE filter as mentioned in literature (Xia et al., 2018). Major reason behind lower air resistance value might be diameters of the nanofibers were comparable to the mean free path of air molecules and led to a higher Knudsen number in the range of Kn 0.1 to 10. In the transitional Knudsen regime, gas slip effect is substantial, hence the air velocity on the nanofiber surface is non-zero (Xia et al., 2018; X. Zhao et al., 2016). That reduced the drag force on the air, so that the air resistance can be reduced significantly as shown in Figure5.3 (b).

5.4 Reproducibility Test

To check the reproducibility of all synthesized electrospun nanofibrous filter mats of PTFE-ZnO with different zinc oxide particles loadings were washed with distilled water after every test run. And afterwards again tested for filtration efficiency (%) for 25 minutes for the removal of PM from polluted air. Pure PTFE filter mats without metal oxide loading showed 91.71 % filtration efficiency for particulate matter 2.5 and 92.83% for particulate matter 10. With the increase in loading of zinc oxide in nano fibrous filter mats filtration efficiency increased from

95.57 to 97.14% for PM $_{2.5}$ whereas for PM $_{10}$ filtration efficiency increased significantly from 97.80 to 99.29%. After 25 minutes of filtration time there was no significant change in the filtration performance of composite nanofibrous filter mats but commercial filters efficiency reduced to 1% as shown in Figure.5.4. The reason might be the higher percentage of porosity and higher hydrophobic nature of the mats (X. Zhao et al., 2016).

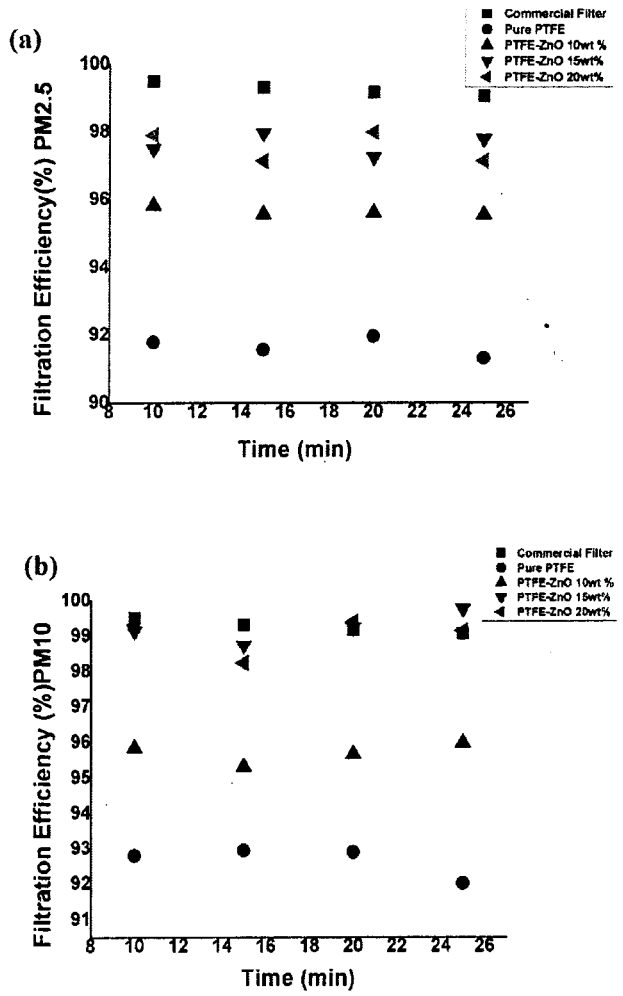

Figure 5.4 (a) Graph showing Filtration Efficiency (E % error ±1.02) of synthesized nanofibrous filter mats for $PM_{2.5}$ **(b)** Graph showing Filtration Efficiency (E % error ±1.14) of synthesized nanofibrous filter mats for PM_{10} with respect to change in time interval.

5.5 Quality Factor measurement

The QF represents a comprehensive evaluation of the air filtering performance by relating the particulate removal efficiency (E (%) of the air filter and the pressure drop (ΔP) due to air flow across the filter. Quality factor of a good air filter should be high representing high pollutants removal efficiency with lower air resistance. Comparison of QF of commercial air filters and fabricated Pure PTFE, PTFE-ZnO nanofibrous filter mats is shown in Figure 5.5.

The QF values of commercial PTFE filters and PTFE/PP support are 0.025 and 0.024(Pa^{-1}) where as QF for synthesized PTFE nanofibrous filter mats range from 0.08 to 0.024(Pa^{-1}). Sintered PTFE-ZnO with 10 and 15wt% showed QF factor of 0.018 and 0.019(Pa^{-1}). PTFE-ZnO with 20wt% showed highest quality factor of 0.024(Pa^{-1}) due to low pressure drop as compared with the commercial PTFE air filter as discussed earlier (Xia et al., 2018). This increase in the quality factor is attributed to Reinforced" slip effect" of the nanofibrous filter mats due to decrease in fiber diameter by increase in loading of zinc oxide in the mats as compared with the pure PTFE mats (Zhao et al., 2016) as mentioned in detail in section 3.1. Taking into consideration the results of PM removal efficiency, pressure drop and quality factor of PTFE-ZnO nanofibrous filter mats, it is suggested that these filter mats can provide best air filtration performance in many fields.

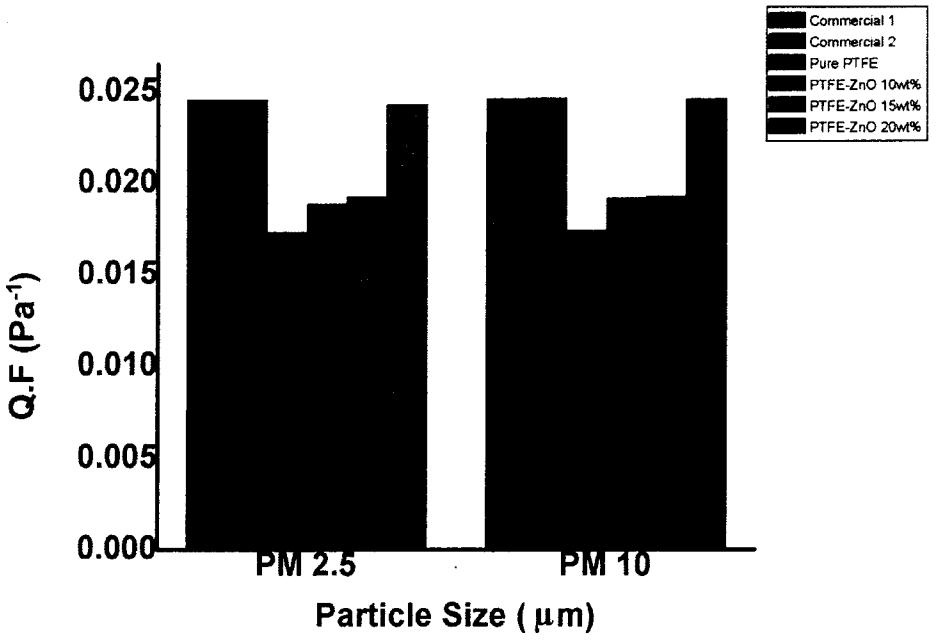

Figure 5.5 Bar graph showing Quality factor (QF) evaluation of commercial filters and PTFE-ZnO nanofibers filter mats with respect to particle size.

5.5 Antibacterial Activity analysis

The antibacterial activity of PTFE-ZnO nanofibrous mats with 10-20 wt% zinc oxide loadings were examined against 2 bacterial strains namely *Escherichia coli (Gram negative)* and *Bacillus subtilis (Gram Positive)*. All experiments were performed in a static state not from air filtration system. The zone of inhibition (ZoI) was determined as the total diameter (mm) of PTFE-ZnO nanofibrous mats. All measurements were performed in PTFE-ZnO with 10µL bacterial solution concentrations and then compared with control as shown in table 7. In case of PTFE-ZnO nanofibrous mats zone of inhibition increased from 1.5 to 6.4 mm in range respectively.

Control (PTFE-PVA) showed 1.5 mm zone of inhibition of E.coli bacterial strain and 1.1 mm for Bacillus subtillis. Bacterial inhibition is less in control due to the absence of antibacterial component in the mat. 15 wt% and 20wt% PTFE-ZnO nanofibrous mats showed significant antibacterial activity by increase in area of inhibition during experiment as shown in Figure3.11. PTFE-ZnO nanofibrous mats with 15wt% zinc oxide particles loadings showed 4.2-5mm zone of inhibition whereas PTFE-ZnO with 20wt% zinc oxide particles showed increase from 6-6.9 mm zone of inhibition respectively.

The increase in the antibacterial activity of PTFE-ZnO nanofibrous mats is due to the presence of zinc oxide particles on mat surface. ZnO reduces the bacteria capability; nevertheless, the exact mechanism of its antibacterial activity has not been well understood so far. There are different possibilities listed in the reported literature for antibacterial activity of zinc oxide particles like; 1) generation of hydrogen peroxide, the accumulation of the particles on the bacteria surface due to the electrostatic forces (Ravindranadh & Mary, 2013). Besides, ROS (Reduced oxygen species) generated due to electrostatic interaction on the surface of the particles, zinc &Nickel ion release, membrane dysfunction and nano particles internalization could also be taken into account as the possible reasons of the cell damage (Hajipour et al., 2012). Moreover, interruption of transmembrane electron transportation has been stated in the case of some metal nanoparticles such as Ag and Zn (L.-H. Li et al., 2013; Atkinson & Winge, 2009).

Table 7. Diameters of Zone of Inhibition (ZoI) for pure PTFE and composite PTFE-ZnO nanofibers filter mats with different ZnO concentrations.

Sample Composition	Sample Diameter (mm)	Zone of Inhibition (mm) *E.coli*	Zone of Inhibition (mm) *Bacillus Subtilis*
Pure PTFE(Control)	10	1.95	1.65
PTFE-ZnO 10wt%	10	2.50	2.95
PTFE-ZnO 15wt%	10	3.95	4.05
PTFE-ZnO 20wt%	10	4.50	4.25

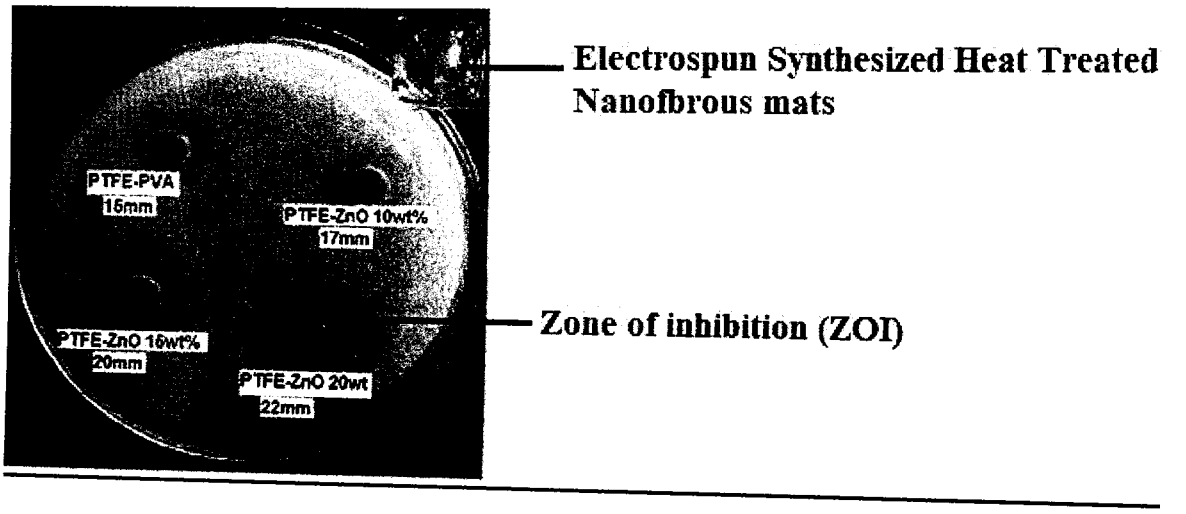

The zone of inhibition (H) was determined by the following formula H= (D-d)/2, D is the overall diameter of the samples and d diameter of zone of inhibition around the sample in mm after antibacterial testing (Veverková & Lovětinská-Šlamborová, 2016).

5.6 Summary:

PTFE-ZnO nanofibrous mats with varying amount of zinc oxide showed significant increase in filtration efficiency 95.04% to 97.01% for $PM_{2.5}$ and 96.53 % to 99.12% for PM_{10} .With the doping of zinc oxide physiochemical properties (specially change in the fibril structure of PTFE/PVA) of the nanofibrous mats improved like pore size increased from 109.47 to 123.47nm while porosity increase from 47.88 to 88.73%. These two parameters are important for increasing filtration efficiency and controlling lower pressure drop across filters. PTFE-ZnO 20wt% showed best results of filtration efficiency; 97.01% for $PM_{2.5}$ and 99.12% for PM_{10}. Antibacterial property of nanofibrous mats demonstrated that PTFE-ZnO 20wt% inhibited 4.25 mm (ZOI) for E.coli and 4.50 mm ZOI for Bacillus bacterial strain. For the adsorption of volatile organic compounds nanofibrous mats were effective in removing formaldehyde and toluene from polluted air while acetone adsorption was the least. The results demonstrated that surface adsorption of these VOCs considerably increased to 10, 07 and 03 folds (64, 141, 62μg/mg) formaldehyde, toluene and acetone respectively for the nanofibrous mats containing 20 wt.% ZnO when compared to pure PTFE mats.

(b) Composite PTFE-NiO Nanofibrous Mats Performance Evaluation

This part of the chapter 3 deals with performance evaluation of synthesized heat treated PTFE-NiO composite nanofibrous filter mats. VOCs adsorption, aerosol filtration and antibacterial activity of mats is studied in detail.

5.7 Adsorption of Volatile Organic Compounds

UV analysis of model VOCs (acetone, toluene and formaldehyde) adsorption by electrospun synthesized PTFE-NiO nanofiber filter mats with varying amount of NiO (2-6 wt %) is shown in Figure 5.7(a-d). The results manifest that adsorption of molecules of model VOCs was deficient on pure PTFE nanofibers filter mats surface; however, with the growing nickel oxide loading in these mats adsorption of VOCs has depicted an increasing trend on the surfaces of PTFE-NiO mats.

Pure PTFE nanofibrous filter mats (without doping) have demonstrated adsorption of 41, 21 and 14 μg/mg of VOCs of toluene, acetone and formaldehyde whereas these adsorptions have been found to 71, 35 and 36 μg/mg; 110, 51 and 52 μg/mg, and 141, 073 and 067 μg/mg for the filter mats containing 2, 4 and 6 wt% NiO respectively. These results revealed that adsorption of formaldehyde acetone and toluene have increased ten, seven and three folds on the surface of nanofiber samples containing 6wt% NiO loading when compared to pure PTFE filter mats. The interaction of PTFE-NiO nanofibers test membrane building blocks with the VOC compounds determines their adsorption capacity and selectivity against the tested VOCs. This can further be analyzed by considering the polar nature of tested VOC compounds and their predisposition towards interaction with the filtration medium of PTFE-NiO nanofibers. Furthermore, selectivity of VOC molecules on the surface of PTFE-NiO nanofibers has been attributed to the fiber structural properties, especially finer mean diameters, internal porous

structure and presence of porous material (metal oxide in present study) on the surface of nanofibers (Y. Wang, Tao, Yu, & Chang, 2018; Kadam et al., 2018).

The sequence of filtration by composite nanofibers filter mats (containing NiO loadings) is attributed to the three steps, firstly, finer diameters of fibers, as adsorption of pollutants takes place on the surface of nanofibers. As shown in Figure 4.1 the mean fiber diameter decreases with an increase in the wt% of NiO in the filter mats, which in turn provides sites of interaction with VOCs molecules. In the second step, adsorption takes place in the internal pores of nanofibers close to the surface (Y. Wang et al., 2018). As depicted in Figure 4.6, porosity increases from 50.21 to 77.36% with the increase in the loading of NiO particles from 0-6wt% which resulted in enhanced VOCs adsorption as shown in Figure 9. Finally, VOC molecules have got adsorbed on the PTFE-NiO nanofibers filter mats with characteristic intermolecular van der Waals forces/H-bonding (Kadam et al., 2018;Y. Wang et al., 2018) revealed in Figure 5.6.

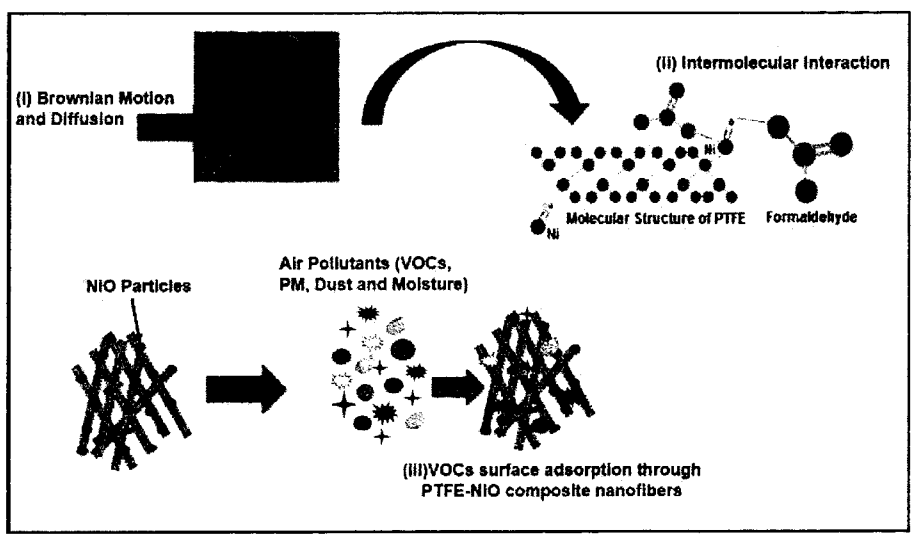

Figure 5.6. (i) Mechanism of adsorption of VOCs on PTFE-NiO composite nanofiber filter mats (i) through Brownian motion and diffusion, (ii) Intermolecular interaction between metal oxide and pollutants on the surface of nanofiber filter mats; **(ii)** VOCs adsorption by PTFE-NiO composite nanofibers.

Physisorption of pollutants on the surface of PTFE-NiO filter mats surface could be of both polar and non-polar. After heat treatment of nanofibers mats at 280 °C in a furnace for 5 minutes some organic species retained on the surface of the mats. The sensitivity of PTFE-NiO filter mats towards VOCs could be due to non-polar interaction of carbonaceous residues species with the VOC molecules. On the other hand, polar oxide surface (NiO) might effectively coordinate with polar organic compounds such as acetone and formaldehyde (Demir et al., 2007) as given in Figure 5.6.

In polar interaction between VOC molecules and NiO molecules, the possible nearest bond (cited calculated bond energy) according to Nugraha (2019) is among oxygen atom of metal oxide (NiO) and hydrogen atom of VOCs on the surface which can be symbolized as O_{surf}-$H_{toluene}$ (Nugraha, Saputro, Agusta, Akbar, & Pramudya, 2019). As it is already mentioned in Figure 4.4 that NiO has two phonon scattering modes (1LO, 2LO) these modes are formed Due to lattice defects, these defects reduce the symmetry around the atoms involved in the formation of phonons in a complete single crystal. Non-stoichiometry in the composition of oxygen is believed to be the main reason for this formation of modes (George & Anandhan, 2014).

Lewis acid-base pairing could be explain the possible interaction between VOCs and the surface metal ions. NiO single crystal structure with 2LO phonon modes has been reported to show surface negative charge due to higher oxygen vacant sites; for that reason, NiO can be considered as Lewis acid (Jiye et al., 2013). Oxygen vacant sites may be considered as trapping sites for interaction with pollutants (VOCs in the present study). Oxygen atoms of nickel oxide particles having two lone pairs and higher electron density can show a tendency to donate electron pairs, thereby acting as Lewis base (Horzum et al., 2014).

Nugraha et al. (2019) demonstrated that benzene, toluene and xylene (BTX) adsorption on metal oxide surface do not originate from the orbital interaction between BTX and metal oxide

surface. Instead, the bonding occurs due to contribution of van der Waals forces between the surface of metal oxide and the VOCs molecule. These authors have verified that toluene adsorption on metal oxide surface is indeed in a physio-sorption state. This weak interaction has been reported to be caused by the donation of 0.09–0.1 e^- to the metal oxide surface from BTX molecules. However, H-atom in acetone ($H_{acetone}$) and formaldehyde ($H_{formaldehyde}$) can easily undergo formation of H-bonding. Thus, acetone and formaldehyde are adsorbed due to H-bonding between O_{surf} and $H_{acetone}$ or $H_{formaldehyde}$ and toluene due to weak van der Waals forces. The quantitative results of improvement in adsorption of VOCs on surfaces of these nanofiber mats was attributed to high percentage of porosity with the increase in concentration of NiO particles in the spinning solution which are given in Figure 4.6.

It is important to mention here that there are two factors affecting surface adsorption of a molecule in the present study; i) size of molecule and ii) the number of atoms involved in VOCs adsorption. The larger molecular size and number of atoms involved in a molecule result in stronger surface interaction (adsorption) (Sharma et al., 2018; Nugraha, Saputro, Agusta, Akbar, & Pramudya, 2019). Similarly, the lower value is of surface energy the stronger interaction (adsorption) is to take place. Furthermore, the high adsorption of acetone and formaldehyde for the same PTFE-NiO 6wt % compositions can be validated on the bases of; 1) higher number of atoms acetone contains for intermolecular interaction with the modified surface of nanofibrous mats, 2) Hydrogen bonding of formaldehyde with the nickel oxide particles on the surface of mats. Toluene adsorption on the surface is low might be due to weak forces for intermolecular interaction in spite of the fact that toluene molecular size is bigger than acetone and formaldehyde (Sharma et al., 2018; Nugraha, Saputro, Agusta, Akbar, & Pramudya, 2019) (please compare the bar charts shown in Figure 5.7).

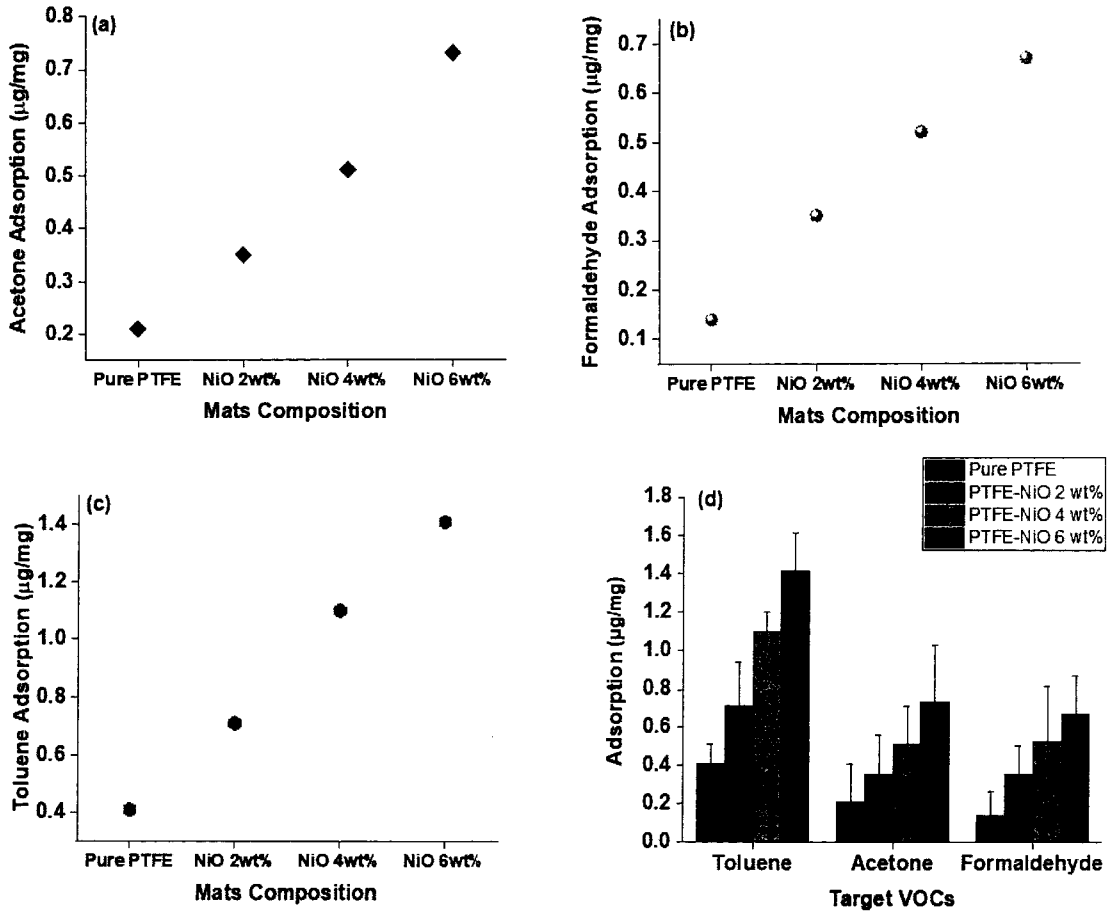

Figure 5.7. Adsorption curves of VOCs at different solvent concentrations. (a-c) Correlation observed by UV-Vis absorbance spectroscopy at 300, 287 and 275nm **(R^2 =0.9999)** for formaldehyde, toluene and acetone (d) Relative adsorption (µg/mg) of three model VOCs.

5.8 Aerosol filtration performance evaluation test

Performance evaluation of heat treated PTFE-NiO nanofibrous filter mats was determined by calculating filtration efficiency and quality factor in comparison with the commercial PTFE air filters. The synthesized nanofibrous filter mats showed filtration efficiency range for all synthesized nanofibrous filter mats (Pure PTFE, PTFE-NiO 2-6 wt%) from 94.31±0.24 to 97.49 %±0.20 for $PM_{2.5}$ and 97.90±1.50 to 99.33 ± 2.25 for PM_{10} as shown in Figure 5.8(a). Pure PTFE nanofibrous mats showed 94.31 % filtration efficiency for particulate matter 2.5 and 97.90 % for particulate matter 10. With the increase in loading of nickel oxide in nano

fibers filtration efficiency significantly increased from 94.31 to 97.49 % for $PM_{2.5}$ whereas for PM_{10} filtration efficiency increased from 97.90 to 99.33 % as shown in Figure 5.8(a). Filtration efficiency of filter mats is dependent on fiber diameter, pore radius, porosity and surface modification with metal oxide (Canalli Bortolassi et al., 2019; W. Liang et al., 2019).

With the increase in the nickel oxide loading in the nanofibers air filtration efficiency increased significantly due to four possible reasons; first fiber diameter decreased that in turn provide more area of interaction to air pollutants, secondly porosity increase by increasing the nickel oxide loading in nanofibers; from 50-78% as shown in Figure 4.6. Results of the present research work clearly indicate that physical size based mechanism is dominant for large size pollutant capturing. In case of smaller particulate matter $PM_{2.5}$ porous fibril structure, pore radius (as shown in Figure 4.6) and nickel oxide particle doping on the surface of filter mats contribution is significant in the present case. Small particulate matters were removed by the interaction based mechanism with the critical contribution from the functional groups in the nickel oxide structure (Souzandeh, 2017). Filtration capability of modified surface nano fibrous filter mats increases in comparison with smooth surface membrane is due to more front area constructed. When pressure gradient is imposed across the bulges of surface modified mats streamlined geometry lowers the pressure drop (Bian, Wang, Ting, Chen, & Zhang, 2018; Zhao, Wang, Yin, Yu, & Ding, 2016). It can safely be conclude from the results that modified surface nanofibrous filter mats have high filtration efficiency due to facilitation of air flow across nanofibers.

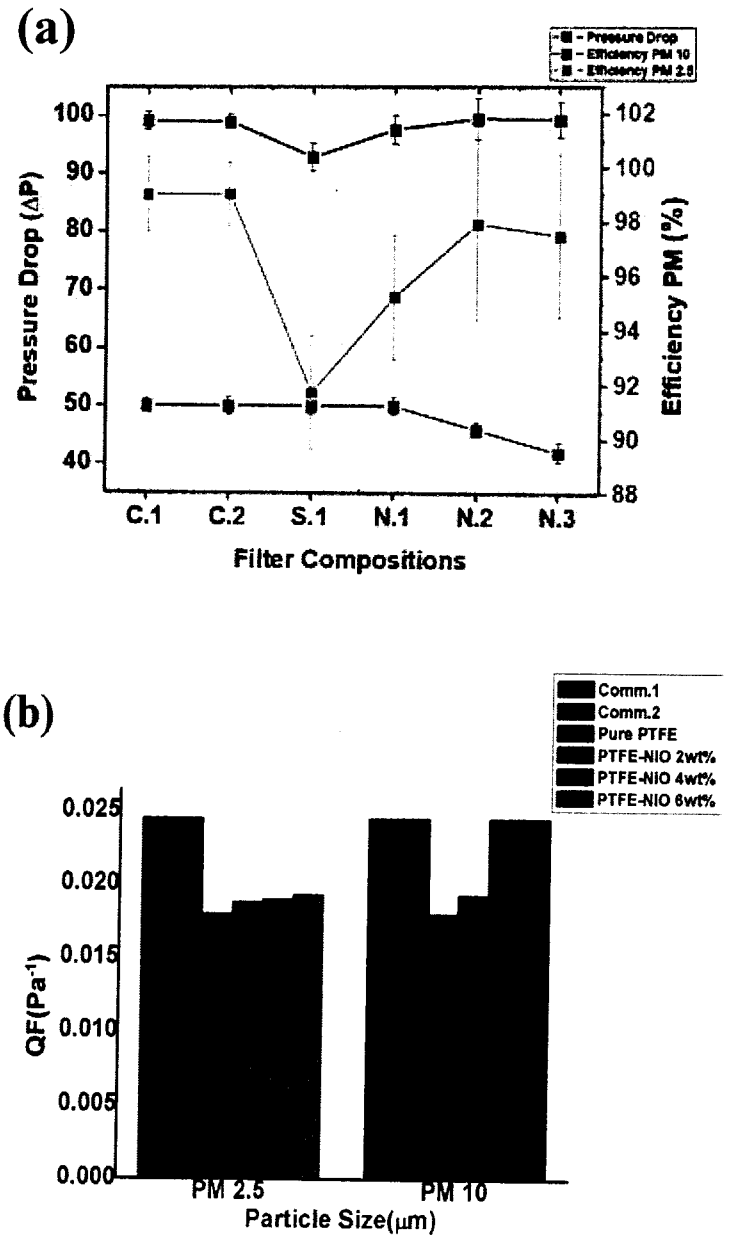

Figure.5.8 (a) Comparative line graph showing change in pressure drop (ΔP) versus collection efficiency (E%) of synthesized nanofibrous filter mats and commercial PTFE air filters, **(S.D ΔP±0.01, S.D ±0.24** $PM_{2.5}$, S.D**±2.25** PM_{10}**).** (ii) Comparative bar graphs showing quality factor with respect to PM particle size.

5.9 Air resistance (AR) Test

Air resistance besides filtration efficiency is another important factor for considering the performance of air filters. Results of the present research work is showing high filtration efficiency of PTFE-NiO filter mats with low pressure drop at 42 Pascal. The AR coefficient was calculated by using the formula in equation 11. Here, we compared the AR coefficient of the PTFE-NiO nanofibers with the commercial PTFE air filter reported in (Xia et al., 2018). The air resistance coefficient of the PTFE-NiO nanofibrous filter mats calculated through equation was 231 Pa s/m with the $PM_{2.5}$ removal efficiency of 97.93% and with the PM_{10} removal efficiency of 99.33%. AR coefficient of the commercial air filter reported in literature (Xia et al., 2018) was 491 Pa s/m with the filtration efficiency of 99.96%. It is obvious that the ARC of the PTFE-NiO nanofibers was lower as compared to the commercial filters.

A major reason might be the diameter of the PTFE-NiO nanofibers which decreased from 0.25 μm to 0.12 μm within increase in nickel oxide doping as shown in Figure 4.1 which could be comparable to the mean free path of air molecules and led to a higher Knudsen number (Kn) in the range of Kn 0.1 to 10 as cited by Xia, 2018. In this transition regime, the gas slip effect is significant, hence the air velocity on the nanofibers surface is non-zero (Xia et al., 2018; Zhao et al., 2016); and second reason is increase in pore size from 100-214 nm of the composite nanofibrous mats as shown in Figure 4.6. That reduced the drag force on the air, so that the air resistance can be reduced significantly as shown in Figure 4.9. In case of PTFE-NiO 6wt% fiber morphology changed to honey combed structure and pore size reduced to 77nm which caused increase in pressure drop a little but still lower than commercial air filters pressure drop as shown in Figure 5.8(a).

5.10 Reproducibility Test

The reproducibility and durability of both commercial PTFE filters and synthesized composite PTFE-NiO filter mats was calculated for the duration of 25 minutes. As shown in Figure 5.9 commercial PTFE filters collective efficiency decrease to 1% after 20 minutes and in case of synthesized composite nanofibrous filter mats filtration efficiency remained the same for $PM_{2.5}$ 97.93% and for PM_{10} removal efficiency of 99.33% after 20 minutes. The reason might be the higher percentage of porosity and higher hydrophobic nature of the filter mats (X. Zhao et al., 2016).

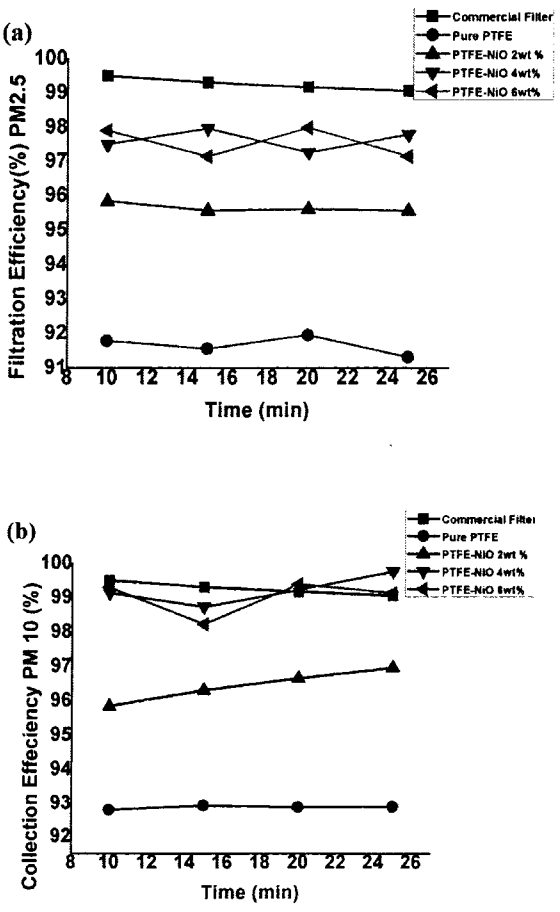

Figure 5.9. Comparative Line Graphs showing PM removal efficiency (E % S.D ±0.24)) of Pure PTFE and PTFE-NiO nanofibers filter mats with respect to time interval.

5.11 Quality Factor Measurement

For a good air filter, the value of QF should be high (high removal efficiency with a low pressure drop). A QF comparison among commercial air filters and the Pure PTFE, PTFE-NiO nanofibrous filter mats is shown in Figure 5.8(b). The QF values of commercial PTFE filters and PTFE/PP support are 0.025 and 0.024 (Pa^{-1}) where as QF for synthesized PTFE-NiO nanofibers range from 0.0188 to 0.0245 (Pa^{-1}). Sintered PTFE-NiO with 2 and 4 wt% NiO showed QF factor of 0.0188 and 0.019 (Pa^{-1}) for $PM_{2.5}$ and 0.0193 to 0.0245 (Pa^{-1}) for PM_{10}. PTFE-NiO with 6wt% showed highest quality factor of 0.019 (Pa^{-1})0.0245(Pa^{-1}) for both particle size as compared with the commercial PTFE air filter. Taking into consideration the results of PM removal efficiency, pressure drop and quality factor of PTFE-NiO nanofibers filter mats, it is suggested that these mats can provide best air filtration performance in wide practical application.

5.12 Antibacterial Analysis of Nanofibers

The antibacterial activity of PTFE-NiO composite nanofibers were examined against 2 bacterial strains namely *Escherichia coli (Gram negative)* and *Bacillus subtilis (Gram Positive)*. All experiments were performed in a static state not from air filtration system. The zone of inhibition (H) was determined by the following formula H= (D-d)/2, D is the overall diameter of the samples and d diameter of zone of inhibition around the sample in mm after antibacterial testing (Veverková & Lovětinská-Šlamborová, 2016). All measurements were performed in PTFE-NiO with 10µL bacterial solution concentrations and then compared with control PTFE-PVA. PTFE-NiO nanofibers showed significantly good bacterial inhibition and the trend of zone of inhibition is 1.9-2 mm for control (PTFE-PVA) for both strains of bacteria and 2.9-4.5 mm for PTFE-NiO with different NiO loadings as shown in table 9. PTFE-NiO with 2wt% nickel oxide loaded particles showed 2.9, 3.05 mm zone of inhibition for E.coli and Bacillus.

Whereas 4 and 6wt% nickel oxide particles loaded PTFE-NiO nanofibers showed an increase in trend of inhibition from 3.8-4.5mm for E.coli and Bacillus bacterial strains. The results showed that PTFE-NiO with 6wt% antibacterial activity for both E.coli and Bacillus was better than 4wt% PTFE-NiO nanofibers. The increase in the zone of inhibition is due to the increase in the amount of metal oxide particles in the nanofibers.

The possibilities behind the mechanism of antibacterial activity of metal oxide particles in nanofibrous mats are; generation of hydrogen peroxide accumulation of the metal oxide particles on bacterial surface due to the electrostatic forces (Ravindranadh & Mary, 2013). ROS (Reduced oxygen species) generated due to electrostatic interaction on the surface of the particles, zinc & Nickel ion release, membrane dysfunction and nano particles internalization could be the possible reasons of the cell damage (Hajipour et al., 2012).

Moreover, interruption of trans-membrane electron transportation has been stated in the case of some metal nanoparticles (L.-H. Li et al., 2013; Atkinson & Winge, 2009). Recently (Peng, Zhang, Aarts, & Dullens, 2018) reported that super paramagnetic nickel colloidal nano crystal clusters has the ability to bind and kill >99.9% of both Gram positive and Gram negative bacteria. Furthermore, bio functionalization of Nickel oxide nanoparticles may synergistically enhance their antibacterial property as shown in table 8.

Table 8. Diameters of Zone of Inhibition (ZoI) for pure PTFE and composite PTFE-NiO nanofibers with different NiO concentrations.

Sample Composition	Sample Diameter (mm)	ZOI (mm) *E.coli*	ZOI(mm) *Bacillus*
Pure PTFE(Control)	10	2	1.9
PTFE-NiO 2wt%	10	3.05	2.90
PTFE-NiO 4wt%	10	3.80	3.95
PTFE-NiO 6wt%	10	4.50	4.49

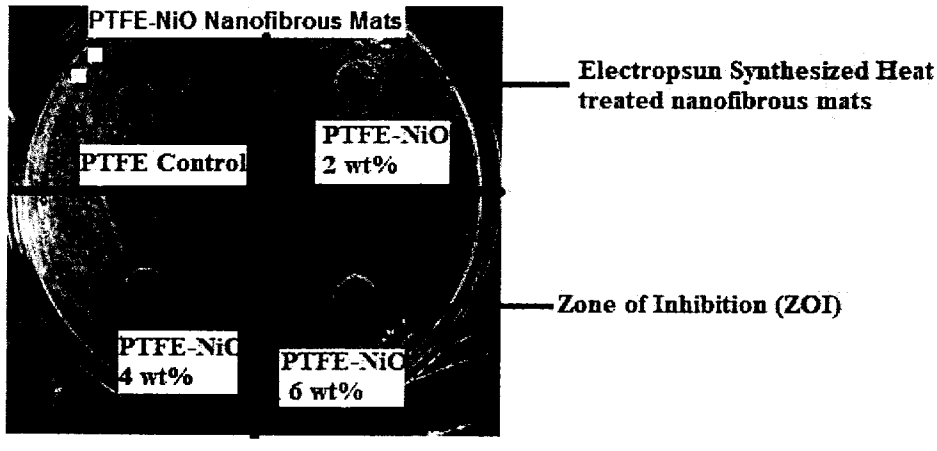

5.13 Summary:

Aerosol filtration efficiency of all the synthesized filter mats was evaluated using three model VOCs, namely, toluene, acetone and formaldehyde that encompasses molecules of both aromatic and aliphatic hydrocarbons. The adsorption of these test VOCs on the surfaces of PTFE-NiO filter mats has been found to increase up to 141, 73 and 67 μg/mg in the samples containing 6 wt% NiO when compared to the pure PTFE filter mats. Results of air filtration experiments revealed that filtration efficiency of PTFE-NiO 6 wt % nanofibrous filter mats reached to 97.49% for $PM_{2.5}$ 99.33% for PM_{10} which was 2 times higher than pure PTFE nanofibrous filter mats under the same pressure drop of 50 Pa. Compared with the commercial PTFE air filters (62Pa). PTFE-NiO nanofibrous filter mats showed reduced air resistance with the same air filtration efficiency. PTFE-NiO nanofibrous filter mats also showed high quality factor of 0.0245(Pa^{-1}) as compared with the (QF) of commercial air filters. The surface property improvements were achieved by the surface modification of PTFE with NiO particles.

Antibacterial property of nanofibrous filter mats demonstrated that PTFE-NiO 6wt% inhibited 4.49 mm of zone of bacterial growth for Bacillus and 4.50 mm ZOI for E.coli bacterial strain.

Conclusion

This doctoral thesis has described the successful fabrication of surface modified PTFE based hydrophobic electrospun composite nanofibrous filter mats with additives metal oxides, like zinc oxide and nickel oxide particles through green electrospinning. These mats can simultaneously capture 2.5 and 10 μm aerosol, VOCs and pathogen agents while offering maximum filtration efficiency (%) and minimum pressure drop mimicing actual conditions of industrial environemt.

Surface morphology of electrospun composite nanofibrous filter mats (PTFE-PVA, PTFE-ZnO and PTFE-NiO) were modified to reduce the pressure drop and enhance filtration efficiency of pollutants. Pure PTFE nanofibrous filter mats showed larger fiber diameter 0.24±15.10μm, low surface roughness of 112.4 nm and low water contact angle of 102.56±2.40 and total surface free energy of 21.03 mN/m. Filtration efficiency of pure PTFE was 91.71% for $PM_{2.5}$ and 92.83% for PM_{10} with the pressure drop of 50 Pa. Quality factor of pure PTFE nanofibrous mats was 0.018 (Pa^{-1}).

PTFE-ZnO composite nanofibrous mats with varying amount of zinc oxide showed increase in filtration efficiency 95.04% to 97.01% for $PM_{2.5}$ and 96.53% to 99.12% for PM_{10} .With the doping of zinc oxide physiochemical properties of the nanofibrous mats improved like pore size increased from 109.47 to 123.47 nm while porosity increase from 47.88 to 88.73%. These two parameters are important for increasing filtration efficiency and controlling lower pressure drop across filters. PTFE-ZnO 20 wt% showed best results of filtration efficiency; 97.01% for $PM_{2.5}$ and 99.12% for PM_{10}. Antibacterial property of nanofibrous mats demonstrated that PTFE-ZnO 20 wt% inhibited 4.25 mm (ZOI) for E.coli and 4.50 mm ZOI for Bacillus bacterial strain. For the adsorption of volatile organic compounds nanofibrous filter mats were effective in removing formaldehyde and toluene from polluted air while acetone adsorption was the least.

The results demonstrated that surface physisorption of these VOCs considerably increased to 10, 07 and 03 folds (70, 140, 57μg/mg) respectively for the nanofibrous filter mats containing 20 wt.% ZnO when compared to pure PTFE filter mats.

In case of PTFE-NiO composite nanofibrous filter mats following results were achieved; fiber diameter range from 0.25± 15.10 to 0.12± 85.75 μm, with the increase in nickel salt doping in suspension, solution conductivity and applied voltage during electrospinning fiber diameter decrease significantly. 6wt% PTFE-NiO composite nanofibrous mats showed high water contact angle of 120.55± 2.20 with surface free energy value of 14.63 mN/m. High hydrophobicity value aid in self-cleaning property of nanofibrous mats. UV analysis showed that PTFE-NiO with 6wt% NiO adsorbed significant amount of volatile organic compounds; 141 of acetone, 73 formaldehyde and 67 μg/mg of toulene. Antibacterial property of nanofibrous mats demonstrated that PTFE-NiO 6wt% inhibited 4.49 mm of zone of bacterial growth for Bacillus and 4.50 mm ZOI for E.Coli bacterial strain.

Filtration efficiency (E%) of synthesized composite PTFE-NiO nanofibrous mats with 6% wt nickel oxide doping range from 97.49% to 99.33% for both $PM_{2.5}$ and PM_{10}. Quality factor was also good as compared with the commercial PTFE filters; 0.0245 (Pa^{-1}) of PTFE-NiO 6wt%. Pressure drop is also low (42 Pa) as compared with the commercial filters (62Pa). Results of self-cleaning test also demonstrated that nanofibrous mats showed excellent self-cleaning property which further aid in air filtration of hazardous pollutants. These composite nanofibrous filter mats has excellent filtration efficiency with low pressure drop and high quality factor. These hydrophobic composite nanofibrous filter mats have wide practical application as far as air filtration is concerned.

Future Perspectives

Human health is continuously deteriorating due to decreasing quality of ambient air. Air quality is declining around the globe due to the adverse effects of human activities; industrialization and urbanization. Based on the experimental results (Hazardous) Polar VOCs and air borne pathogenic agents filtration through PTFE based green polymer composite identified as worthy of further research.

Nanofibers have been found efficient for removal of fine aerosol particles. At present, the particulate capture mechanism is described mostly through two models; diffusion and interception models. There is a need of further elaboration about particles capturing during air filtration through seiving and electrostatic attraction mechansim models. The elaboration of modelling work can be extended to composite nanofibrous membranes surface enabled with different nanoparticles for multifunction air filtration.

References:

Abdul Mannan, H., Yih, T. M., Nasir, R., Muhktar, H., & Mohshim, D. F. (2019). Fabrication and characterization of polyetherimide/polyvinyl acetate polymer blend membranes for CO2/CH4 separation. *Polymer Engineering & Science, 59*(S1), E293-E301.

Aluigi, A., Vineis, C., Tonin, C., Tonetti, C., Varesano, A., & Mazzuchetti, G. (2009). Wool keratin-based nanofibres for active filtration of air and water. *Journal of Biobased Materials and Bioenergy, 3*(3), 311-319.

Balgis, R., Kartikowati, C. W., Ogi, T., Gradon, L., Bao, L., Seki, K., & Okuyama, K. (2015). Synthesis and evaluation of straight and bead-free nanofibers for improved aerosol filtration. *Chemical Engineering Science, 137*, 947-954.

Betha, R., Behera, S. N., & Balasubramanian, R. (2014). 2013 Southeast Asian smoke haze: fractionation of particulate-bound elements and associated health risk. *Environmental Science & Technology, 48*(8), 4327-4335.

Brook, R. D., Rajagopalan, S., Pope III, C. A., Brook, J. R., Bhatnagar, A., Diez-Roux, A. V., Mittleman, M. A. (2010). Particulate matter air pollution and cardiovascular disease: an update to the scientific statement from the American Heart Association. *Circulation, 121*(21), 2331-2378.

Brown, E. N., & Dattelbaum, D. M. (2005). The role of crystalline phase on fracture and microstructure evolution of polytetrafluoroethylene (PTFE). *Polymer, 46*(9), 3056-3068.

Brown, R. (1993). Air Filtration, 77–119. 231–236. In: Oxford: Pergamon Press.

Brown, R., & Thorpe, A. (2001). Glass-fibre filters with bimodal fibre size distributions. *Powder Technology, 118*(1-2), 3-9.

Brown, R. C. (2001). Filtration in industrial hygiene. *AIHAJ-American Industrial Hygiene Association, 62*(5), 633-643.

Casper, C. L., Stephens, J. S., Tassi, N. G., Chase, D. B., & Rabolt, J. F. (2004). Controlling surface morphology of electrospun polystyrene fibers: effect of humidity and molecular weight in the electrospinning process. *Macromolecules, 37*(2), 573-578.

Chuang, Y.-H., Hong, G.-B., & Chang, C.-T. (2014). Study on particulates and volatile organic compounds removal with TiO2 nonwoven filter prepared by electrospinning. *Journal of the Air & Waste Management Association, 64*(6), 738-742.

De Vrieze, S., Westbroek, P., Van Camp, T., & Van Langenhove, L. (2007). Electrospinning of chitosan nanofibrous structures: feasibility study. *Journal of Materials Science, 42*(19), 8029-8034.

DeCoste, J.B. and G.W. Peterson, *Metal–organic frameworks for air purification of toxic chemicals.* Chemical Reviews, 2014. **114**(11): p. 5695-5727.

DOE, U. (2005). Specification for HEPA filters used by DOE contractors. In: DOE Tech. Stand. DOE-STD-3020-2005, US DOE, Washington, DC.

Dotti, F., Varesano, A., Montarsolo, A., Aluigi, A., Tonin, C., & Mazzuchetti, G. (2007). Electrospun porous mats for high efficiency filtration. *Journal of Industrial Textiles, 37*(2), 151-162.

Guibo, Y., Qing, Z., Yahong, Z., Yin, Y., & Yumin, Y. (2013). The electrospun polyamide 6 nanofiber membranes used as high efficiency filter materials: Filtration potential, thermal treatment, and their continuous production. *Journal of Applied Polymer Science, 128*(2), 1061-1069.

Hailin, W., Zhuang, Y., Ying, W., Yele, S., Hui, Y., Zhuang, G., & Zhengping, H. (2008). Long-term monitoring and source apportionment of PM2. 5/PM10 in Beijing, China. *Journal of Environmental Sciences, 20*(11), 1323-1327.

Han, X., & Naeher, L. P. (2006). A review of traffic-related air pollution exposure assessment studies in the developing world. *Environment International, 32*(1), 106-120.

Hassan, M. A., Yeom, B. Y., Wilkie, A., Pourdeyhimi, B., & Khan, S. A. (2013). Fabrication of nanofiber meltblown membranes and their filtration properties. *Journal of Membrane Science, 427*, 336-344.

Horton, D. E., Skinner, C. B., Singh, D., & Diffenbaugh, N. S. (2014). Occurrence and persistence of future atmospheric stagnation events. *Nature Climate Change, 4*(8), 698-703.

Huang, Q.-L., Huang, Y., Xiao, C.-F., You, Y.-W., & Zhang, C.-X. (2017). Electrospun ultrafine fibrous PTFE-supported ZnO porous membrane with self-cleaning function for vacuum membrane distillation. *Journal of Membrane Science, 534*, 73-82.

Huang, Q.-l., Xiao, C.-f., Hu, X.-y., & Li, X.-f. (2011). Study on the effects and properties of hydrophobic poly (tetrafluoroethylene) membrane. *Desalination, 277*(1-3), 187-192.

Huang, Y., Huang, Q.-L., Liu, H., Zhang, C.-X., You, Y.-W., Li, N.-N., & Xiao, C.-F. (2017). Preparation, characterization, and applications of electrospun ultrafine fibrous PTFE porous membranes. *Journal of Membrane Science, 523*, 317-326.

Hung, C.H. and W.W.F. Leung, *Filtration of nano-aerosol using nanofiber filter under low Peclet number and transitional flow regime.* Separation and Purification Technology, 2011. **79**(1): p. 34-42.

Huang, Z.-M., Zhang, Y.-Z., Kotaki, M., & Ramakrishna, S. (2003). A review on polymer nanofibers by electrospinning and their applications in nanocomposites. *Composites Science and Technology, 63*(15), 2223-2253.

Hohman, M. M., Shin, M., Rutledge, G., & Brenner, M. P. (2001). Electrospinning and electrically forced jets. II. Applications. *Physics of Fluids, 13*(8), 2221-2236.

Ignacz, G., Fei, F., & Szekely, G. (2018). Ion-stabilized membranes for demanding environments fabricated from polybenzimidazole and its blends with polymers of intrinsic microporosity. *ACS Applied Nano Materials, 1*(11), 6349-6356.

Jang, S., Yoon, Y.-G., Lee, Y.-S., & Choi, Y.-W. (2018). One-step fabrication and characterization of reinforced microcomposite membranes for polymer electrolyte membrane fuel cells. *Journal of Membrane Science, 563*, 896-902.

Jaworek, A., Krupa, A., & Czech, T. (2007). Modern electrostatic devices and methods for exhaust gas cleaning: A brief review. *Journal of Electrostatics, 65*(3), 133-155.

Jin, M., Zhang, X., Nishimoto, S., Liu, Z., Tryk, D. A., Emeline, A. V., Fujishima, A. (2007). Light-stimulated composition conversion in TiO2-based nanofibers. *The Journal of Physical Chemistry C, 111*(2), 658-665.

Jin, W.-J., Jeon, H. J., Kim, J. H., & Youk, J. H. (2007). A study on the preparation of poly (vinyl alcohol) nanofibers containing silver nanoparticles. *Synthetic Metals, 157*(10-12), 454-459.

Jung, J. H., Hwang, G. B., Park, S. Y., Lee, J. E., Nho, C. W., Lee, B. U., & Bae, G.-N. (2011). Antimicrobial air filtration using airborne Sophora flavescens natural-product nanoparticles. *Aerosol Science and Technology, 45*(12), 1510-1518.

Jung, J. H., Lee, J. E., & Kim, S. S. (2009). Thermal effects on bacterial bioaerosols in continuous air flow. *Science of the Total Environment, 407*(16), 4723-4730.

Kadam, V., Jadhav, A., Nayak, R., Wang, L., & Padhye, R. (2016). Air permeability and moisture management properties of electrospun nanofiber Membranes. *Journal of Fiber Bioengineering and Informatics, 9*(3), 167-176.

Kadam, V. V., Wang, L., & Padhye, R. (2018). Electrospun nanofibre materials to filter air pollutants–A review. *Journal of Industrial Textiles, 47*(8), 2253-2280.

Kang, W., Li, F., Zhao, Y., Qiao, C., Ju, J., & Cheng, B. (2016). Fabrication of porous Fe2O3/PTFE nanofiber membranes and their application as a catalyst for dye degradation. *RSC advances, 6*(39), 32646-32652. doi:10.1039/C5RA27879A.

Kang, Y. O., Im, J. N., & Park, W. H. (2015). Morphological and permeable properties of antibacterial double-layered composite nonwovens consisting of microfibers and nanofibers. *Composites Part B: Engineering, 75*, 256-263.

Kayaci, F., & Uyar, T. (2014). Electrospun polyester/cyclodextrin nanofibers for entrapment of volatile organic compounds. *Polymer Engineering & Science, 54*(12), 2970-2978.

Kelly, T. L., Gao, T., & Sailor, M. J. (2011). Carbon and carbon/silicon composites templated in rugate filters for the adsorption and detection of organic vapors. *Advanced Materials, 23*(15), 1776-1781.

Khajavi, R., Abbasipour, M., & Bahador, A. (2016). Electrospun biodegradable nanofibers scaffolds for bone tissue engineering. *Journal of Applied Polymer Science, 133*(3).

Kurose, T., Takahashi, T., & Koyama, K. (2004). A new process to make a porous PTFE structure from aqueous PTFE dispersion with the help of hydrogel. *Journal of Porous Materials, 11*(3), 173-181.

Lala, N. L., Ramaseshan, R., Bojun, L., Sundarrajan, S., Barhate, R., Ying-jun, L., & Ramakrishna, S. (2007). Fabrication of nanofibers with antimicrobial functionality used as filters: protection against bacterial contaminants. *Biotechnology and Bioengineering, 97*(6), 1357-1365.

Leibold, H., Dirks, F., & Rüdinger, V. (1989). Particulate emissions from a LLW incinerator and off-gas cleaning with a new type of ceramic candle filter. *Waste Management, 9*(2), 87-94.

Li, D., & Xia, Y. (2004). Electrospinning of nanofibers: reinventing the wheel? *Advanced Materials, 16*(14), 1151-1170.

Li, L., Lin, G.-Z., Liu, H.-Z., Guo, Y., Ou, C.-Q., & Chen, P.-Y. (2015). Can the Air Pollution Index be used to communicate the health risks of air pollution? *Environmental Pollution, 205*, 153-160.

Liang, Y., Ju, J., Deng, N., Zhou, X., Yan, J., Kang, W., & Cheng, B. (2018). Super-hydrophobic self-cleaning bead-like SiO2@PTFE nanofiber membranes for waterproof-breathable applications. *Applied Surface Science, 442*, 54-64. doi:https://doi.org/10.1016/j.apsusc.2018.02.126

Liu, C., Hsu, P.-C., Lee, H.-W., Ye, M., Zheng, G., Liu, N., Cui, Y. (2015). Transparent air filter for high-efficiency PM 2.5 capture. *Nature communications, 6*(1), 1-9.

Ma, P. X. (2004). Scaffolds for tissue fabrication. *Materials Today, 7*(5), 30-40.

Main, C. E. (2003). Aerobiological, ecological, and health linkages. *Environment International, 29*(2-3), 347-349.

Mao, N., Liu, J., Chang, D., & Sun, X. (2015). *Discussion of influencing factors on filtration performances of PTFE membrane filters.* Paper presented at the 2015 International Symposium on Computers & Informatics.

Maricq, M. M. (2007). Chemical characterization of particulate emissions from diesel engines: A review. *Journal of Aerosol Science, 38*(11), 1079-1118.

Martin, C. R. (1994). Nanomaterials: a membrane-based synthetic approach. *Science, 266*(5193), 1961-1966.

Matthews, J. A., Wnek, G. E., Simpson, D. G., & Bowlin, G. L. (2002). Electrospinning of collagen nanofibers. *Biomacromolecules, 3*(2), 232-238.

Maze, B., Tafreshi, H. V., Wang, Q., & Pourdeyhimi, B. (2007). A simulation of unsteady-state filtration via nanofiber media at reduced operating pressures. *Journal of Aerosol Science, 38*(5), 550-571.

Meng, S., Ye, Y., Mansouri, J., & Chen, V. (2014). Fouling and crystallisation behaviour of superhydrophobic nano-composite PVDF membranes in direct contact membrane distillation. *Journal of Membrane Science, 463*, 102-112.

Meringolo, C., Poerio, T., Fontananova, E., Mastropietro, T. F., Nicoletta, F. P., De Filpo, G., . . . Profio, G. D. (2019). Exploiting Fluoropolymers Immiscibility to Tune Surface Properties and Mass Transfer in Blend Membranes for Membrane Contactor Applications. *ACS Applied Polymer Materials, 1*(3), 326-334.

Mukhopadhyay, A. (2010). Pulse-jet filtration: An effective way to control industrial pollution Part II: Process characterization and evaluation of filter media. *Textile Progress, 42*(1), 1-97.

Nan, Z., Xiang-yu, J., Chen, H., & Qin-fei, K. (2017). Improved filtration properties of hydroentangled PTFE/PPS fabric filters caused by fibrillation.

Nayak, R., Padhye, R., Kyratzis, I. L., Truong, Y. B., & Arnold, L. (2012). Recent advances in nanofibre fabrication techniques. *Textile Research Journal, 82*(2), 129-147.

Nataraj, S., Kim, B., Yun, J., Lee, D., Aminabhavi, T., & Yang, K. (2008). Electrospun nanocomposite fiber mats of zinc-oxide loaded polyacrylonitrile. *Carbon letters, 9*(2), 108-114.

Pope III, C. A., & Dockery, D. W. (2006). Health effects of fine particulate air pollution: lines that connect. *Journal of the Air & Waste Management Association, 56*(6), 709-742.

Park, B. H., Kim, S. B., Jo, Y. M., & Lee, M.-H. (2012). Filtration characteristics of fine particulate matters in a PTFE/glass composite bag filter. *Aerosol Air Quality Res, 12*(5), 1030-1036.

Patanaik, A., Jacobs, V., & Anandjiwala, R. D. (2010). Performance evaluation of electrospun nanofibrous membrane. *Journal of Membrane Science, 352*(1-2), 136-142.

Podgorski, A., Bałazy, A., & Gradoń, L. (2006). Application of nanofibers to improve the filtration efficiency of the most penetrating aerosol particles in fibrous filters. *Chemical Engineering Science, 61*(20), 6804-6815.

Reneker, D. H., & Chun, I. (1996). Nanometre diameter fibres of polymer, produced by electrospinning. *Nanotechnology, 7*(3), 216.

Reshmi, C., Sundaran, S. P., Juraij, A., & Athiyanathil, S. (2017). Fabrication of superhydrophobic polycaprolactone/beeswax electrospun membranes for high-efficiency oil/water separation. *RSC Advances, 7*(4), 2092-2102.

Rwei, S.-P., & Huang, C.-C. (2012). Electrospinning PVA solution-rheology and morphology analyses. *Fibers and Polymers, 13*(1), 44-50.

Repace, J. L., Jiang, R.-T., Acevedo-Bolton, V., Cheng, K.-C., Klepeis, N. E., Ott, W. R., & Hildemann, L. M. (2011). Fine particle air pollution and secondhand smoke exposures and risks inside 66 US casinos. *Environmental Research, 111*(4), 473-484.

Riboldi, S. A., Sampaolesi, M., Neuenschwander, P., Cossu, G., & Mantero, S. (2005). Electrospun degradable polyesterurethane membranes: potential scaffolds for skeletal muscle tissue engineering. *Biomaterials, 26*(22), 4606-4615.

Ryi, S.-K., Park, J.-S., Park, S.-J., Lee, D.-G., & Kim, S.-H. (2007). Fabrication of nickel filter made by uniaxial pressing process for gas purification: Fabrication pressure effect. *Journal of Membrane Science, 299*(1-2), 174-180.

Senturk Parreidt, T., Schmid, M., & Hauser, C. (2017). Validation of a novel technique and evaluation of the surface free energy of food. *Foods, 6*(4), 31.

Simpson, J. T., Hunter, S. R., & Aytug, T. (2015). Superhydrophobic materials and coatings: a review. *Reports on Progress in Physics, 78*(8), 086501.

Sambaer, W., Zatloukal, M., & Kimmer, D. (2012). 3D air filtration modeling for nanofiber based filters in the ultrafine particle size range. *Chemical Engineering Science, 82*, 299-311.

Sharifi, F., Sooriyarachchi, A. C., Altural, H., Montazami, R., Rylander, M. N., & Hashemi, N. (2016). Fiber based approaches as medicine delivery systems. *ACS Biomaterials Science & Engineering, 2*(9), 1411-1431.

Sim, K. M., Park, H.-S., Bae, G.-N., & Jung, J. H. (2015). Antimicrobial nanoparticle-coated electrostatic air filter with high filtration efficiency and low pressure drop. *Science of the Total Environment, 533*, 266-274.

Souzandeh, H. (2017). Protein-Based Nanofabrics for Multifunctional Air Filtering. Washington State University.

Souzandeh, H., Johnson, K. S., Wang, Y., Bhamidipaty, K., & Zhong, W.-H. (2016). Soy-protein-based nanofabrics for highly efficient and multifunctional air filtration. *ACS Applied Materials & Interfaces, 8*(31), 20023-20031.

Souzandeh, H., Wang, Y., & Zhong, W.-H. (2016). "Green" nano-filters: fine nanofibers of natural protein for high efficiency filtration of particulate pollutants and toxic gases. *RSC advances, 6*(107), 105948-105956.

Sundarrajan, S., Tan, K. L., Lim, S. H., & Ramakrishna, S. (2014). Electrospun nanofibers for air filtration applications. *Procedia Engineering, 75*, 159-163.

Tanthapanichakoon, W., Hata, M., Nitta, K.-h., Furuuchi, M., & Otani, Y. (2006). Mechanical degradation of filter polymer materials: Polyphenylene sulfide. *Polymer Degradation and Stability, 91*(11), 2614-2621.

Tsai, P., & Schreuder-Gibson, H. (2003). The role of fiber charging on co-electrospinning and resilient life of the residual charge from the electrospinning process. *Advances in Filtration and Separation Technology, 16*, 340-353.

Tran, P. A., & Webster, T. J. (2013). Understanding the wetting properties of nanostructured selenium coatings: the role of nanostructured surface roughness and air-pocket formation. *International Journal of Nanomedicine, 8*, 2001-2009. doi:10.2147/ijn.s42970.

Uppal, R., Bhat, G., Eash, C., & Akato, K. (2013). Meltblown nanofiber media for enhanced quality factor. *Fibers and Polymers, 14*(4), 660-668.

Uyar, T., Havelund, R., Nur, Y., Balan, A., Hacaloglu, J., Toppare, L., Kingshott, P. (2010). Cyclodextrin functionalized poly (methyl methacrylate)(PMMA) electrospun nanofibers for organic vapors waste treatment. *Journal of Membrane Science, 365*(1-2), 409-417.

Vanangamudi, A., Hamzah, S., & Singh, G. (2015). Synthesis of hybrid hydrophobic composite air filtration membranes for antibacterial activity and chemical detoxification with high particulate filtration efficiency (PFE). *Chemical Engineering Journal, 260*, 801-808.

Verdenelli, M., Cecchini, C., Orpianesi, C., Dadea, G., & Cresci, A. (2003). Efficacy of antimicrobial filter treatments on microbial colonization of air panel filters. *Journal of Applied Microbiology, 94*(1), 9-15.

Vitchuli, N., Shi, Q., Nowak, J., McCord, M., Bourham, M., & Zhang, X. (2010). Electrospun ultrathin nylon fibers for protective applications. *Journal of Applied Polymer Science, 116*(4), 2181-2187.

Wang, F., Zhu, H., Zhang, H., Tang, H., Chen, J., & Guo, Y. (2016). An elastic microporous material with tunable optical property. *Materials Letters, 164*, 376-379.

Wang, B., Zhang, Y., Shi, L., Li, J., & Guo, Z. (2012). Advances in the theory of superhydrophobic surfaces. *Journal of Materials Chemistry, 22*(38), 20112-20127. doi:10.1039/c2jm32780e

Wang, X., Li, Y., Lin, J., Hodgson, P., & Wen, C. (2008). Apatite-inducing ability of titanium oxide layer on titanium surface: the effect of surface energy. *Journal of Materials Research, 23*(6), 1682-1688.

Wang, Y., Tao, H., Yu, D., & Chang, C. (2018). Performance Assessment of Ordered Porous Electrospun Honeycomb Fibers for the Removal of Atmospheric Polar Volatile Organic Compounds. *Nanomaterials (Basel, Switzerland), 8*(5), 350. doi:10.3390/nano8050350.

Woo, C. G., Kang, J.-S., Kim, H.-J., Kim, Y.-J., & Han, B. (2015). Treatment of air filters using the antimicrobial natural products propolis and grapefruit seed extract for deactivation of bioaerosols. *Aerosol Science and Technology, 49*(8), 611-619.

Wu, S., Deng, F., Wei, H., Huang, J., Wang, X., Hao, Y., Shima, M. (2014). Association of cardiopulmonary health effects with source-appointed ambient fine particulate in Beijing, China: a combined analysis from the Healthy Volunteer Natural Relocation (HVNR) study. *Environmental Science & Technology, 48*(6), 3438-3448.

Xiao, K., Sun, J., Mo, Y., Fang, Z., Liang, P., Huang, X., Ma, B. (2014). Effect of membrane pore morphology on microfiltration organic fouling: PTFE/PVDF blend membranes compared with PVDF membranes. *Desalination, 343*, 217-225.

Xu, J., Liu, C., Hsu, P.-C., Liu, K., Zhang, R., Liu, Y., & Cui, Y. (2016). Roll-to-roll transfer of electrospun nanofiber film for high-efficiency transparent air filter. *Nano Letters, 16*(2), 1270-1275.

Xia, T., Bian, Y., Zhang, L., & Chen, C. (2018). Relationship between pressure drop and face velocity for electrospun nanofiber filters. *Energy and Buildings, 158*, 987-999.

Xu, H., Jin, W., Wang, F., Liu, G., Li, C., Wang, J., Guo, Y. (2019). Formation and characterization of polytetrafluoroethylene nanofiber membranes for high-efficiency fine particulate filtration. *Rsc Advances, 9*(24), 13631-13645. doi:10.1039/c9ra01643k

Yang, F., Xu, C., Kotaki, M., Wang, S., & Ramakrishna, S. (2004). Characterization of neural stem cells on electrospun poly (L-lactic acid) nanofibrous scaffold. *Journal of Biomaterials Science, Polymer Edition, 15*(12), 1483-1497.

Zhang, B., Kang, F., Tarascon, J.-M., & Kim, J.-K. (2016). Recent advances in electrospun carbon nanofibers and their application in electrochemical energy storage. *Progress in Materials Science, 76*, 319-380.

Zhang, C., Xue, X., Luo, Q., Li, Y., Yang, K., Zhuang, X., Zou, G. (2014). Self-assembled peptide nanofibers designed as biological enzymes for catalyzing ester hydrolysis. *Acs Nano, 8*(11), 11715-11723.

Zhang, R., Jing, J., Tao, J., Hsu, S.-C., Wang, G., Cao, J., Zhao, Y. (2013). Chemical characterization and source apportionment of PM 2.5 in Beijing: seasonal perspective. *Atmospheric Chemistry and Physics Discussions, 13*(4), 9953-10007.

Zhang, R., Liu, C., Hsu, P.-C., Zhang, C., Liu, N., Zhang, J., Chu, S. (2016). Nanofiber air filters with high-temperature stability for efficient PM2. 5 removal from the pollution sources. *Nano Letters, 16*(6), 3642-3649.

Zhang, S., Shim, W. S., & Kim, J. (2009). Design of ultra-fine nonwovens via electrospinning of Nylon 6: Spinning parameters and filtration efficiency. *Materials & Design, 30*(9), 3659-3666.

Zhao, D., Kim, J. F., Ignacz, G., Pogany, P., Lee, Y. M., & Szekely, G. (2019). Bio-inspired robust membranes nanoengineered from interpenetrating polymer networks of polybenzimidazole/polydopamine. *Acs Nano, 13*(1), 125-133.

Zhou, T., Yao, Y., Xiang, R., & Wu, Y. (2014). Formation and characterization of polytetrafluoroethylene nanofiber membranes for vacuum membrane distillation. *Journal of Membrane Science, 453*, 40.

Development of Polymer Based Electrospun Nano fiber Filters for Removal of Aerosols from the Petrochemical Industrial Exhaust

ORIGINALITY REPORT

14%	8%	11%	%
SIMILARITY INDEX	INTERNET SOURCES	PUBLICATIONS	STUDENT PAPERS

PRIMARY SOURCES

1	researchbank.rmit.edu.au Internet Source	2%
2	Ye Bian, Rutao Wang, Sin Hang Ting, Chun Chen, Li Zhang. "Electrospun SF/PVA nanofiber filters for highly-efficient PM $_{2.5}$ capture", IEEE Transactions on Nanotechnology, 2018 Publication	1%
3	Dan Lv, Miaomiao Zhu, Zhicheng Jiang, Shaohua Jiang, Qilu Zhang, Ranhua Xiong, Chaobo Huang. "Green Electrospun Nanofibers and Their Application in Air Filtration", Macromolecular Materials and Engineering, 2018 Publication	1%
4	scholarscompass.vcu.edu Internet Source	1%
5	www.tandfonline.com Internet Source	1%

Journal of Polymer Research (2020) 27:222
https://doi.org/10.1007/s10965-020-02218-x

ORIGINAL PAPER

Synthesis of surface modified hydrophobic PTFE-ZnO electrospun nanofibrous mats for removal of volatile organic compounds (VOCs) from air

Syeda Irsa Mazhar[1] · Hafiz Zahid Shafi[2] · Attaullah Shah[2] · Maliha Asma[1] · Seema Gul[1] · Muhammad Raffi[2]

Received: 21 December 2019 / Accepted: 17 July 2020
© The Polymer Society, Taipei 2020

Abstract
The article reports a two-step synthesis of composite nanofibrous mats of polytetrafluoroethylene/zinc oxide (PTFE-ZnO); first, emulsion electrospinning of precursor solution was performed to yield as-spun mats followed by heat treatment at 280 °C. The surface of pure PTFE nanofibrous mats was modified by varying the amount of ZnO loadings in the electrospinning solution from 10 to 20 wt.%. Physiochemical characterization of synthesized mats was performed by FESEM, EDX, AFM, FTIR, Raman, TGA and contact angle goniometry. It was observed that fiber mean diameter decreased from 0.243 ± 15.10 μm to 0.17 ± 30.50 μm, RMS roughness increased from 112 to 627 nm and CA improved from 102.56° to 121.55° with the rise in ZnO content up to 20 wt% compared to the pure PTFE mats. Higher surface area, roughness and hydrophobicity of PTFE-ZnO mats resulted into significantly enhanced adsorption ability of VOCs on their surfaces against three model VOCs, namely, toluene, acetone and formaldehyde. The results have demonstrated that surface adsorption capacity of tested VOCs has considerably increased to 10, 07 and 03 folds respectively for the nanofibrous mats containing 20 wt.% ZnO, compared to pure PTFE mats. Based on these findings, these nanofibrous mats can potentially be used as filters for VOCs and particulate removal from air in the processing industries.

Keywords Poly-tetrafluoroethylene · Nanofibrous mats · Hydrophobicity · VOCs filters · Surface adsorption

Introduction

There are numerous types of volatile organic compounds (VOCs), varied and ubiquitous, which are considered as one of the major sources of air pollution. These VOCs are of about 300 different kinds; mainly released by chemical process industries involved in manufacturing of paints, lubricants and liquid fuels which constitute their primary sources [1]. These pollutants are often discharged due to loading issues from the pipes, heat exchangers and vents of processing vessels in storage tanks. VOCs sources are not only natural but of man-made too like volatilization of building materials, pesticides detergents, cleaning agents, cosmetics containing liquid fuels, solvent thinners, lubricants and degreasers [2]. The most common toxic VOCs are benzene, formaldehyde, toluene, xylene, ethylene, styrene, acetone and acetaldehyde. Prolonged exposure to these compounds may cause carcinogenic effects on the humans, animals, plants and environment. Furthermore, these VOCs have acute catastrophic effects, specifically, on the human central nervous system, liver, respiratory system, eyes and throat [3, 4]. Therefore, it is highly essential to effectively control and reduce the adverse effects of VOCs by removing them from the environment to the safe regulatory limits. Prominent techniques used to control concentration of VOCs in the environment are condensation, thermal oxidation, catalytic oxidation, absorption and adsorption etc. Among these, adsorption has been considered as an efficient method used for the removal of VOCs from the environment to low-concentration levels (ppm) while other conventional techniques are not only expensive but exhibit lower efficiency [5]. Removal of VOCs through conventional adsorbents; activated carbon, GO and metal organic frameworks (MOFs) [6–8] is considered problematic for substantial industrial

✉ Muhammad Raffi
muhammad_raffi@hotmail.com

[1] Department of Environmental Science, International Islamic University, Islamabad, Pakistan

[2] Department of Materials Engineering, National Institute of Lasers and Optronics (NILOP) College, Pakistan Institute of Engineering and Applied Sciences (PIEAS), Islamabad 45650, Pakistan

Published online: 20 July 2020

Journal of Hazardous Materials 395 (2020) 122687

Contents lists available at ScienceDirect

Journal of Hazardous Materials

journal homepage: www.elsevier.com/locate/jhazmat

Mimicking the human respiratory system: Online *in vitro* cell exposure for toxicity assessment of welding fume aerosol

Ryan X. Ward[a,1], Trevor B. Tilly[a], Syeda Irsa Mazhar[a,b], Sarah E. Robinson[c], Arantzazu Eiguren-Fernandez[d], Jun Wang[e], Tara Sabo-Attwood[c], Chang-Yu Wu[a,*]

[a] Department of Environmental Engineering Sciences, Engineering School of Sustainable Infrastructure & Environment, University of Florida, 1128 Center Dr, 220 Black Hall, Gainesville, FL, 32611, USA
[b] Department of Environmental Science, International Islamic University, Female Campus, Room No. 23, Hazrat Maryam Block, H-10 Islamabad, Pakistan
[c] Department of Environmental & Global Health, College of Public Health and Health Professions, University of Florida, HPNP 4157, 1225 Center Dr, PO Box 100188, Gainesville, FL, 32610, USA
[d] Aerosol Dynamics Inc., 935 Grayson St., Berkeley, CA, 94710, USA
[e] Department of Occupational and Environmental Health, Hudson College of Public Health, University of Oklahoma Health Sciences Center, 801 Northeast 13thSt, Oklahoma City, OK, 73104, USA

GRAPHICAL ABSTRACT

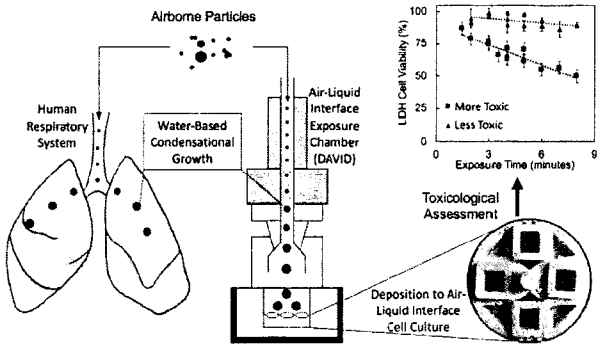

ARTICLE INFO

Editor: R. Debora

Keywords:
Air-liquid interface
Ultrafine particles
Condensation

ABSTRACT

In assessing the biological impact of airborne particles *in vitro*, air-liquid interface (ALI) exposure chambers are increasingly preferred over classical submerged exposure techniques, albeit historically limited by their inability to deliver sufficient aerosolized dose. A novel ALI system, the Dosimetric Aerosol *in Vitro* Inhalation Device (DAVID), bioinspired by the human respiratory system, uses water-based condensation for highly efficient aerosol deposition to ALI cell culture. Here, welding fumes (well-studied and inherently toxic ultrafine particles)

* Corresponding author.
E-mail addresses: rward425@ufl.edu (R.X. Ward), tillytb@ufl.edu (T.B. Tilly), irsa.phdes7@iiu.edu.pk (S.I. Mazhar), sarah.robinson@phhp.ufl.edu (S.E. Robinson), arantza@aerosol.us (A. Eiguren-Fernandez), junwang@ouhsc.edu (J. Wang), sabo@phhp.ufl.edu (T. Sabo-Attwood), cywu@essie.ufl.edu (C.-Y. Wu).
[1] Currently at Division of Geological and Planetary Science, California Institute of Technology, Address: 1200 E California Blvd, Linde + Robinson Laboratory MC 131-24, Pasadena, CA, 91125, USA.

https://doi.org/10.1016/j.jhazmat.2020.122687
Received 20 December 2019; Received in revised form 3 March 2020; Accepted 7 April 2020
Available online 13 April 2020
0304-3894/ © 2020 Elsevier B.V. All rights reserved.